131-04
GEMS 1288209

Consequence Assessment Methods for Incidents Involving Releases from Liquefied Natural Gas Carriers

May 13, 2004

This work was performed by ABSG Consulting Inc. for the Federal Energy Regulatory Commission under contract number FERC04C40196.

ABS Consulting
RISK CONSULTING DIVISION

NOTICE

This report was prepared by ABSG Consulting Inc. (ABS Consulting) solely for the benefit of the Federal Energy Regulatory Commission (FERC). Neither ABS Consulting, FERC, nor any person acting in their behalf makes any warranty (express or implied), or assumes any liability to any third party, with respect to the use of any information or methods disclosed in this report. Any third-party recipient of this report, by acceptance or use of this report, releases ABS Consulting and FERC from liability for any direct, indirect, consequential, or special loss or damage, whether arising in contract, tort (including negligence), or otherwise.

ABS Consulting and its employees, subcontractors, consultants, and other assigns cannot, individually or collectively, predict what will happen in the future. We have made a reasonable effort to review the available consequence assessment methods for some types of incidents involving liquefied natural gas spills and to recommend modeling approaches for use by FERC. Appropriate application of the presented methods will require selection of scenarios to model and selection of some site-specific and scenario-specific modeling parameters. Such application of the models should be done by an experienced consequence analyst. However, as described in this report, the recommended methods have limitations, including uncertainty in the results that they produce. Even when applied appropriately, the recommended methods will provide only estimates of the consequences of postulated scenarios involving LNG spills on water. ABS Consulting accepts no liability for any adverse impacts stemming from use of information in this report.

EXECUTIVE SUMMARY

Liquefied natural gas (LNG) has been transported by sea since 1959 in specially designed LNG carriers. These vessels have a remarkable safety record and provide an essential link in the movement of LNG from production locations to consumer locations. However, stakeholders recognize that there are possibilities for some serious incidents involving LNG carriers, particularly in light of increased awareness and concern about potential terrorist actions.

The Federal Energy Regulatory Commission (FERC) sponsored this study with the goal of identifying appropriate consequence analysis methods for estimating flammable vapor and thermal radiation hazard distances for potential LNG vessel cargo releases during transit and while at berth.

This work considers the flammable vapor and thermal radiation hazards created by unconfined LNG spills on water resulting from an LNG cargo release. This includes review of literature on experimental LNG spills and on consequence assessment methodologies that are applicable to modeling of incidents involving LNG spills on water.

The key modeling issues addressed in this report are:

- Rate of release of LNG from a ship
- Spread of an unconfined pool on water
- Vapor generation for unconfined spills on water
- Thermal radiation from pool fires on water
- Distance for flammable vapor dispersion following spills on water
- Rapid phase transitions (RPTs)
- Effects of thermal radiation on people and structures

Where possible, methods are recommended for assessing carrier spills on water; however, in the case of RPTs no available consequence methods could be identified.

The descriptions of the recommended analysis methods are left to the body of this report. In general these methods can provide only rough estimates of the magnitude of effects for incidents involving large LNG releases on water. This is typically the case with consequence assessments, and it is important to keep in mind that the recommended methods cannot provide precise estimates of effects because of variability in actual incident circumstances as well as uncertainty inherent in the methods used.

In the particular case of the methods of interest here (i.e., methods for large releases from LNG carriers), some important issues include:

- No release models are available that take into account the true structure of an LNG carrier, in particular the multiple barriers that the combination of cargo tanks and the double hulls in current LNG carriers provide
- No pool spread models are available that account for wave action or currents

- Relatively few experimental data are available for validation of models involving LNG spills on water, and there are no data available for spills as large as the spills considered in this study

In making the modeling recommendations in this report, our goal was to select methods that provide the most accurate estimates possible; however, we recognize the limitations of the models we suggest. As a result of these limitations, the project team made some selections that we believe lead to conservative estimates (i.e., tend to overestimate the consequences of LNG releases). Clearly there is an opportunity to develop pool spread models that consider more realistic analysis of the spill behavior on the water surface. In the long term, additional research will need to be performed to develop more refined models, and additional large-scale spill tests would be useful for providing better data for validation of models. However, definition of the specific research tasks and objectives needed to accomplish that research was not in the scope of this project.

No release models were identified that account for the multi-hull structure of an LNG carrier and the physics of a release of cryogenic LNG. In the absence of models specifically for LNG carriers, the orifice model is recommended.

Several models for spreading of pools on water were found in the literature, most of which are based on the assumption that spreading is dominated by the balance of the gravitational spreading force and inertial resistance to spreading. One methodology, developed by Webber and his colleagues (as described in TNO 1997), also accounts for resistance to spreading as a result of frictional forces. Our analysis of these methodologies indicates that frictional effects are important for scenarios involving large releases in short periods of time. Therefore, Webber's methodology is recommended.

For a given hole size (or release rate), the upper limit on pool spread depends on the duration of release. For long duration releases, the pool will spread to the point where evaporation rate (or burning rate in case of a fire) matches the release rate into the pool. This is based on a simple mass and heat balance for the pool, and effectively defines an upper limit for long-term releases. For short duration releases, the dynamics of the release are more important in identifying the upper limit. The pool spread is slowed by inertial and frictional effects but is only stopped once the pool is thin enough for surface tension effects to become important. During the spread, evaporation reduces the volume of the pool, and therefore also slows the spread. As a result of these dynamics, it is difficult to establish an upper limit for short duration releases without modeling the full spread process.

Two methods are identified for estimating heat flux to a boiling LNG pool on water: (1) select a value estimated from spill tests or (2) calculate a value based on heat transfer theory. Based on review of the literature, it is recommended to estimate heat flux using heat transfer theory. Key reasons for this choice are that (1) the experimental data show significant spread, (2) the experimental data for heat flux were typically calculated from other data (rather than measured directly), and (3) a viable theoretical model from heat transfer theory is available to help fill the gap in experimental data.

Available pool fire models for hazard assessment purposes are predominantly based on the solid flame model. The fire is represented as gray-body emitter, and the geometry is approximated by an upright cylinder that is tilted as a result of wind. The point source model is also sometimes used. In this model, energy generated by combustion is assumed to emanate from a single point at the center of the pool fire. The calculated energy is multiplied by a fraction that accounts for the fact that only part of the energy will be emitted as thermal radiation. In some circumstances the point source model can be appropriate, but its chief disadvantage is that it does not produce valid estimates for receptors close to the fire. Therefore, the solid flame model is recommended.

The extent to which people are injured by exposure to thermal radiation depends on both the incident heat flux and the exposure time. A variety of data are available for estimating effects on people, including data from experiments with humans and animals and review of historical data. Section 2.7.1 summarizes some of the injury criteria developed based on these data. Like effects of thermal radiation on people, effects on structures also depend on incident heat flux and the exposure time. With structures, effects also depend strongly on the materials of construction (e.g., wood, steel, concrete). Section 2.8 presents some criteria from various sources for structural damage.

The body of the report also presents some example consequence calculations, which are intended to illustrate use of the various analysis methods recommended. Input parameter values (e.g., atmospheric conditions, surface roughness) were chosen to allow comparison with other methods (Fay [2003], Lehr [2004], and Quest [2001]) or to match values specified by federal regulations for LNG facility siting (49 Code of Federal Regulations [CFR] 193). When using the presented analysis methods for evaluating a specific facility, input parameter values based on actual site conditions should be used.

For the example dispersion calculations presented in this report, the DEGADIS software was used. This model accounts for dense-gas effects and was originally developed for simulation of cryogenic flammable gas dispersion, particularly for LNG. It has been validated against a wide range of available laboratory and field test data.

It is also important to note that this study addresses the potential consequences of large scale LNG cargo releases without regard to the sequence of events leading to such an incident or their probabilities of occurrence. As such, this report does not and was not intended to provide a measure of risk to the public. A thorough risk assessment would consider both the probabilities and consequences of hazardous events. And finally it should not be assumed that the levels of hazards presented in this study are the assured outcome of an LNG vessel release, given the conservatisms in the models and the level of damage required to yield such large-scale releases.

Consistent with the scope of work defined by FERC, this report is highly technical and is focused on the currently available methods for modeling potential releases from LNG vessels. In the scientific community, there is room for debate and different opinions about the most appropriate way to model possible outcomes of incidents. The state of the science will continue to evolve, leading to ongoing iterations of better models/approaches in coming years. However, practical and defendable guidance is needed now to help understand the currently available modeling methods, including their limitations, so that reasonable decision-making processes are

used. This work ultimately recommends practical models/approaches (with appropriate caveats) for use in guiding facility siting decisions.

While studying the results of this report, readers should keep the following key points in mind:

Models have limitations. The recommended models/approaches represent a reasonable set of tools to aid decision making. However, it should be recognized that modelshave an inherent level of uncertainty, as described in this report. In some cases, the scientific community's understanding of the fundamental physical phenomena is better than its ability to simulate such phenomena. Also, models cannot make decisions for us. They inform decision makers, who must integrate information on many different factors in their decision-making process.

Consequence assessment is only one piece of the risk picture. Understanding risk requires an understanding of (1) what can go wrong, (2) what the consequences might be, and (3) how likely the losses are to occur. This report focuses only on consequence modeling of potential release scenarios, not how likely such scenarios are to occur. Decision making related to scenario risks should be considered in the context of both potential consequence and expected likelihood (or frequency). With regard to potential attack scenarios, the expected likelihood is a function of both threat (the likelihood that someone would try to carry out a specific type of attack) and vulnerability (the likelihood that a specific type of attack would be successful and produce the expected consequences of concern). As noted in the report, LNG vessel and associated facility operations are highly regulated and closely monitored/controlled by authorities, so many layers of protection exist against losses. The dependability of these layers of protection was not addressed in this project, but are important considerations in understanding the total risk picture.

Risk perception and risk acceptance are complex issues. How individuals and groups of individuals perceive or accept risks depends on many factors, which are often subjective with no clear right and wrong answers. Even when very precise/certain risk information is available, different people often react to the information in different ways. This project made no attempt to place value judgments on what risks people should or should not accept.

TABLE OF CONTENTS

TABLE OF CONTENTS (cont'd)

LIST OF TABLES

Table **Page**

LIST OF FIGURES

Figure **Page**

ACRONYMS

AIChE	American Institute of Chemical Engineers
AIS	automatic identification system
ANOA	Advanced Notice of Arrival
API	American Petroleum Institute
CFD	computational fluid dynamics
CFR	Code of Federal Regulations
COTP	Captain of the Port
DoS	declaration of security
EPA	Environmental Protection Agency
FERC	Federal Energy Regulatory Commission
GRI	Gas Research Institute
IGC Code	International Code for Ships Carrying Liquefied Gases in Bulk
IMO	International Maritime Organization
ISM Code	International Management Code for the Safe Operation of Ships and for Pollution Prevention
ISPS Code	International Ship and Port Facility Security Code
LFL	lower flammability limit
LNG	liquefied natural gas
LPG	liquefied petroleum gas
MARVS	maximum allowable relief valve setting
MIE	minimum ignition energy
MSO	Marine Safety Office
NFPA	National Fire Protection Association
PSC	Port State Control
RPT	rapid phase transition
SIGTTO	Society of International Gas Tanker and Terminal Operators
SOLAS	Safety of Life at Sea
SSA	ship security alarm
STCW	Standards of Training, Certification, and Watchkeeping
TNT	trinitrotoluene
UFL	upper flammability limit
USCG	United States Coast Guard

SCIENTIFIC SYMBOLS

C_d	discharge coefficient
C_F	turbulent or laminar resistance force
F_G	gravitational force
F_I	inertial resisting force
g	gravitational acceleration
g_r	reduced gravitational acceleration
h	mean pool height
h_f	pool height at the leading edge
H	liquid height above hull breach
Q	flow rate
r	pool radius
R	radius of hull breach
Φ	coefficient for gravity term
ρ_l	density of LNG
ρ_w	water density

UNITS

BTU	British thermal unit
BTU/ft^2	British thermal unit per square foot
BTU/hr/ft^2	British thermal unit per hour per square foot
°C	Celsius
cm	centimeter
°F	Fahrenheit
ft	foot
ft/s	feet per second
ft^3	cubic feet
K	Kelvin
kg	kilogram
kg/m^2/s	kilogram per square meter per second
kg/s	kilograms per second
kJ	kilojoule
kJ/m^2	kilojoule per square meter
kW	kilowatt
kW/m^2	kilowatt per square meter
lb/ft^2/s	pound per square foot per second
lb/s	pounds per second
m	meter
m/s	meter per second
m^3	cubic meter
m^3/s	cubic meter per second
min	minute
mph	miles per hour
psi	pounds per square inch
sec	second

1 INTRODUCTION

1.1 BACKGROUND

Liquefied natural gas (LNG) has been transported by sea since 1959 in specially designed LNG carriers. These vessels have a remarkable safety record and provide an essential link in the movement of LNG from production locations to consumer locations.

The combination of recent interest in expanding or building new facilities to receive LNG carriers (i.e., as a result of increases in demand for LNG in the United States), along with increased awareness and concern about potential terrorist actions, has caused stakeholders to raise questions about the potential consequences of incidents involving LNG carrier operations. For example, the size and extent of a possible fire or the distance a vapor cloud may extend are important factors in gauging the acceptability of a new facility.

Several recently published studies on releases or spills from LNG carriers employ varying methodologies and assumptions. As a result, these studies report some widely varying estimates of potential flammable vapor and thermal radiation hazard distances.

In this context, the Federal Energy Regulatory Commission (FERC) sponsored this study with the goal of identifying appropriate analysis methods for estimating flammable vapor and thermal radiation hazard distances for potential LNG vessel cargo releases during transit and while at berth.

1.2 SCOPE OF WORK

This work considers the flammable vapor and thermal radiation hazards created by unconfined LNG spills on water resulting from an LNG cargo release. This includes a search for and review of literature on experimental LNG spills and on consequence assessment methodologies that are applicable to modeling of incidents involving LNG spills on water. Key consequences of concern include the distance from a spill that flammable vapors might travel and, in the case of a pool fire, the distance from a spill that might receive harmful thermal radiation.

The specific scope of work, as defined by FERC, is as follows:

- An evaluation of published models to calculate the rate of cargo release and the spread of unconfined LNG spills on water;
- A determination of the effect of cargo tank hole diameter on cargo release and pool spread (including establishment of an upper limit on pool spread);
- An evaluation of these models to calculate the rate of vapor generation for unconfined LNG spills on water;
- An evaluation of the models to calculate thermal radiation distances from fires involving unconfined LNG spills on water;
- An evaluation of the models to calculate the distance traveled by flammable vapors from unconfined LNG spills on water;
- An evaluation of the theoretical basis for current models used to calculate each of the above, and a review of the applicability of existing computer modeling to field test data;
- A review of the effects of thermal radiation levels on population and structures;

- A recommendation, including the selection rationale, of specific methods and a model FERC staff may use to calculate the flammable vapor and thermal radiation hazards associated with marine transportation of LNG; and
- A comprehensive review of design, operational, safety, and security features and possible mitigating measures that an LNG facility and/or vessel operator employs or could provide to minimize impacts from: accidents; attacks; leaks; spills; fire; rapid phase transitions; or the spread of negatively buoyant, flammable vapor clouds.

A key goal of this work is to search for and review published methodologies for consequence assessment that are applicable to LNG spills on water. As part of this review, FERC requested the project specifically address the methods applied in four reports: Fay (2003), Lehr (2004), Quest (2001), and Vallejo (2003). Section 2 of this report discusses the modeling approaches in Fay (2003), Lehr (2004), and Quest (2001). However, the Vallejo (2003) report does not provide sufficient technical information and is not discussed.

1.3 PROPERTIES OF LNG

LNG is transported and stored at temperatures as low as -259 ºF (-162 ºC). LNG is typically 85 to 96% methane on a volume basis, with the balance being mostly other light hydrocarbons such as ethane, propane, butane, and up to 1% nitrogen. Methane is flammable in air at 5 to 15% (by volume). At a pressure of 1 atmosphere and temperature of -259 ºF (-162 ºC), its normal boiling point, LNG can evaporate, forming vapor, which has a specific gravity of 1.7. However, LNG vapor at ambient temperatures is lighter than air, and its specific gravity relative to air is 0.55 (once thermal equilibrium is reached). Hence, LNG vapor from a liquid release will tend to stay near the surface of the ground or water until it mixes with air and warms to a temperature of approximately -162 °F (-108 ºC), at which point it will become less dense than air and tend to rise and disperse more rapidly.

1.4 LNG HAZARDS

LNG's principal hazards result from its (1) cryogenic temperature -259 ºF (-162 ºC), (2) flammability, and (3) vapor dispersion characteristics. As a liquid, LNG will neither burn nor explode. Methane, the primary component of LNG, is colorless, odorless, and tasteless, and is classified as a simple asphyxiant for human exposure. LNG vaporizes rapidly when exposed to ambient heat sources such as water, producing 620 to 630 standard cubic feet of natural gas for each cubic foot of liquid.

When spilled onto water, LNG will initially produce a negatively buoyant vapor cloud (i.e., the cold vapors are more dense than air and stay close to the water or ground). As this cloud mixes with air, it will warm up and disperse into the atmosphere. If not ignited, the flammable vapor cloud would drift downwind until the effects of dispersion dilute the vapors below a flammable concentration. At a 5 percent concentration of gas in air, LNG vapors are at their lower flammability limit (LFL). Below this vapor/air ratio, the cloud is too dilute for ignition. At a 15 percent concentration of gas in air, LNG vapors are at their upper flammability limit (UFL). Above this vapor/air ratio, the cloud is too rich in LNG for ignition.

The downwind distance that flammable vapors might reach is a function of the volume of LNG spilled, the rate of the spill, and the prevailing weather conditions. Also, in order to disperse to

significant downwind distances, a vapor cloud must avoid ignition. Evaluation of ignition probability is beyond the scope of this study; however, it is noted that the large releases from an LNG carrier would likely require a significant energy source to initiate (i.e., to puncture the outer hull, inner hull, and cargo tank). An event of sufficient magnitude to rupture an LNG cargo tank may also provide ignition sources. If a flammable cloud is ignited by the initiating event or by other ignition sources (e.g., on the ship, on other nearby vessels, or on shore), the flame will burn back to the vapor source, and the flammable cloud would not travel a significant distance over land.

If a flammable vapor-air mixture from an LNG spill is ignited, it may result in a flash fire, which is a short duration fire burning the vapors already mixed with air in flammable concentrations. The flame front will burn back through the vapor cloud to the spill site, provided the vapor concentration along this path is high enough to continue burning. The rate at which this flame front travels relative to the unburned gas is called the laminar burning velocity. An unconfined methane-air mixture will burn slowly, tending to ignite combustible materials within the vapor cloud, whereas fast flame speeds tend to produce flash burns rather than self-sustaining ignition.

Although LNG vapors can explode (i.e., create large overpressures) if ignited within a confined space, such as a building or structure, there is no evidence suggesting that LNG is explosive when ignited in unconfined open areas. Experiments to determine whether unconfined methane-air mixtures will explode have been conducted and, to date, have been negative.

The principal LNG hazards of interest for this study are those posed by flammable vapor dispersion and thermal radiation. Secondary hazards, such as cryogenic burns and asphyxiation, are typically localized to LNG transport and storage areas and are outside the scope of this study.

LNG is less hazardous than liquefied petroleum gas (LPG) and liquefied ethylene, which have (1) higher specific gravities, (2) a greater tendency to form explosive vapor clouds, (3) lower minimum ignition energies (MIEs), and (4) higher fundamental burning velocities. LNG is not toxic, and it rapidly evaporates; therefore, long-term environmental impacts from a release are negligible if there is no ignition of natural gas vapors.

1.4.1 Fire Hazards

LNG vaporizes quickly as it absorbs heat from the environment, and the resulting vapor is flammable when mixed in air at concentrations from 5 to 15% (volume basis). Its fire-related properties are comparable to other light hydrocarbon fuels (see Table 1.1). The only significant difference is that its molecular weight is considerably less than air, so once it warms above approximately -162 ºF (-108 ºC) it will become less dense than air and tend to rise and disperse more rapidly. However, LNG vapor at its normal boiling point -259 ºF (-162 ºC) is 1.5 times more dense than air at 77 ºF (25 ºC). Typically, LNG released into the atmosphere will remain negatively buoyant until after it disperses below its LFL.

Three types of fires — pool fires, jet fires, and flash fires — are postulated for the purposes of this study.

Pool Fire – When a flammable liquid is released from a storage tank or pipeline, a liquid pool may form. As the pool forms, some of the liquid will evaporate and, if flammable vapor finds an ignition source, the flame can travel back to the spill, resulting in a pool fire, which involves burning of vapor above the liquid pool as it evaporates from the pool and mixes with air.

Jet Fire – If compressed or liquefied gases are released from storage tanks or pipelines, the materials discharging through the hole will form a gas jet that entrains and mixes with the ambient air. If the material encounters an ignition source while it is in the flammable range, a jet fire may occur. For LNG stored at low pressure as a liquid, as it is in an LNG carrier, this type of fire is unlikely. Jet fires could occur during unloading or transfer operations when pressures are increased by pumping. Such fires could cause severe damage but will generally affect only the local area. This report focuses on large spills on water, and analysis of jet fires is outside the scope.

Flash Fire – When a volatile, flammable material is released to the atmosphere, a vapor cloud forms and disperses (mixes with air). If the resultant vapor cloud is ignited before the cloud is diluted below its LFL, a flash fire may occur. The combustion normally occurs within only portions of the vapor cloud (where mixed with air in flammable concentrations), rather than the entire cloud. A flash fire may burn back to the release point, resulting in a pool or jet fire but is unlikely to generate damaging overpressures (explode) when unconfined.

Table 1.1 Fire-related Properties of LNG and Other Light Hydrocarbon Fuels

Material		**Ethylene**[1,2]	**Gasoline**[1,3]	**LNG/methane**[1,2]	**Propane (LPG)**[1,2]
Flash Point (°F)		-186	-40 to -49	<-259	<-155
Flammability Limits (% in air)	**LFL**	2.7	1.3	5	2.1
	UFL	36	7.1	15	9.5
Autoignition Temperature (°F)		910	820	1000	840
Minimum Ignition Energy (BTU)		6.6×10^{-8}	Not reported	2.5×10^{-7}	2.4×10^{-7}
Fundamental Burning Velocity[4] **(ft/s)**		2.6	1.3	1.3	1.5
Vapor Specific Gravity		0.97	< 2	0.55	1.5

Data sources:

1. NFPA (1995)
2. Lees (1980)
3. NFPA (2001)
4. NFPA (2002)

Terms:

Flash Point – The minimum temperature at which a liquid gives off vapor in sufficient concentration to form an ignitable mixture with air near the surface of a liquid, as specified by test.

Flammability Limits – The lowest (LFL) and highest (UFL) concentrations of a combustible substance in a gaseous oxidizer that will support burning.

Autoignition Temperature – Temperature at which a flammable mixture will spontaneously ignite.

Minimum Ignition Energy – The minimum amount of energy released at a point in a combustible mixture that causes flame propagation away from the point, under specified test conditions.

Fundamental Burning Velocity – The burning velocity of a laminar flame under test conditions. When ignited in a flammable vapor cloud, substances with lower fundamental burning velocities will tend to generate lower overpressures.

Vapor Specific Gravity – Ratio of the molecular weight of the material/compound to the molecular weight of air (based on an assumed composition of 79 vol% N_2 and 21 vol% O_2).

1.4.2 Explosions

As discussed in the previous section, a flash fire can occur if LNG is released into the atmosphere and ignited. If ignited in open (unconfined) areas, pure methane is not known to generate damaging overpressures (explode). However, if some confinement of the vapor cloud is present, methane can produce damaging overpressures. Confinement can be provided by spaces within the ship or nearby structures, such as a building on shore or another ship. Areas congested with equipment and structures can also facilitate damaging overpressures if a vapor cloud is ignited within such an area. For example if a vapor cloud infiltrates a chemical process plant in an area with various vessels, structures, and piping and the cloud ignites, the portion of the cloud within that congested area may generate damaging overpressures.

A larger volume fraction of heavier hydrocarbons in the LNG (1) reduces the minimum ignition energy required for detonation and (2) increases the specific gravity of the hydrocarbon mixture (and hence reduces the tendency to rapidly disperse). Both of these effects increase the likelihood of generation of damaging overpressures.

1.4.3 Rapid Phase Transition (RPT)

RPT is the term used to describe a phenomenon recognized in some LNG release experiments involving the nearly instantaneous transition from the liquid to vapor phase and an associated rapid pressure increase. This topic is further discussed in Section 2.6.

When LNG forms a pool on water, the heat from the water rapidly vaporizes the LNG; however, this boiling is not the phenomenon referred to as RPT. In an RPT, a portion of the spilled LNG changes from liquid to gas virtually instantaneously.

Although the physical mechanism is not well understood, RPT is attributed to the superheating of the LNG due to the lack of nucleation sites (sites that help with the formation of gas bubbles and promote boiling). An RPT may result in two types of effects: (1) overpressure resulting from the rapid phase change and (2) dispersion of the "puff" of LNG expelled into the atmosphere. Rapid phase changes have caused numerous steam explosions in foundries and other industrial operations, but have not resulted in any known major mishaps involving transport of LNG.

1.4.4 Cryogenic Effects

LNG carriers are designed to prevent LNG from contacting the inner and outer hulls, but incidents can be postulated that would place LNG in contact with the hulls. It is possible that a release of liquid LNG to the inner hull would cause low temperatures for areas of the hull structure that are not designed for cryogenic temperatures. (The international ship design rules require areas where cargo tank leakage might be expected to be designed for contact with cryogenic LNG.) Assessing the likelihood or result of cold temperature on hull structural members was not within the scope of this study.

A study by Lloyds (2001) includes brief descriptions of 10 LNG spills involving LNG carriers that occurred between 1965 and 1989. Seven of these ten spills led to brittle fracture of the deck or tank covers, but none of them caused serious structural damage. Given where the damage occurred (i.e., to the deck or tank cover), it is likely that all of these releases occurred from piping systems

used during LNG transfers. Also, vessels built since 1976 have to comply with current ship design rules and are designed with steel rated for low temperature in areas where LNG leakage might be expected to contact decking or internal structures. (See Section 4.3.1.2 for a discussion of the design requirements for LNG tankers.)

2 CONSEQUENCE ASSESSMENT METHODS

This section presents a review of available methods for modeling some specific aspects of events involving large releases of LNG on water. Also presented are recommended approaches for modeling, which are based on:

- The reviews of available methods,
- The types of events of interest (e.g., large LNG releases on water leading to pool fires and/or flash fires), and
- The intended uses for the consequence assessment results (e.g., facility siting decision making, emergency planning).

Section 3 presents some example calculations that follow the methods recommended in this section.

2.1 RATE OF RELEASE OF LNG FROM A SHIP

If an LNG cargo tank is punctured below the liquid level, the LNG will flow through the hole. This section presents an evaluation of methods to calculate how fast the liquid will spill.

2.1.1 Review of Modeling Approaches

Fay (2003) – Fay presents two release rate models, one for holes above the seawater level and one for holes below the seawater level. The model for holes above the seawater level is equivalent to the well-known relationships for flow through an orifice, driven by gravity. The orifice model is presented in many references on consequence assessment, such as AIChE (2000) and TNO (1997), as well as most basic textbooks on fluid mechanics. This model represents flow from a hole in the side of a single hull cargo tank that allows the LNG to flow directly from the tank into the water. A discharge coefficient is often used to represent the frictional loss accompanying flow through the orifice; Fay does not include a discharge coefficient, which is equivalent to assuming a value of 1.0 (no frictional loss). This model does not attempt to account for the multi-hull construction of LNG carriers, and therefore may overestimate the rate at which LNG would escape through a breach.

Fay's model for holes below the seawater level is an idealistic approach in which the difference in density of the fluids causes (1) the LNG to flow out the hole to the water surface and (2) water to flow into the ship. However, this method ignores the fact that the boiling point of LNG is well below the water temperature. In reality, the LNG would flash to vapor as it exited the hole and came into contact with the water, rapidly rising to the surface. Water that did enter the ship would likely freeze and might affect the rate of LNG release. This model also does not attempt to account for the multi-hull construction of LNG carriers.

Lehr (2004) – Lehr neither presents nor uses release rate models. This paper presents a single release example that is an instantaneous release of 500 m^3 of LNG.

Quest (2001, 2003) – This study postulates 1-m and 5-m diameter holes but does not describe the method used to calculate the flow rate from the holes.

Other Methods – Our literature review did not identify any additional methods for estimating release rates for spills from LNG carriers. No methods were identified that attempt to account for the multiple barriers to release that are present in LNG carriers.

2.1.2 Modeling Recommendations

In LNG carriers, the LNG is contained inside an insulated cargo tank that is contained within the inner hull of the ship. The scenarios of interest for this study involve incidents that puncture both the inner and outer hulls, the insulation layer, and the LNG cargo tank. No existing release model accounts for these multiple barriers to release or for a ship's possible response to a large release of LNG (e.g., into the inner compartments of a ship).

In addition, the existing models assume that air can enter the space at the top of the LNG compartment or LNG can be vaporized to replace the exiting liquid at a volumetric rate equal to the discharge rate from a hole in the side wall of the tank. That is, they ignore the possibility of low pressure in the vessel reducing the rate of outflow. For small diameter holes, or for scenarios where a hole extends above the liquid level, this may be a valid assumption. For large diameter holes, the liquid release rate may be higher than the rate at which vapor can be generated or at which air can enter through the vacuum relief valve. If this occurs, a partial vacuum may be created in the tank, reducing the outflow rate and possibly further damaging the compartment (if it is not designed for full vacuum).

In the absence of models that account for the true structure of an LNG carrier and the physics of a release of cryogenic LNG, the simple orifice model is recommended:

$$Q = C_d \pi \rho_l R^2 \sqrt{2gH}$$

where Q = flow rate
C_d = discharge coefficient (taken as 1.0)
ρ_l = density of LNG
R = radius of hull breach
H = liquid height above hull breach

When using this model it is vital to keep in mind that the model does not reflect actual carrier construction very well, and the results should be interpreted as a rough guide to the rate of release for a given hole size. It is also important to note that cargo spilling between hulls is not accounted for. The orifice model represents the double-hulled ship as a single-wall vessel, and therefore will tend to overestimate the LNG outflow for many scenarios.

The orifice model is presented in many references on consequence assessment, such as AIChE (2000) and TNO (1997), as well as most basic textbooks on fluid mechanics.

There are no appropriate models available for releases through a hole in the tank wall that is below the seawater level. As described above, Fay (2003) does present a model for underwater punctures, but his model does not account for the (1) actual physics of a release of cryogenic liquid directly into seawater or (2) actual geometry of an LNG carrier. In the absence of an appropriate model, the orifice model may be applied to provide a rough guide to the rate of release.

A qualitative discussion of what might happen in a release below water level is useful in understanding the difficulty in accurately modeling such a situation. To a certain level below the seawater surface, the LNG pressure will exceed the water pressure, so the LNG will tend to flow out the hole and vaporize rapidly as it contacts the water. For holes further below seawater level (or once the LNG level drops), a point will be reached where the LNG pressure and water pressure match, and seawater may begin entering the hole. Any seawater that entered the vessel would tend to freeze rapidly, and the heat it transfers to LNG within the vessel will vaporize LNG, possibly increasing pressure in the vessel and forcing LNG and/or water out the breach. Other possible scenarios might involve both LNG and seawater spilling into the void space between the tank and outer hull.

For many scenarios, the orifice flow model is expected to overestimate the release rate because it does not account for factors such as (1) a reduction in tank pressure as liquid exits (i.e., when outflow exceeds rate at which volume can be replaced by air or LNG vaporization) or (2) the additional barriers to release provided by the design of the cargo system and the structure of the ship. On the other hand, the orifice model does not address any additional ship damage that might occur as a result of a postulated release.

Two other aspects of LNG spills were also considered in this review:

Effects of LNG Composition – Cumber (2002) assessed the discrepancy between estimates of outflow for LNG using the correct composition and using an approximation of the material as pure methane. This report finds that composition can "change the shape and location of the boundary of the two-phase envelope," which can significantly affect outflow. He presents an example with LNG that is 90% methane held at 44 psi (3 bar) and –244 ºF (120 K). For this example, the pure methane approximation underpredicts initial outflow by nearly a factor of two. Within roughly 300 seconds, the estimated flow rates converge to approximately the same value. In the case of an LNG carrier, LNG is stored very near the normal boiling point, so two-phase flow effects are expected to be minimal. Considering the overall uncertainty introduced by applying the orifice model to postulated LNG release scenarios, approximating the outflow using pure methane properties will introduce negligible additional uncertainty.

Transient Nature of Spills – For the idealized case of a gravity-driven release of liquid from a hole in a vessel, the flow rate will decrease as the height of the liquid above the hole decreases, and the flow will stop once the liquid level reaches the bottom of the hole. If appropriate for the scenario postulated, this transient flow rate should be applied when modeling LNG carrier releases. For other scenarios, it may be more appropriate to conservatively assume a constant outflow rate (i.e., at the initial rate predicted by the orifice model).

2.2 SPREAD OF AN UNCONFINED POOL ON WATER

LNG is less dense than water and when spilled on water will form a floating pool that will spread and evaporate. This section presents an evaluation of the methods for estimating the rate and extent of LNG pool spread on water.

2.2.1 Review of Modeling Approaches

Fay (2003) – Fay presents a model based on a balance of fluid inertia and gravity force. This model assumes the water surface is smooth.

Lehr (2004) – Lehr applies a model based on a balance of fluid inertia and gravity force; the model includes empirical constants, which he takes from Briscoe (1980). For large spills, Lehr points out that spread may become controlled by a balance of viscous and gravity forces. However, he concludes that the time at which this would occur would likely be longer than the expected burn time for an LNG pool fire. This model assumes the water surface is smooth.

Quest (2001, 2003) – Quest also applied a model for spread based on a balance of fluid inertia and gravity force. In addition, Quest attempted to account for the effects of waves on spread. The waves were approximated by a cycloid function, and computations were performed to apply boundary conditions on the basic gravitational spreading model. The effect of these boundary conditions is that the pool stops spreading once the height of the LNG above the water level drops below 60% of the wave height. An adjustment was also made for the increased water surface area caused by the waves, which results in an increase in vaporization flux of 27%.

Other Methods – Several pool spread models are currently in use. Early spread models published by Hoult (1972), Fay (1973), Shaw (1978), and others are based on the steady state Bernoulli equation and approximate axisymmetric spread on water by:

$$\frac{dr}{dt} = \sqrt{2 g_r h}$$

where r = pool radius

$$g_r = g \frac{\rho_w - \rho_l}{\rho_w}$$

h = mean pool height

ρ_w = water density

ρ_l = density of liquid in pool

With this approach, spread is driven strictly by gravity, and the rate is given as a function of pool height only.

Raj and Kalelkar (1974) derived a different spreading relationship, based directly on equating gravitational force (F_G) and inertial resisting force (F_I), given by:

$$F_G = \pi r h^2 \rho g_r \qquad \text{and} \qquad F_I = -C(\pi r^2 h \rho)\frac{d^2 r}{dt^2}$$

The constant C is introduced to account for the fact that the inertia of the entire pool is a fraction of that given by use of the acceleration of the leading edge ($\frac{d^2 r}{dt^2}$). Equating these forces and solving for acceleration gives:

$$\frac{d^2 r}{dt^2} = -\frac{g_r h}{C r \rho}$$

This approach also defines spread as driven strictly by gravity.

Both of these approaches effectively ignore resistance to spreading as a result of friction. Some authors acknowledge this fact and mention that viscous effects may be important for "large" LNG spills on water.

One method, developed by Webber (as described in TNO 1997), does account for friction effects. This approach is based on self-similar solutions of the shallow water equations and lubrication theory. Webber's formulation results in the following description of spreading:

$$\underset{\text{inertia}}{\frac{d^2 r}{dt^2}} = \underset{\text{gravity}}{\frac{4 g_r \Phi h}{r}} - \underset{\text{resistance}}{C_F}$$

where:

Φ = coefficient, which is a function of $\frac{h_f}{h}$

h_f = pool height at the leading edge

C_F = turbulent or laminar resistance force

In this formulation, resistance by turbulent or laminar friction effects is included, and Webber provides methods for estimating the various values needed (e.g., Φ , C_F).

To better understand the characteristics of these methods and to assess the importance of friction effects for spills of interest in this report, two of these methods were implemented using an integral solution approach. The methods implemented are those of Shaw (1978) and Webber (TNO 1997). The method of Webber was chosen because it is the only one that includes friction effects. The method of Shaw was chosen as representative of the methods based solely on gravitational spreading. As shown by Otterman (1975), while the formulations of these gravitational spread methods vary, they give very similar results. Otterman's analysis included methods of Fay, Hoult, and Raj/ Kalelkar; note that the methods of Fay and Hoult included are equivalent to the method of Shaw as presented above.

Implementation of the Shaw and Webber methods was accomplished with the assistance of the Mathcad computer software (©1986-2000 MathSoft, Inc.). For the case of an LNG spill on water, the solutions are simplified by the fact that pool temperature remains constant (at the boiling point) and the evaporation heat flux is constant (based on either film boiling heat flux or burning rate). The numerical solutions applied here also allow accounting for various types of spill sources, including those that are transient.

Example pool spread scenarios and results from both the Shaw and Webber methods are shown below. These scenarios involve spills of 4.4×10^5 ft^3 (12,500 m^3) through 3.3-ft (1-m) and 16-ft (5-m) diameter holes. These hole diameters were selected for the sensitivity analysis since they are representative of potential ship damage as found in other vulnerability assessments. Results are provided for two cases (1) assuming that a fire occurs immediately (at the beginning of the release) and (2) assuming that no fire occurs. The spill duration is the time required to empty the volume of liquid that is above the hole in the cargo tank.

Pool Spread Scenario for Comparison of Shaw and Webber Models – Fire Case

Hole diameters: 3.3 ft (1 m) and 16 ft (5 m)

Initial liquid height above hole: 43 ft (13 m)

Total spill quantity: 4.4×10^5 ft^3 (12,500 m^3)

Burning rate: 0.058 lb/s/ft^2 (0.282 kg/s/m^2)

Pool Spread Results for Comparison of Shaw and Webber Models – Fire Case

Hole diameter	3.3 ft (1 m)		16 ft (5 m)	
Initial spill rate	11,700 lb/s (5,300 kg/s)		290,000 lb/s (130,000 kg/s)	
Total spill duration	33 min		1.3 min	
Spread model	Shaw	Webber	Shaw	Webber
Maximum pool radius	250 ft (76 m)	240 ft (74 m)	790 ft (240 m)	440 ft (130 m)
Total duration of fire	33 min	33 min	3.2 min	6.9 min

Pool Spread Scenario for Comparison of Shaw and Webber Models – Nonfire Case

Hole diameters: 3.3 ft (1 m) and 16 ft (5 m)

Total spill quantity: 4.4×10^5 ft^3 (12,500 m^3)

Air temperature: 71 °F (22 °C)

Water temperature: 70 °F (21 °C)

Pool Spread Results for Comparison of Shaw and Webber Models – Nonfire Case

Hole diameter	3.3 ft (1 m)		3.3 ft (5 m)	
Initial spill rate	11,700 lb/s (5,300 kg/s)		290,000 lb/s (130,000 kg/s)	
Total spill duration	33 min		1.3 min	
Heat transfer to LNG pool	11,700 BTU/hr/ft^2 (37 kW/m^2)			
Spread model	Shaw	Webber	Shaw	Webber
Maximum pool radius	450 ft (140 m)	430 ft (130 m)	1,100 ft (340 m)	550 ft (170 m)
Total evaporation duration	34 min	34 min	6.1 min	18 min

Conclusions from the analysis of the Shaw and Webber methods are that:

- For some of the LNG spills of interest in this report, Webber's methods indicate that friction effects on the LNG pool spreading over water are important, in particular, for large, short-term releases. In a scenario involving a release of 4.4×10^5 ft^3 (12,500 m^3) through a 16-ft (5-m) diameter hole, Webber's method predicts a maximum pool radius that is approximately

half that predicted by the method of Shaw. On the other hand, for longer duration spills, friction effects appear much less important. For a scenario involving a release of 4.4×10^5 ft^3 (12,500 m^3) through a 3.3-ft (1-m) diameter hole, the methods provide very similar results.

- When Webber's method is modified to ignore friction effects, it produces results very similar to those of Shaw. As TNO (1997) points out for this special case, Webber's method reduces to the same form as the basic gravitational methods (like Shaw), differing only by the coefficient on the right side. Shaw effectively has a coefficient of $\sqrt{2} = 1.41$, and Webber uses a coefficient of 1.64 (empirically derived).
- Webber's method for determining the turbulent resistance term, C_F, involves taking the larger of estimates for laminar or turbulent flow. The implementation here included both factors, but for all of the scenarios examined, the turbulent factor dominated.
- A numerical solution to the spreading problem is desirable because it allows handling transient spill sources, and therefore avoids artificially characterizing a spill as either "instantaneous" or "continuous."

2.2.2 Modeling Recommendations

Based on review of the literature and example implementation of the Shaw and Webber spread methodologies, the method of Webber (as described in TNO 1997) is recommended. For many scenarios (e.g., long duration releases), this method will provide results that are very similar to those from the various methods based solely on gravity-driven spread. However, for some scenarios (e.g., large, short-duration releases), Webber's method predicts significantly slower pool spread (as friction effects become more important). Because Webber's method (1) has a more sound theoretical basis and (2) accounts for friction effects, these results are believed to be more realistic than those from the simpler gravitational models that ignore friction effects.

It is also recommended that pool spread modeling be implemented in a way that avoids the need to characterize spills as either "instantaneous" or "continuous." The integral approach taken in the example implementation for this report accomplishes this. If desired, it can accommodate an "instantaneous" release (i.e., a specified pool volume in the water at time zero) and/or a fixed or transient release rate into the pool.

It is also useful to note that for some scenarios, detailed modeling of pool spreading is not necessary. In particular, with a long-term (i.e., "continuous") release, the pool will spread until the evaporation rate (or burn rate, in the case of a pool fire) matches the rate of addition from the spill. In a case such as this, the pool area can be estimated using the spill rate and the evaporation rate per unit area. Of course, as with the Webber model, this is predicated on the assumption of smooth, quiescent water.

Because the recommended spread model does not account for wave action or currents, it can only provide an approximation of pool behavior. All LNG tankers transit waterways in tidal contact with the ocean, and therefore are usually subject to tidal currents and wave action. However, when unloading cargo at a marine terminal (in a protected slip or turning basin) tidal currents and wave action may at times be minimal. Wave action will tend to increase the rate of heat transfer to the spreading pool of LNG, which will increase the rate of LNG vaporization and limit the size of the pool area. Water currents (tidal, river, etc.) and wave movement will tend to stretch the pool in the direction of current flow and increase the size of the spill. Likewise, winds will tend to drag the LNG

liquid pool in the direction of the wind flow, increasing the size of the spill area. However, increasing wind will also increase the wave action on the spill. No existing model for an LNG spill accounts for the simultaneous impacts of wind, current, and wave action on the spread of the spill.

The wave model of Quest (2001, 2003) appears to take a step in the right direction, but is not recommended at this time. This method may lead to low estimates of pool area and evaporation because it models waves as stationary objects, effectively assuming that the effects of wave movement, wind, and currents are negligible. In the examples presented by Quest for wave heights from 0.575 to 1.24 m, the pool (circle) area was reduced by more than 90%. The model does recognize the increased water surface area within the circle, which Quest states results in an increase in vaporization flux of 27%. However, because the pool radius is reduced so dramatically, the model results in lower estimates for both pool radius and total evaporation rate (i.e., mass per unit time). These results may be correct, but until the model is better developed and supported (experimentally and/or theoretically), a more conservative approach is recommended.

This work did not include a comprehensive review of computer software for performing spreading calculations. However, several available software programs implement gravitational spreading methods and would be expected to provide reasonable results for scenarios where friction effects are minimal. Examples of such software include SOURCE5, which implements the methods of Raj and Kalelkar (1974) and LPOOL (part of HGSYSTEM), which implements the methods of Cavanaugh (1994). However, without applying a more complete model (like Webber's), it may be difficult to determine if friction effects are important. Webber's work included development of a computer model called GASP for the Health and Safety Executive in the U.K., but this software is neither publicly or commercially available.

As a general rule, it may often be difficult to apply existing computer models if they provide limited ability to specify input parameters. For example, if a software package is designed to calculate heat transfer itself and does not calculate an appropriate value for LNG on water (as discussed in Section 2.3), then the software could not be used for modeling the scenarios considered in this study.

2.3 VAPOR GENERATION FOR UNCONFINED SPILLS ON WATER

As an LNG pool spreads on a water surface, the heat transferred from the water and other sources will cause the liquid to evaporate. This section presents an evaluation of the methods for estimating the rate of evaporation for spills on water.

2.3.1 Review of Modeling Approaches

Fay (2003) – This paper does not address vapor generation in a detailed manner, but for the example calculations presented, a burn regression rate for pool fires is taken as 8×10^{-4} m/s (evaporation rate of 0.34 kg/m^2/s). This value is based on contributions to evaporation caused by heat from the fire, giving a regression rate of 1.9×10^{-4} m/s (evaporation rate of 0.080 kg/m^2/s), and heat from the water, giving a regression rate of 5×10^{-4} to 7×10^{-4} m/s (evaporation rate of 0.21 to 0.30 kg/m^2/s).

Lehr (2004) – This report primarily addresses pool fires and provides information about vaporization only in the context of fire.

Quest (2001, 2003) – Evaporation is assumed to be controlled by film boiling. Calculations provide a heat flux to the LNG of 92 kW/m^2 and evaporation rate of 0.18 kg/m^2/s. As mentioned in Section 2.2, Quest attempted to account for the effects of waves on vapor generation by approximating the waves as a cycloid function. Boundary conditions were applied to the spread model, which resulted in smaller pool diameters. An adjustment was also made for the increased water surface area caused by the waves, which results in an increase in vaporization flux of 27%.

Other Methods – One method available for estimating vapor generation for an LNG pool on water is to calculate the heat transfer into the pool. Because the pool is at its normal boiling point, heat added goes directly to vaporize a portion of the LNG. Those who have taken this approach assume film boiling of the LNG and use correlations from heat transfer theory, such as that given by Klimenko (1981), to calculate the heat transfer. During film boiling, a layer (or film) of pure methane vapor forms between the liquid LNG pool and the water surface beneath it. Heat transfer between the water and the LNG occurs by conduction and radiation through the vapor layer.

Models reviewed also assume that the water remains at a constant temperature that does not decrease with time. Consequently, heat transfer from the water to the LNG pool can be assumed to remain constant. No models were identified that attempt to quantify the convection heat transfer in the water.

A second method for estimating vaporization from an LNG pool is simply to select a value from the available experimental data. Some of the available data for spills of LNG on water are provided in Table 2.1.

Table 2.1 Summary of Test Data for LNG Spilled on Water

Reference	Description	Vaporization Rate (kg/m^2/s)	Associated Heat Flux (kW/m^2)
Burgess (1970)	U.S. Bureau of Mines tests Tests in an aquarium (2 ft by 1 ft by 1 ft) Ice film formed after approximately 20 seconds	0.181	92
Burgess (1972)	U.S. Bureau of Mines tests Tests on a pond (70 m diameter and 8 m deep) No ice formed	0.155	79
Boyle (1972)	Shell Research Tests Laboratory scale	0.024 to 0.195	12 to 99
McQueen (1972)	Esso Tests Spill volumes from 0.8 to 10.8 m^3	0.195	99
Koopman (1979)	5 m^3 LNG spill tests at China Lake Pool sizes ranged from 6.8 to 7.8 m radius	0.12 to 0.15	61 to 78

Table 2.1 Summary of Test Data for LNG Spilled on Water (cont'd)

Reference	Description	Vaporization Rate ($kg/m^2/s$)	Associated Heat Flux (kW/m^2)
Valencia-Chavez (1979)	LNG Research Center at MIT Laboratory scale Pure methane Range is over a period of 100 seconds Ice began to form	0.05 to 0.23	25 to 120
	Tertiary LNG (82.9% C1, 10.1% C2, and 7% C3) Range is over a period of 90 seconds Ice began to form	0.02 to 0.28	10 to 140

2.3.2 Modeling Recommendations

The literature reviewed consistently agrees that the rate of vaporization for a spill of a cryogenic liquid on water will be controlled by the rate of heat transfer from the water into the LNG. Because the pool is already at its normal boiling point, any heat added will go directly to vaporize the liquid. Factors that affect the heat flux from the water include:

- Convective heat transfer cells formed in the water below the spill
- Water currents below the spill
- Waves that could increase surface area
- Ice formation between the spill and the water
- The degree of spill confinement
- The heat transfer phenomenon occurring at the surface (e.g., the boiling mechanism)

None of the literature reviewed attempt to account for all of these factors.

Regarding convection and water currents, the consensus approach is to assume that convection and water currents are sufficient to keep the water well mixed and maintain the water temperature at its initial level. As long as the quantity of water available is large compared to the spill volume, this is a reasonable assumption.

Regarding waves, the wave model of Quest (2001, 2003) is not recommended at this time (see discussion in Section 2.2.2), and no other models were identified.

Regarding ice formation, the literature consistently indicates that ice can form when cryogenic material is spilled on water in laboratory-scale experiments. However, in larger-scale experiments (such as those on ponds), ice formation is minimal. For large LNG spills from carriers, it is recommended to assume no ice formation.

Confinement should be considered on a site-specific basis. For most scenarios involving large spills from LNG carriers, it is assumed that the spill will be unconfined. However, for narrow

shipping channels, the spill will be confined by the shoreline, and the predicted unconfined pool radius may exceed the width of the channel.

The literature indicates that LNG will boil on water in the film boiling regime for the majority of the evaporation time, until almost all of the methane is evaporated. The film is a thin layer of pure methane vapor between the liquid LNG pool and water surface below.

Chemical composition can also significantly impact LNG vaporization, as concluded by Conrado (2000). However, this work, which simulated vaporization of (1) pure methane and (2) a 90% methane and 10% ethane mixture, indicated that assuming pure methane underestimates total evaporation time by 10 to 15%. In addition, the vaporization rates for pure methane and the methane/ethane mixture match closely until much of the methane is evaporated. Given the overall uncertainty in the analysis of large LNG spills on water, attempting to include effects of composition is not warranted, at least for currently typical LNG compositions.

Considering all of the factors discussed above, it is recommended that vaporization be estimated directly from the film boiling heat flux from the water to the LNG. The heat flux is the rate at which heat is transferred from the water to the LNG. The water temperature is assumed constant and the pool remains at the normal boiling point, so a constant heat flux value can be used. The evaporation rate is then calculated directly from the heat flux and heat of vaporization for LNG.

The heat flux could be taken directly from experimental data; however, the available data for LNG show significant spread. As noted by Waite (1983) regarding experimental work, "estimates of the heat flux from water to liquefied gas pools have ranged over a factor of 4, from 25 kW/m^2 to 100 kW/m^2." Our review here showed some even higher estimates. Notable reasons for wide variation in experimental results include the (1) differences in the experimental setups, (2) differences in measurement techniques, and (3) fact that evaporation rates were typically inferred from other data (rather than measured directly).

Because of (1) the uncertainty in the experimental data and (2) the availability of a viable theoretical model from heat transfer theory to help fill the gap in experimental data, it is recommended that heat flux be estimated using film boiling heat transfer theory. This choice is also supported by Waite (1983), who performed a simulation of some of the experiments for which data are available, using a "typical film boiling heat flux of 25 kW/m^2" and using a heat flux of 100 kW/m^2, "often used in LNG spill simulations," for comparison. The conclusion of that comparison was that the simulation using a film boiling heat flux better matched the experimental data than the simulation with 100 kW/m^2.

A correlation developed by Klimenko (1981) can be used to estimate the film boiling heat flux. This method is also presented in TNO (1997) and Conrado (2000), and Appendix A provides a sample calculation. In addition to the thermophysical properties of the substance, this method depends upon the water temperature. For a water temperature of 68 ºF (20 ºC), the method estimates a heat flux of 11,600 $BTU/ft^2/hr$ (37 kW/m^2), which will generate an evaporation rate of 0.015 $lb/ft^2/s$ (0.072 $kg/m^2/s$).

Of course, the heat transfer rate must also be used along with an appropriate method for estimating pool spread, as discussed in Section 2.2. In the recommended spread model, heat flux to the pool directly drives evaporation and, since the evaporation removes material from the pool, it also

affects the rate and extent of pool spread, which in turn affects the downwind distance for flammable vapor travel.

Given the relative uncertainty in the choice of heat flux, it is useful to examine the sensitivity of final consequence analysis results (such as distance to the LFL predicted by an atmospheric dispersion model) to the heat flux. To examine the sensitivity, calculations were performed with three different heat flux values to see the effects on pool radius, evaporation time, and dispersion distance. The heat flux values examined are 7,900 BTU/ft^2/hr (25 kW/m^2), 11,600 BTU/ft^2/hr (37 kW/m^2), and 31,700 BTU/ft^2/hr (100 kW/m^2). The scenario and results are as follows:

Scenario for Evaporation Heat Flux Sensitivity Analysis

Hole diameter: 3.3 ft (1 m)

Initial liquid height above hole: 43 ft (13 m)

Total spill quantity: 4.4×10^5 ft^3 (12,500 m^3)

Air temperature: 71 °F (22 °C)

Relative humidity: 50%

Wind speed: 6.7 mph (3.0 m/s) and 4.5 mph (2.0 m/s)

Surface roughness: 0.03 ft (0.01 m)

Pasquill-Turner stability class: D and F

Averaging time: 0 sec (i.e., peak concentrations are used)

Results for Evaporation Heat Flux Sensitivity Analysis

Hole diameter	3.3 ft (1 m)		
Initial spill rate	11,700 lb/s (5,300 kg/s)		
Total spill duration	33 min		
Spread model	Webber		
Film boiling heat flux to pool	7,900 BTU/hr/ft^2 (25 kW/m^2)	11,700 BTU/hr/ft^2 (37 kW/m^2)	31,700 BTU/hr/ft^2 (100 kW/m^2)
Evaporation rate	0.010 lb/ft^2/s (0.049 kg/m^2/s)	0.015 lb/ft^2/s (0.072 kg/m^2/s)	0.040 lb/ft^2/s (0.20 kg/m^2/s)
Maximum pool radius	500 ft (150 m)	430 ft (130 m)	280 ft (87 m)
Total evaporation duration	34 min	34 min	34 min
Wind speed and stability class	**6.7 mph (3.0 m/s) and D stability**		
Downwind distance to LFL	6,200 ft (1,900 m)	6,600 ft (2,000 m)	4,300 ft (1,300 m)
Time at which LFL reaches maximum distance	38 min	33 min	33 min
Time at which entire cloud drops below LFL	42 min	37 min	37 min

Results for Evaporation Heat Flux Sensitivity Analysis (cont'd)

Wind speed and stability class	**4.5 mph (2.0 m/s) and F stability**		
Downwind distance to LFL	9,200 ft (2,800 m)	11,000 ft (3,300 m)	5,600 ft (1,700 m)
Time at which LFL reaches maximum distance	38 min	44 min	26 min
Time at which entire cloud drops below LFL	43 min	48 min	29 min

The downwind distance to the LFL is the maximum distance at which some of the released LNG vapor is within the flammable range. Note that the vapor cloud continues to travel downwind and disperse even after the spill stops and the pool completely evaporates.

This example shows that the chosen heat flux affects the distance to the LFL and the time at which the maximum distance is reached.. For the heat flux values examined, downwind distances to the LFL vary by approximately 54% in the case with D stability and approximately 94% in the case with F stability. This example also illustrates the importance of selecting a best-estimate value for the heat flux (as opposed to a "conservatively high" estimate). In this case, the heat flux value of 11,700 BTU/hr/ft^2 (37 kW/m^2), as calculated using heat transfer theory, results in the longest downwind distances.

This example also illustrates the importance of carefully characterizing the release source. Dispersion results are sensitive to mass evaporation rate, source area, and release duration. In addition, the example shows the importance of considering the transient nature of the large spills addressed in this report. In this case, the total evaporation duration is approximately the same in all three cases, but with the higher heat flux values, mass evaporation increases more rapidly, and the majority of the total quantity is released in a shorter period of time. This effect is particularly evident in this example because the spill rate decreases with time (i.e., a large fraction of the total spill amount is added to the pool early in the release).

While this example provides valuable insights about the recommended methodology, it is important to note that it does not represent a comprehensive sensitivity analysis; sensitivity may be different for other types of scenarios and with other input parameter values.

2.4 THERMAL RADIATION FROM POOL FIRES ON WATER

A pool fire can result when LNG is spilled on water, forming a pool, and vapor evolving from the pool is ignited. The fire above the pool continues to be fueled by evaporation from the pool. The flames that form the pool fire emit thermal radiation, which can injure people and damage structures. On water, LNG will spread and burn rapidly, so the fire will typically burn out shortly following the end of the spill into the pool, at which time the thermal radiation hazard will cease. This section presents an evaluation of the methods for estimating the distances at which thermal radiation levels of concern might be reached if an LNG pool fire occurs.

2.4.1 Review of Modeling Approaches

Fay (2003) – For the example calculations presented in this paper, the point source model is employed. In this model, the energy generated by combustion is assumed to emanate from a single point at the center of the pool fire. A key parameter for this model is the fraction of heat that is emitted as thermal radiation. As Fay correctly points out, this point source model only applies at large distances from the pool fire. A burn regression rate for pool fires is taken as 8×10^{-4} m/s (evaporation rate of 0.34 kg/m^2/s). This value is based on contributions to evaporation caused by heat from the fire, giving a regression rate of 1.9×10^{-4} m/s (evaporation rate of 0.080 kg/m^2/s), and heat from the water, giving a regression rate of 5×10^{-4} to 7×10^{-4} m/s (evaporation rate of 0.21 to 0.30 kg/m^2/s). The fraction of heat that is emitted as thermal radiation is taken as 0.15.

Lehr (2004) – Lehr employs the solid flame model. The fire is represented as an upright cylinder, and a form of the Thomas equation (Brown, 1974) is used to estimate the flame (cylinder) height. Geometric view factors are used to compute the heat flux at a given receptor location, and attenuation of the thermal radiation by the atmosphere is estimated using the work of Glastone (1977). The paper states that experiments involving LNG pool fires on water show burn regression rates that vary from 4×10^{-4} to 1×10^{-3} m/s (evaporation rate of 0.17 to 0.42 kg/m^2/s) and references Raj (1979). It further states that for larger continuous releases, the burn rate has been estimated as 2.5×10^{-4} m/s (evaporation rate of 0.11 kg/m^2/s); for this value, the report references an unpublished internal memo.

Quest (2001) – Quest also employs the solid flame model; however, in this case the fire is represented as an upright (but tilted) elliptical cylinder. The elliptical shape and tilt attempt to account for the effects of wind on the fire, which can increase the distance that damaging thermal radiation can reach in the downwind direction. The Thomas (1965) correlation is used to calculate flame length. Flame tilt is estimated using an empirical correlation from Welker (1970), and flame drag (increasing the downwind dimension of the base of the flame) is calculated based on the work of Moorhouse (1982). Quest also divides the flame into two zones: a clear zone and a smoky zone, in which a portion of the flame is obscured by smoke. The length of the clear zone is calculated based on work by Prichard (1992). The surface flux is calculated using an equation that depends on the maximum surface flux, an extinction coefficient, and the pool diameter; however, no information is given on the values used for the maximum surface flux or extinction coefficient. In the smoky zone, the surface flux for the smoky areas is taken as 20 kW/m^2, and the clear areas are taken as having the same surface flux as the clean burning zone. The fraction of smoke in the smoky zone is taken as 10%. Geometric view factors are used to compute the heat flux at a given receptor location, and attenuation of the thermal radiation by the atmosphere is estimated using the work of Wayne (1991).

Other Methods – Available pool fire models for hazard assessment purposes are predominantly based on the solid flame model. The fire is represented as gray-body emitter, and the geometry is approximated by an upright cylinder that is tilted as a result of wind. Geometric view factors are available to calculate the thermal radiation that a given receptor would be exposed to, based on the geometry of the cylinder. For hazard assessment purposes, hazard zones are often depicted as circles, based on the maximum downwind distance to the level of concern (i.e., in the direction that the flame is tilted) and centered on the base of the pool. However, it can be noted that in an actual fire, flame tilt will result in a hazard zone with a roughly elliptical pattern, with upwind distances being shorter than downwind distances.

Detailed descriptions of solid flame models are available in many references. Perhaps the best overall reference on the topic is Section 3/Chapter 11 of NFPA (1995); others include TNO (1997) and Rew (1996).

The point source model is also sometimes used in hazard analysis. As mentioned above, in this model the energy generated by combustion is assumed to emanate from a single point at the center of the pool fire. The calculated energy is multiplied by a fraction that accounts for the fact that only part of the energy will be emitted as thermal radiation.

Fire modeling can also be performed using computational fluid dynamics (CFD) methods (e.g., finite element analysis). These methods are often based on numerical solutions to the Navier-Stokes equations but also often require use of some empirical data. CFD models are not normally used for typical pool fire hazard assessments because they require significantly more effort to apply but provide little or no benefit over the solid flame model when the goal is prediction of heat flux at significant distances from the fire. CFD models do have a distinct advantage in cases where it is necessary to model effects on objects engulfed in fire and in modeling fires with irregular geometry. Detailed examination of CFD methods is beyond the scope of this study.

While LNG has been studied more than many substances, there are still relatively few data available for use in determining the behavior of LNG pool fires. This is particularly true for very large pool fires on water. No correlations are available to predict burning rate or surface emission power for various pool sizes.

The data identified in this review are as follows:

From TNO (1997)

- Thomas (1963) correlation for flame length
- For an experimental LNG pool fire of 16.8-m diameter, a mass burning flux of 0.255 kg/s/m^2 is given (TNO Table 6.10)
- Mass burning fluxes for several flammable materials vs. pool diameter on water (TNO Table 6.11)
    - LNG on water – up to 13.7-m diameter: 0.94 kg/s/m^2
    - LNG on water – 20-m diameter: 0.106 kg/s/m^2
    - LNG on water – 35-m diameter: 0.14 kg/s/m^2

From NFPA (1995)

- For unconfined, continuous spills, diameter will increase until burning rate matches spill rate
- Summary of Radiation Data on Hydrocarbon Pool Fires (NFPA Table 3-11.2)
    - Raj (1979) – 10 to 15 m pools: burning rate 4 to 10 x 10^{-4} m/s, 1400 K, average emissive power of 220 kW/m^2
    - Mizner (1983) – 20 m (diameter), LNG and LPG, burning rate 2.4 x 10^{-4} m/s
- Measured Emissive Powers and Radiation Temperatures for Various Liquid Hydrocarbon Pool Fires (NFPA Table 3-11.4)
    - LNG on water: 8.5 to 15.0 m, emissive power 210 to 280 kW/m^2, radiation temperature 1500 K (estimated using narrow-angle radiometer data and spectral data)

From Mizner (1983)

- Regarding China Lake tests, states that "From the LNG tests, surface emissive powers were determined to be about 210 kW/m^2 for both the pool and cloud fires"
- Data reported for four tests at Maplin Sands in 1989: three continuous and one instantaneous. All tests involved a cloud fire, and only one involved a pool fire. Report indicates that the one pool fire probably did not last long enough to become fully developed. Continuous releases were 3.2, 5.8, and 4.7 m^3/s. Instantaneous release was 12 m^3. Wind speeds ranged from 4 to 6 m/s
- Surface emissive powers reported in "range from 137 kW/m^2 to 225 kW/m^2 with an overall mean of 174 kW/m^2"
- For Trial 39 (the only pool fire), emissive powers ranged from 178 kW/m^2 to 248 kW/m^2, with a mean of 203 kW/m^2. Estimated pool diameter was approximately 30 m, flame length ranged from 50 to 78 m, and tilt angle from 27 to 35 degrees

From Rew (1996)

- Work included a review of recent developments in hydrocarbon pool fire modeling and development of a computer program called POOLFIRE6
- For LNG on water, they chose the following parameters, based on a review of available test data:
    - Maximum burning rate: 0.282 kg/s/m^2
    - Emissive power: 265 kW/m^2

2.4.2 Modeling Recommendations

While the point source model is computationally easier to apply, its chief disadvantage is that it does not produce valid estimates for receptors close to the fire. At long distances (and assuming other parameters such as burning rate, emissive power, and fraction of heat radiated are matched), both the point source model and the solid flame model will provide equivalent results. Therefore, the solid flame model is recommended, with the pool fire represented as a tilted cylinder.

Based on the literature reviewed, the values chosen by Rew (1996) for burning rate and emissive power are recommended, namely a burning rate of 0.058 lb/s/ft^2 (0.282 kg/s/m^2) and emissive power of 84,000 BTU/hr/ft^2 (265 kW/m^2). The authors performed a reasonable review of the experimental data, and our review for this work concurs with their choices. Comparisons only to data for the larger scale spill tests tend to indicate that these are relatively conservative choices. Remaining details of the recommended approach (e.g., correlations for flame height and tilt) are given in the example calculations in Appendix C.

It is also important to note that the methods recommended here have generally been validated against a broad range of the available experimental data. However, there are no experimental data for pool fires as large as some of the sizes postulated for LNG carrier incidents. These are the best currently available methods, but it is important to keep in mind that the methods are being used well outside the range where they have been validated.

For rapid releases onto an unconfined water surface, pool spread can be estimated using a pool spread model, as described in Section 2.2. However, in the case of a fire, heat transfer to the pool from both the water and the fire itself must be included. The additional heat transfer (from the fire) results in greater evaporation than in the nonfire case; this greater evaporation rate can affect pool

spread. The chosen burning rate of 0.058 lb/s/ft^2 (0.282 kg/s/m^2) already accounts for both of these contributions and corresponds to a heat transfer rate of approximately 46,000 BTU/ft^2/hr (140 kW/m^2). The model accounts for the resulting evaporation in estimating the pool spread. Given the relative uncertainty in the choices of burning rate and surface emitted flux, it is useful to examine the sensitivity of final consequence analysis results (such as distance to a heat flux level of concern) to the values of these parameters. To examine the sensitivity, calculations were performed using the methods recommended in this report for an example scenario. The burning rates examined are 0.041 lb/s/ft^2 (0.20 kg/s/m^2), 0.057 lb/s/ft^2 (0.28 kg/s/m^2), and 0.074 lb/s/ft^2 (0.36 kg/s/m^2). The surface emitted fluxes examined are 63,000 BTU/ft^2/hr (200 kW/m^2), 84,000 BTU/ft^2/hr (265 kW/m^2), and 95,000 BTU/ft^2/hr (300 kW/m^2). The scenario and results are as follows:

Scenario for Burning Rate and Surface Emitted Flux Sensitivity Analysis

Hole diameter: 3.3 ft (1 m)

Initial liquid height above hole: 43 ft (13 m)

Total spill quantity: 4.4×10^5 ft^3 (12,500 m^3)

Air temperature: 80 °F (27 °C)

Relative humidity: 70%

Wind speed: 20 mph (8.9 m/s)

Results for Burning Rate Sensitivity Analysis

Hole diameter	3.3 ft (1 m)		
Initial spill rate	11,700 lb/s (5,300 kg/s)		
Total spill duration	33 min		
Spread model	Webber		
Flame surface emitted flux	84,000 BTU/ft^2/hr (265 kW/m^2)		
Burning rate	0.041 lb/s/ft^2 (0.20 kg/s/m^2)	0.057 lb/s/ft^2 (0.28 kg/s/m^2)	0.074 lb/s/ft^2 (0.36 kg/s/m^2)
Maximum pool radius	280 ft (90 m)	240 ft (74 m)	220 ft (66 m)
Total fire duration	33 min	33 min	33 min
Flame length (height)	790 ft (240 m)	910 ft (280 m)	1,000 ft (310 m)
Flame tilt at maximum radius	34 deg	35 deg	37 deg
Downwind distance to 12,000 BTU/hr/ft^2 (38 kW/m^2)	1,300 ft (380 m)	1,200 ft (370 m)	1,200 ft (370 m)
Downwind distance to 7,900 BTU/hr/ft^2 (25 kW/m^2)	1,500 ft (450 m)	1,500 ft (450 m)	1,500 ft (440 m)
Downwind distance to 3,800 BTU/hr/ft^2 (12 kW/m^2)	2,000 ft (600 m)	2,000 ft (600 m)	2,000 ft (600 m)
Downwind distance to 1,600 BTU/hr/ft^2 (5 kW/m^2)	2,800 ft (860 m)	2,800 ft (860 m)	2,800 ft (850 m)

Results for Surface Emitted Flux Sensitivity Analysis

Hole diameter	3.3 ft (1 m)		
Initial spill rate	11,700 lb/s (5,300 kg/s)		
Total spill duration	33 min		
Spread model	Webber		
Burning rate	0.057 lb/s/ft^2 (0.28 kg/s/m^2)		
Maximum pool radius	240 ft (74 m)		
Total fire duration	33 min		
Flame length (height)	910 ft (280 m)		
Flame tilt at maximum radius	36 deg		
Flame surface emitted flux	63,000 BTU/ft^2/hr (200 kW/m^2)	84,000 BTU/ft^2/hr (265 kW/m^2)	95,000 BTU/ft^2/hr (300 kW/m^2)
Downwind distance to 12,000 BTU/hr/ft^2 (38 kW/m^2)	1,100 ft (330 m)	1,200 ft (370 m)	1,300 ft (400 m)
Downwind distance to 7,900 BTU/hr/ft^2 (25 kW/m^2)	1,300 ft (400 m)	1,500 ft (450 m)	1,600 ft (470 m)
Downwind distance to 3,800 BTU/hr/ft^2 (12 kW/m^2)	1,800 ft (540 m)	2,000 ft (600 m)	2,100 ft (630 m)
Downwind distance to 1,600 BTU/hr/ft^2 (5 kW/m^2)	2,500 ft (760 m)	2,800 ft (860 m)	3,000 ft (900 m)

The results for burning rate sensitivity show that the distance estimates are not highly sensitive to burning rate. There are competing factors at work here:

- As the burning rate rises, the maximum pool radius drops (since the LNG evaporates more quickly, reducing the opportunity for spread).
- Flame length is a function of both burning rate and pool radius. Increasing either of these results in a longer flame length. In the example above, the effect of burning rate dominates this competition, and flame length drops with burning rate.

In the example above, increasing burning rate also increases flame length but decreases pool radius. These are competing effects on estimated flux at downwind distances, and in this example, the effect of increased pool diameter slightly dominates this competition. As a result, increasing burning rate causes a decrease in the estimated distances to thermal flux levels of concern. For other scenarios, distances may increase with increased burning rate, but as in this example, the distances are expected to vary by relatively small percentages over this range of burning rates.

The results for surface emitted flux sensitivity show that the distance estimates are affected by the value chosen. However, increasing the value by 50%, from 63,000 BTU/ft^2/hr (200 kW/m^2) to 95,000 BTU/ft^2/hr (300 kW/m^2), increases the distance estimates by only 18% to 21%.

So, while the burning rate and surface emitted flux are important parameters in the pool fire analysis, it is useful to note that the distance results are not highly sensitive to the values chosen.

In these examples, it can also be noted that the total fire duration matches the total spill duration. This occurs because the pool spreads to the point where the burn rate matches the spill rate into the pool, so following the initial spreading of the pool, the LNG burns at the same rate that it is spilled.

While this example provides valuable insights about the recommended methodology, it is important to note that it does not represent a comprehensive sensitivity analysis; sensitivity may be different for other types of scenarios and with other input parameter values.

This work did not include a comprehensive review of computer software for performing pool fire consequence assessment. However, the majority of software currently available for modeling pool fires is based on the same basic approach recommended here (solid flame model, tilted cylinder). This includes software packages like LNGFIRE and POOLFIRE6. However, as was stated in the case of software for pool spread estimation in Section 2.2.2, existing software for pool fire modeling may be difficult to apply to large LNG spills on water if they provide limited ability to specify input parameters.

2.5 FLAMMABLE VAPOR DISPERSION FOLLOWING SPILLS ON WATER

If LNG is spilled on water but not ignited immediately or soon after the spill, the LNG will evaporate. The vapor will mix with air and move downwind. The resulting vapor cloud could cause a flash fire if ignited before it is diluted below the LFL. This section presents an evaluation of the methods for estimating distances that flammable vapors might reach.

2.5.1 Review of Modeling Approaches

Fay (2003) – This paper does not address vapor dispersion.

Lehr (2004) – This paper does not address vapor dispersion.

Quest (2001) – To estimate the distance to the LFL, Quest used a dispersion modeling software package that it sells commercially, which it states is based on the SLAB model. The DEGADIS dispersion model was also used.

Other Methods – For flash fires, the level of concern is typically defined as either the LFL or ½ the LFL for the substance. Therefore, modeling of flash fires is primarily a matter of applying a dispersion model. This work did not involve a detailed review of dispersion models, but it is clear that for large releases of LNG, dense-gas effects will be important and must be accounted for in the model used. Several such models are available in the form of freely available software, including DEGADIS, SLAB, and HGSYSTEM. In addition, several commercial software packages include models for dense-gas effects.

For further information, reviews and validation studies for various dispersion models have been conducted by a variety of organizations. Examples include EPA (1991) and API (1992).

2.5.2 Modeling Recommendations

When considering large releases of LNG, dense-gas effects are important and must be accounted for in any model selected. Among the dispersion models appropriate for large LNG spills,

DEGADIS was selected for use (see example problems in Section 3). DEGADIS accounts for dense-gas effects and was originally developed for simulation of cryogenic flammable gas dispersion, particularly for LNG. It has been validated against a wide range of laboratory and field test data. Chapter 6 of GRI (1990) provides information on the comparison of DEGADIS predictions with field test data from the Burro and Maplin Sands tests. In addition, API (1992) indicates that DEGADIS tends to overpredict by less than a factor of two for simulations with short averaging times. This is based on comparisons with field test data, including data from the Burro, Coyote, Desert Tortoise, Goldfish, Maplin Sands, and Thorney Island tests.

Furthermore, the federal siting requirements for onshore LNG facilities (49 CFR 193) specify the use of DEGADIS for the determination of dispersion distances. As recognized by 49 CFR 193, DEGADIS does not account for additional dispersion caused by "the complex flow patterns induced by tank and dike structure(s)." For cases where dense gas flow obstructions are a concern, the regulation allows dispersion distances to be calculated with the FEM3A model (see GRI 1997). However, for most hazard assessment purposes, including facility siting analyses, modeling of complex terrain is not necessary.

For flammable vapor dispersion distance calculations, the level of concern is sometimes taken as the LFL, and there is some regulatory basis for this choice in EPA's risk management program rule (40 CFR 68). However, the level of concern is also often defined as ½ the LFL to account for localized pockets of higher gas concentrations that may occur in an actual release. Use of ½ the LFL for LNG is also supported by 49 CFR 193, which specifies use of an average gas concentration in air of 2.5 percent for onshore exclusion zones. For the example calculations presented in Section 3, distances are provided for both the LFL and ½ the LFL.

As is the case any time one models dispersion of flammables, it is recommended that a short averaging time (not more than a few seconds) be used because a flammable cloud need only be within the flammable range for a very short time to be ignited. It is also important to appropriately represent the topography downwind of the release point. For many dispersion models, topography is characterized by a surface roughness value, which the model uses in accounting for the effects of terrain on dispersion of the cloud. In general, a rougher surface will tend to cause more mixing with ambient air, and therefore more rapid dispersion of a vapor cloud.

2.6 RAPID PHASE TRANSITIONS

An RPT may occur during an LNG spill when a portion of the pool changes from liquid to gas, virtually instantaneously. This vaporization will rapidly expel LNG vapor into the atmosphere and can generate an overpressure. The vaporization may also increase the downwind distance where the LFL is reached or it may affect the size of a pool fire. RPTs have occurred during LNG spill tests on water. An RPT is a physical explosion of a liquid that does not involve fire or other chemical reactions.

2.6.1 Literature Review

Fay (2003), Lehr (2004), and Quest (2001) – These documents do not address RPTs.

Other Literature – The literature reveals that RPTs are a poorly understood phenomenon. They have occurred in small and large simulated spill releases of LNG on water. The water is very hot with respect to the LNG, which has a normal boiling point of approximately -260 °F. Typical sea water temperatures range from 30 °F to 80 °F. The large temperature difference between the sea water and the LNG results in a very rapid vaporization of the LNG.

Sometimes, the RPT occurs after the spill, as the LNG vaporizes. Some have speculated that the differential boiling (i.e., change in composition as methane boils off first) may play a role in the RPT initiation. In some incidents, more than one RPT has occurred during a single spill event.

Although the physical mechanism for the rapid vaporization is not well understood, if it proceeds fast enough, an overpressure wave may be formed. In some test cases, overpressures generated were strong enough to damage test equipment in the immediate vicinity of the LNG release point. The sizes of the overpressure events have been generally small, with a maximum TNT equivalence estimated at several pounds of TNT. Such a small overpressure event is not expected to cause significant damage to an LNG vessel. However, the RPT may increase the rate of LNG pool spreading and the LNG vaporization rate.

Atallah (1997) surveyed the literature on RPTs for the Gas Research Institute. Atallah's study reviewed available experimental and theoretical studies of RPTs for liquid metal-water and LNG-water systems. Atallah's work provides a good summary of what is known about RPTs.

The survey of the LNG-water releases yields the following conclusions:

1. Rapid phase transitions have been observed in many field tests of spills of LNG on a water surface
2. Increasing the spill rate increases the effective explosive yield of an RPT event (Atallah, pg. 3-17, Figure 3.7)
3. The largest explosive yield of an RPT event observed in a field test was equivalent to an explosion of 5.5 kg of TNT (Atallah, pg. 3-21, Table 3.11)
4. RPT events did not occur in every spill test
5. No existing theory for RPT events can account for all of the observed test data
6. There is no existing theoretical method to predict the severity of an RPT event involving the release of the LNG from an LNG carrier onto water

2.6.2 Modeling Recommendations

Modeling of RPTs could be useful for two types of effects: (1) overpressure resulting from the rapid phase change and (2) dispersion of the "puff" of LNG expelled into the atmosphere by the RPT.

Although the possibility of an RPT igniting a vapor cloud was mentioned by Vallejo (2003), the experimental results reviewed do not indicate that ignition is likely. Unfortunately, no theoretical or experimental basis could be identified for modeling either the overpressure or source term effects. Regarding overpressure, the literature suggests that damage might be limited to the immediate vicinity of the RPT event; that is, that overpressures decrease rapidly with distance. On the other hand, none of the spill tests reported involve spills of the magnitude of interest in this report.

Regarding the "puff" of LNG entering the atmosphere in an RPT, an example dispersion analysis was performed. The purpose of this analysis is to examine the importance of an RPT in estimating

downwind flammable concentrations. The analysis looks at three scenarios: (1) a base case releasing 1.8×10^5 ft^3 (5,000 m^3) through a 9.8-ft (3-m) hole without an RPT occurring, (2) the base case modified by assuming that an RPT occurs at 2 minutes and the entire mass remaining in the pool is released to the atmosphere within 30 seconds and that the source area used as input into a dispersion model is twice the pool area at the time of the RPT, and (3) the base case modified by assuming that an RPT occurs at 2 minutes and the entire mass remaining in the pool is released to the atmosphere within 30 seconds with the source area remaining equal to the pool area at the time of the RPT. The source area is the area over which the vapor cloud originates; in the case of an evaporating pool (without an RPT), this is simply the pool area.

These scenarios are designed to at least roughly follow some of the anecdotal information from the literature, in particular, the cases where a spill occurs and the RPT follows within a couple of minutes. This example is pursued simply to explore the possible effects of RPT on dispersion of a flammable cloud; there is no precedent in the literature for the chosen modeling approach.

The scenario parameters and results are as follows:

Scenario for Analysis of RPT Influence on Vapor Dispersion

Hole diameter: 9.8 ft (3 m)

Total spill quantity: 1.8×10^5 ft^3 (5,000 m^3)

Air temperature: 70 °F (21 °C)

Water temperature: 70 °F (21 °C)

Relative humidity: 50%

Wind speed: 6.7 mph (3.0 m/s)

Surface roughness: 0.03 ft (0.01 m)

Pasquill-Turner stability class: D

Averaging time: 0 sec (i.e., peak concentrations are used)

Results for Analysis of RPT Influence on Vapor Dispersion

Scenario	Base Case (No RPT)	RPT at 2 min with Pool Radius Doubled	RPT at 2 min with Pool Radius Held Constant
Maximum pool radius (from spread calculations)	410 ft (125 m)	310 ft (93 m) spread at 2 min	310 ft (93 m) spread at 2 min
Maximum source radius for dispersion modeling	410 ft (125 m)	610 ft (186 m) twice pool radius at 2 min	310 ft (93 m) pool radius at 2 min
Total evaporation duration	13 min	2.5 min	2.5 min
Downwind distance to LFL	6,600 ft (2,000 m)	7,500 ft (2,300 m)	7,500 ft (2,300 m)

In this example, the "puff" of LNG released into the atmosphere by the RPT does have some impact on downwind distances since it generates vapor more rapidly and results in longer distances to the LFL. However, the assumptions here are probably more severe than would be expected in an actual RPT since the majority of the original volume goes into the atmosphere in a 30-second period. This is not a comprehensive analysis; results could be different for different scenarios and/or input parameters. However, it gives some indication that for scenarios like this short-term release, an RPT may not result in estimates of dispersion distances that are much longer than what is expected with similar scenarios that do not involve RPTs.

2.7 EFFECTS OF THERMAL RADIATION ON PEOPLE

This section provides an overview of data and methods for estimating the effects on people and structures that result from thermal radiation exposure.

2.7.1 Review of Data and Effects Models

The extent to which people are injured by exposure to thermal radiation depends on both the incident heat flux and the exposure time. The data used in estimating effects on people include those from:

- Experiments with humans (at lower levels of thermal radiation)
- Experiments with animals
- Review of historical data from actual thermal radiation burn incidents

Based on these data, various researchers have presented estimates of effects primarily in the form of (1) tabulated radiation levels and exposure times for various effects and (2) probability unit (probit) models that allow estimating the probability of various effects, typically based on a thermal load (i.e., the time integral of radiation intensity to an empirically derived power).

Detailed summaries of available data and models are provided in references such as Lees (1996) and TNO (1992). This report does not provide as detailed a summary as these references; rather, it presents examples of data that are appropriate for hydrocarbon fires and are frequently used when selecting levels of concern for hazard assessment purposes, such as facility siting analyses.

Tabulated effects for various radiation levels and exposure times include the following:

- Table 2.2 – Burn injury criteria from the Federal Emergency Management Agency (FEMA, 1990)
- Table 2.3 – Exposure limits recommended by API (1997) for exposure of workers to thermal radiation from flares
- Table 2.4 – Burn injury estimates for fireballs given by Prugh (1994). Note that these data are based on thermal dose, which is the time integral of radiation intensity. These data are also based on short-duration exposures (i.e., on the order of a minute or less)

Table 2.2 Thermal Radiation Burn Injury Criteria from FEMA (1990)

Thermal Radiation Intensity		Time for Severe Pain (sec)	Time for Second-degree Burns (sec)
BTU/hr/ft^2	kW/m^2		
300	1	115	663
600	2	45	187
1000	3	27	92
1300	4	18	57
1600	5	13	40
1900	6	11	30
2500	8	7	20
3200	10	5	14
3800	12	4	11

Table 2.3 Permissible Thermal Radiation Exposure for Flares from API 521 (1997)

Thermal Radiation Intensity		Type of Damage
BTU/hr/ft^2	kW/m^2	
500	1.6	Permissible level at any location where personnel are continuously exposed
1,500	4.7	Permissible level in areas where emergency actions lasting several minutes may be required by personnel without shielding but with appropriate clothing
2,000	6.3	Permissible level in areas where emergency actions lasting up to 1 minute may be required by personnel without shielding but with appropriate clothing
3,000	9.5	Permissible level in areas where exposure to personnel is limited to a few seconds, sufficient for escape only

The values shown in Table 2.3 are measures of heat per unit area as a function of time. Table 2.4 shows cumulative heat received over time. For example, exposure to a flux level of 5 kW/m^2 (approx. 1,500 BTU/hr/ft^2) for 30 seconds results in a thermal dose of 150 kJ/m^2 and causes second-degree burns.

Table 2.4 Thermal Dose Data for Exposure to Fireballs from Prugh (1994)

Thermal Dose $\int I(t)dt$		Type of Injury
kJ/m^2	BTU/ft^2	
40	3.5	Threshold of pain
100	8.8	Sunburn (first-degree burn)
150	13	Blisters (second-degree burn)
250	22	1% fatal (third-degree burn)
500	44	50% fatal (third-degree burn)
1200	106	99% fatal (third-degree burn)

Available probit models include the relations shown in Table 2.5 (TNO, 1992). In these empirically derived relations, $tI^{\frac{4}{3}}$ is referred to as the thermal load. The probit value (Pr) is a Gaussian-distributed, random variable with a mean value of 5.0 and a standard deviation of 1.0. The probit value is related to probability by the following:

$$\text{Probability} = \frac{1}{\sqrt{2\pi}} \int_{-\infty}^{\text{Pr}-5} e^{\frac{-u^2}{2}}\, du$$

Table 2.5 Probit Models for Injury by Thermal Radiation from TNO (1992)

Probit Equation	Effects
$\text{Pr} = -39.83 + 3.0186 \ln(tI^{\frac{4}{3}})$	First-degree burns
$\text{Pr} = -43.14 + 3.0186 \ln(tI^{\frac{4}{3}})$	Second-degree burns
$\text{Pr} = -36.38 + 2.56 \ln(tI^{\frac{4}{3}})$	Lethality

In addition to radiation intensity and time, it is important to keep in mind that other factors can strongly affect the extent of injury to people that is caused by thermal radiation:

- Protection afforded by shelter
- Protection afforded by clothing
- Contribution of solar radiation to total exposure (250-330 Btu/hr-ft^2)
- Susceptibility of individual exposed
- Response of individual (e.g., ability to take shelter)

2.7.2 Selecting Levels of Concern

As in all hazard assessment activities, thermal radiation levels of concern must be chosen with the nature of (1) the potentially exposed population and (2) the potential fire events. For example, permissible levels could be defined differently for (1) workers in a process plant who are wearing protective clothing, (2) areas where people are generally not present but could have access, or (3) sensitive populations, such as the elderly.

For purposes of onshore facility siting analysis, 49 CFR 193 and NFPA 59A specify a level of concern of 1,600 BTU/hr/ft^2 (5 kW/m^2). Based on the information presented in Section 2.7.1, 1,600 BTU/hr/ft^2 (5 kW/m^2) could be expected to cause the effects summarized in Table 2.6.

Table 2.6 Effects on People for 1,600 BTU/hr/ft^2 (5 kW/m^2) Thermal Radiation

Effect	Exposure Time (seconds)	Data Source
Severe pain	13	Table 2.2
First-degree burns	20	Table 2.4 (5 kW/m^2 for 20 seconds corresponds to a thermal dose of 100 kJ/m^2)
Second-degree burns	30	Table 2.4 (5 kW/m^2 for 30 seconds corresponds to a thermal dose of 150 kJ/m2)
	40	Table 2.2
Third-degree burns (1% fatality)	50	Table 2.4 (5 kW/m^2 for 50 seconds corresponds to a thermal dose of 250 kJ/m^2)
72% probability of first-degree burns	40	Table 2.5

This level of 1,600 BTU/hr/ft^2 (5 kW/m^2) is applicable to short duration events, such as fireballs. It is also applicable to the early stages of longer duration events, such as pool fires, provided that the potentially exposed population will have both opportunity and capability to quickly take cover.

2.8 EFFECTS OF THERMAL RADIATION ON STRUCTURES

2.8.1 Review of Data and Effects Models

Like effects of thermal radiation on people, effects on structures also depend on incident heat flux and the exposure time. With structures, effects also depend strongly on the materials of construction (e.g., wood, steel, concrete).

Tabulated effects for various radiation levels and exposure times include the following:

- Table 2.7 – Damage criteria from the World Bank (1988) based on observations of large fires
- Table 2.8 – Critical intensity levels presented by TNO (1992)
- Table 2.9 – Various thermal radiation limits presented by Lees (1996)

Unless otherwise noted, these tabulated intensity levels and effects are applicable for long-term exposure, which is very generally considered to be on the order of 30 minutes or more.

Table 2.7 Structure Damage Criteria for Thermal Radiation Exposure from World Bank (1988)

Thermal Radiation Intensity		Type of Damage
BTU/hr/ft^2	kW/m^2	
11,890	37.5	Sufficient to cause damage to process equipment (e.g., steel structures and equipment)
7,930	25.0	Minimum energy required to ignite wood at indefinitely long exposures without a flame
3,960	12.5	Minimum energy required to ignite wood with a flame or cause melting of plastic tubing

Table 2.8 Damage Resulting from Thermal Radiation for Various Materials from TNO (1992)

Type of Damage	Critical Radiation Intensity[1] (kW/m^2)	
	Damage Level 1[2]	Damage Level 2[3]
Steel	100	25
Wood	15	2
Synthetic materials	15	2
Glass	4	–

[1] Radiation intensity that can cause damage from long-term exposure.
[2] Damage Level 1: Surfaces of exposed materials catch fire and structural elements collapse or rupture.
[3] Damage Level 2: Surfaces of exposed materials experience serious discoloration as well as paint peeling, and structural elements undergo substantial deformation.

A more accurate assessment of structural damage requires performing heat balance calculations to determine the resulting surface temperature for comparison with acceptable temperatures for the particular structure. TNO (1992) presents a discussion and example of such calculations. In addition, Chapters 9, 10, and 11 of NFPA (1995) present analytical methods for determining fire resistance of steel, concrete, and timber members.

2.8.2 Selecting Levels of Concern

For large incidents involving LNG spills on water, selection of levels of concern is complicated by the fact that fire incidents may be brief, perhaps on the order of 5 minutes for a pool fire involving a rapid spill of the contents of a single membrane tank from a carrier. However, the general guidance on damage to structures (e.g., intensity levels presented in Section 2.8.1) is based on long-term exposure (perhaps 30 minutes or more).

Table 2.9 Various Thermal Radiation Limits for Structures from Lees (1996)

Thermal Radiation Intensity Limit		Limit Description
(BTU/hr/ft^2)	(kW/m^2)	
Design Guidance from Kletz (1980)		
12,000	38	Intensity on storage tanks
4,000	12.5	Intensity on wood or plastics
1,600	5	Intensity on people performing emergency operations
Design and Assessment Guidance from British Standard 5908 (BS 5908, 1990)		
12,000	37.5	Intensity at which damage is caused to process equipment
7,900	25	Intensity at which nonpiloted ignition of wood occurs
4,000	12.5	Intensity at which piloted ignition of wood occurs
Design and Assessment Guidance from Mecklenburgh (1985)		
4,400	14	Intensity which normal buildings should be designed to withstand
3,200 – 3,800	10-12	Intensity at which vegetation ignites
Assessment Guidance from Dinenno (1982)		
9,500	30	Spontaneous ignition of wood
4,800	15	Piloted ignition of wood
6,300	20	Ignition of No. 2 fuel oil in 40 seconds
3,200	10	Ignition of No. 2 fuel oil in 120 seconds
5,700 - 6,300	18-20	Cable insulation degrades
3,800	12	Plastic melts
12,000	37.5	Equipment damage
2,900	9	Equipment damage – conservative value used in flare system design

The data presented in Section 2.8.1 show some variations in intensity levels and associated effects. However, the data are relatively consistent, and for long-term exposure, some reasonable choices for levels of concern and associated types of damage are as follows:

- 12,000 BTU/hr/ft^2 (38 kW/m^2) – Damage to process equipment and storage tanks
- 7,900 BTU/hr/ft^2 (25 kW/m^2) – Ignition of wood without direct flame exposure
- 3,800 BTU/hr/ft^2 (12 kW/m^2) – Piloted ignition of wood, melting of plastic, ignition of vegetation

Of course, the appropriate levels of concern for a specific site depend on the materials present. For example, in an area with a wooden structure, a value of 7,900 BTU/hr/ft^2 (25 kW/m^2) might be appropriate if there are no combustibles in the area that are more vulnerable. However, if vegetation or other more vulnerable combustibles are present, a level of 3,800 BTU/hr/ft^2 (12 kW/m^2) may be more appropriate, particularly if ignition of these materials could initiate a larger fire.

These levels could be used as general guidelines for fire events of any duration, but they will tend to be very conservative for short-duration fires. For example, some steel structures could be exposed to much higher intensities for short durations without their temperatures rising to damaging levels. However, as noted previously, heat balance calculations are generally required to evaluate the intensities/durations that a specific structure can withstand. To minimize the need for heat balance calculations, the above levels of concern could be employed, and detailed analysis could be used on a case-by-case basis when structures have the potential for exposure to fires of shorter duration.

3 CONSEQUENCE ASSESSMENT EXAMPLES

This section presents some example consequence analysis results using the methods recommended in Section 2. The scenarios presented here are chosen to illustrate the various analysis methods and are not intended to model any specific facility. For these examples, site-specific parameters (e.g., atmospheric conditions, surface roughness) were chosen either to match values used in other studies (for comparison purposes) or values required by 49 CFR 193 for LNG facility siting. For actual analysis of a site, these parameters must be selected based on site conditions and the goals of the analysis.

Detailed computations and computer output data for the samples in this section are provided in Appendices B (release rates), C (pool fires), and D (vapor dispersion). The computations presented in those appendices were performed with the assistance of the Mathcad computer software (©1986-2000 MathSoft, Inc.).

3.1 RELEASE RATES

As mentioned in Section 2, the orifice model is recommended, although only for providing a rough guide to the rate of release for a given hole size. As an example, Figure 3.1 presents estimated release rates for a few hole sizes.

For these calculations, the height of the LNG above the hole was taken as 43 ft (13 m). This is an approximate value for the height of the LNG above the water level in a membrane-type carrier. The discharge coefficient was assumed to be 1.0. The calculations of these values are presented in Appendix B.

3.2 POOL FIRES

This section presents the results of example pool fire calculations for an LNG spill on water. The scenarios examined are fires following spills from 3.3-ft (1-m) and 16-ft (5-m) holes in an LNG carrier just above the waterline. In both cases, the holes are assumed to be uniform in diameter and to penetrate through the outer and inner hulls and the cargo tank. The 3.3-ft (1-m) diameter hole represents a relatively long duration event, and the 16-ft (5-m) diameter hole represents a more rapid, short duration release. These example calculations are intended only as demonstrations of the modeling methods. The results should not be taken as a consequence assessment for any specific facility. Evaluation of a specific facility requires input parameter values based on site-specific conditions, and analysis of different or additional scenarios may be appropriate.

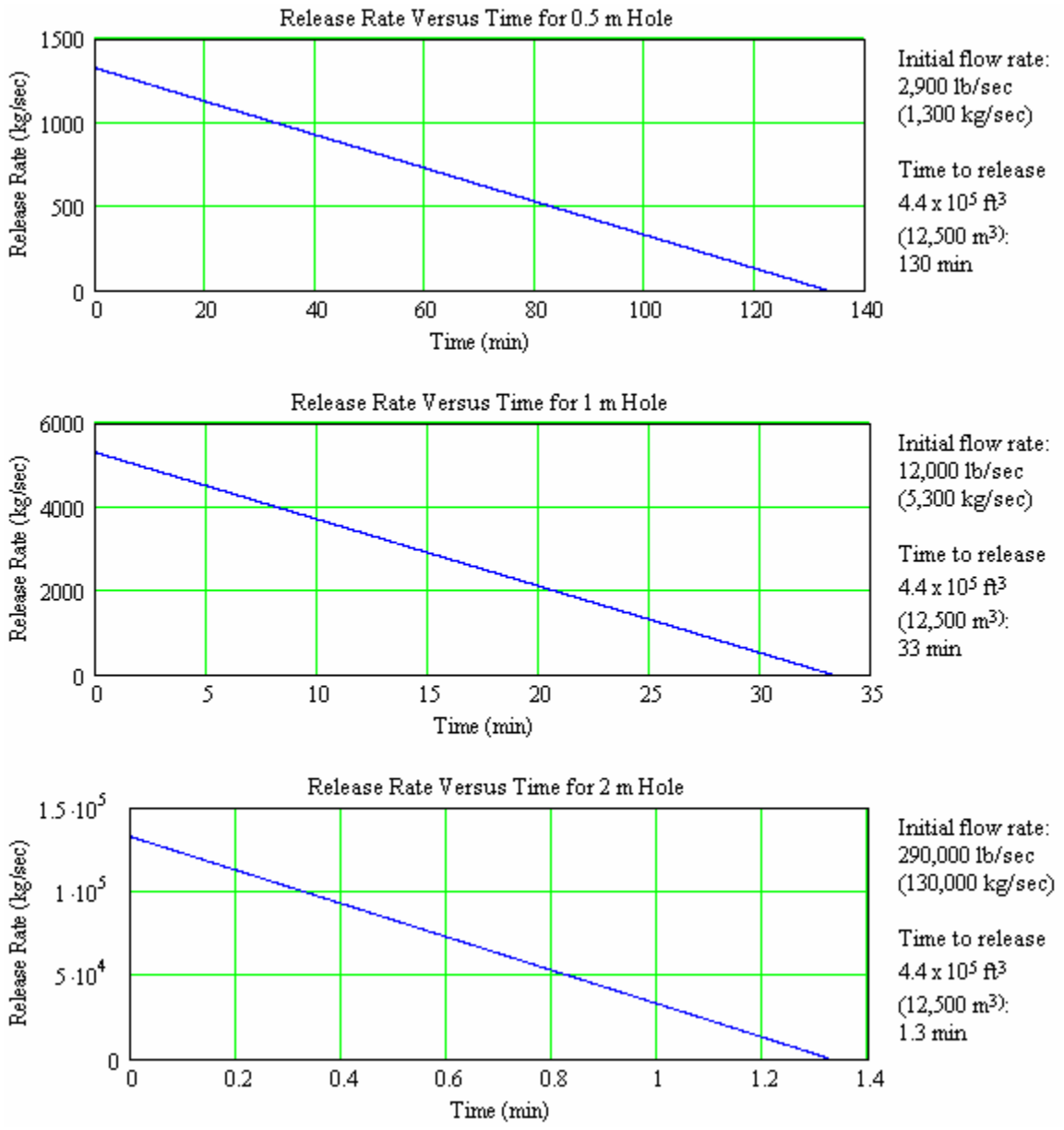

Figure 3.1 Estimated LNG Release Rates Based on Orifice Model

For these examples, it is assumed that the amount of LNG above the hole is 4.4×10^5 ft^3 (12,500 m^3), and the orifice model is used to estimate outflow, with flow rate dropping as the liquid level above the hole drops. It is assumed that the spill is ignited immediately upon release. The scenarios and input parameter are summarized as follows:

Scenarios

Hole diameters: 3.3 ft (1 m) and 16 ft (5 m)

Initial liquid height above hole: 43 ft (13 m)

Total spill quantity: 4.4×10^5 ft^3 (12,500 m^3)

Air temperature: 80 °F (27 °C)

Relative humidity: 70%

Wind speed: 20 mph (8.9 m/s)

Flame surface emitted flux: 84,000 BTU/hr/ft^2 (265 kW/m^2)

Burning rate: 0.058 lb/s/ft^2 (0.282 kg/s/m^2)

Table 3.1 summarizes the results of the pool fire calculations for these scenarios. The detailed calculations are provided in Appendix C. Note that the results for the 3.3-ft (1-m) hole show that the total fire duration matches the total spill duration. This occurs because the pool spreads until the burning rate matches the spill rate into the pool. For the 16-ft (5-m) hole, the spill is much more rapid, lasting only 1.3 minutes, and the pool does not have enough time to spread to the point where the burn rate matches the spill rate. However, the large mass in the pool does result in a much larger pool, and therefore the spilled material burns in a much shorter time.

Table 3.1 Summary of Results for Example Pool Fire Calculations

Hole diameter	3.3 ft (1 m)	16 ft (5 m)
Initial spill rate	11,700 lb/s (5,300 kg/s)	290,000 lb/s (130,000 kg/s)
Total spill duration	33 min	1.3 min
Maximum pool radius	240 ft (74 m)	440 ft (130 m)
Total fire duration	33 min	6.9 min
Flame length (height)	910 ft (280 m)	1,400 ft (430 m)
Flame tilt at maximum radius	35 deg	31 deg
Downwind distance to 12,000 BTU/hr/ft^2 (38 kW/m^2)	1,200 ft (370 m)	2,000 ft (600 m)
Downwind distance to 7,900 BTU/hr/ft^2 (25 kW/m^2)	1,500 ft (450 m)	2,400 ft (720 m)
Downwind distance to 3,800 BTU/hr/ft^2 (12 kW/m^2)	2,000 ft (600 m)	3,200 ft (980 m)
Downwind distance to 1,600 BTU/hr/ft^2 (5 kW/m^2)	2,800 ft (860 m)	4,600 ft (1,400 m)

3.3 FLAMMABLE VAPOR DISPERSION

This section presents the results of example dispersion calculations for an LNG spill on water. The scenarios examined are spills that are not immediately ignited and disperse downwind. Spills are from 3.3-ft (1-m) and 16-ft (5-m) holes in an LNG carrier just above the waterline. For these examples, it is assumed that the amount of LNG above the hole is 4.4×10^5 ft^3 (12,500 m^3) and the orifice model is used to estimate outflow, with flow rate dropping as the liquid level above the hole drops.

These are the same scenarios presented in Section 3.2 for pool fires, except in this case it is assumed that ignition does not occur immediately and ambient conditions are different. Also, as stated above for pool fires, these example calculations are intended only as demonstrations of the modeling methods. The results should not be taken as a consequence assessment for any specific facility. Evaluation of a specific facility requires input parameter values based on site-specific conditions, and analysis of different or additional scenarios may be appropriate.

The scenarios and input parameters are summarized as follows:

Scenarios

Hole diameters: 3.3 ft (1 m) and 16 ft (5 m)

Total spill quantity: 4.4×10^5 ft^3 (12,500 m^3)

Air temperature: 71 °F (22 °C)

Water temperature: 70 °F (21 °C)

Relative humidity: 50%

Wind speed: 4.5 mph (2.0 m/s)

Surface roughness: 0.03 ft (0.01 m)

Pasquill-Turner stability class: F

Averaging time: 0 sec (i.e., peak concentrations are used)

Table 3.2 summarizes the results of the source term and dispersion calculations for these scenarios. The detailed source term calculations are provided in Appendix D, and dispersion calculations were performed using DEGADIS.

Table 3.2 Summary of Results for Example Dispersion Calculations

Hole diameter	3.3 ft (1 m)	16 ft (5 m)
Initial spill rate	11,700 lb/s (5,300 kg/s)	290,000 lb/s (130,000 kg/s)
Total spill duration	33 min	1.3 min
Heat transfer to LNG pool	11,700 BTU/hr/ft^2 (37 kW/m^2)	
Maximum pool radius	430 ft (130 m)	550 ft (170 m)
Total evaporation duration	34 min	18 min
Downwind distance to LFL	11,000 ft (3,300 m)	13,000 ft (3,900 m)
Time at which LFL reaches maximum distance	44 min	35 min
Time at which entire cloud drops below LFL	48 min	38 min
Downwind distance to ½ LFL	16,000 ft (4,800 m)	18,000 ft (5,500 m)
Time at which ½ LFL reaches maximum distance	53 min	45 min
Time at which entire cloud drops below ½ LFL	58 min	48 min

4 LNG RELEASE PREVENTION AND MITIGATION MEASURES

4.1 INTRODUCTION

This section outlines current measures that the international community, individual governments, shipping companies, and associated facilities employ to prevent and mitigate potential LNG releases from LNG carriers. Specifically, the section covers the following areas:

- Equipment overview
  - Brief descriptions of the basic types of LNG carriers (Section 4.2)
- Prevention measures
  - Regulatory and industry approaches for LNG carrier design (Section 4.3.1)
  - Design and operational features pertinent to release prevention (Sections 4.3.2 and 4.3.3)
  - Security measures pertinent to release prevention (Section 4.3.4)
- Mitigation measures
  - Measures that can help mitigate releases once they occur, whether they are accidental releases or releases caused by security incidents (Section 4.4)

4.2 EQUIPMENT OVERVIEW

LNG is transported at sea in three basic types of carriers – membrane ships, independent prismatic tank ships, and independent spherical tank ships. Each of these types of carriers must meet international and U.S. Coast Guard (USCG) requirements before they receive the various approvals that are required to allow them to operate in U.S. waters. Because there are different cargo tank designs that fall into the three classes of LNG carriers referenced above, this report does not describe the specifics of LNG carrier tank design. Since this report was not developed to reflect a specific cargo tank design, that information is not within the scope of this study.

However, all current LNG cargo tanks either provide two barriers designed for cargo containment at low temperature (i.e., membrane type designs) or a more robust single barrier with provisions to handle potential leakage (including international requirements specifically for hull structures in locations where they could be exposed to potential leaks and USCG rules that require crack-arresting steel in specific locations). Also, the LNG cargo tanks for all three types of LNG tanks are separated from the external environment by a double hull. This means external damage to an LNG carrier hull would not result in an LNG release unless the damage was extensive enough to puncture the inner hull and then the cargo tank.

4.3 INCIDENT PREVENTION MEASURES

4.3.1 Regulatory and Industry Approaches for LNG Carrier Design

LNG carriers and most other oceangoing vessels are governed by rules and regulations established by many different entities. Those entities are generally categorized as the International Maritime Organization, the flag state, the port state, and classification societies. Each of the entities

has specific areas of responsibility, and in some cases the responsibilities overlap. The result of these various rules and regulations is that most aspects of the design, construction, and operation of LNG tankers are addressed by the various entities. LNG carriers are unique in that LNG is a cryogenic liquid; accordingly, specialized materials, construction methods, and operating procedures are needed to safely handle LNG. The general rules and regulations that govern ships at sea do not address the particular concerns of LNG; therefore, specific rules and regulations have been developed by the various entities in order to ensure the safety of LNG tankers and their ports of call.

4.3.1.1 Definitions

The International Maritime Organization (IMO): A branch of the United Nations that operates under the auspices of the United Nations Convention on the Law of the Sea. The IMO Convention entered into force in 1958, and the new Organization met for the first time the following year. The purposes of the Organization, as summarized by Article 1(a) of the Convention, are "to provide machinery for cooperation among Governments in the field of governmental regulation and practices relating to technical matters of all kinds affecting shipping engaged in international trade; to encourage and facilitate the general adoption of the highest practicable standards in matters concerning maritime safety, efficiency of navigation and prevention and control of marine pollution from ships." The Organization is also empowered to deal with administrative and legal matters related to these purposes. IMO serves to write international requirements for safety and pollution prevention for ships in international service. These rules are then administered in various ways by Flag and Port States.

Flag States: The country of registry for the vessel, such as the United States, Panama, Bahamas, etc. The flag state is the country of the national flag the vessel flies. In IMO Conventions, the flag state is sometimes referred to as the "Administration." The flag state establishes regulations for the construction and operation of vessels registered under its flag. Many of the flag state requirements are based on the vessel complying with regulations of the IMO.

Port State: The authority that has jurisdiction over the port area and waters under national control. In the United States, this is typically the USCG, supplemented by state and local authorities. As defined by IMO, Port State Control (PSC) is the inspection of foreign ships in national ports to verify that the condition of the ship and its equipment comply with the requirements of international regulations and that the ship is manned and operated in compliance with these rules. The USCG defines Port State Control as “the process by which a nation exercises its domestic and or international authority over foreign vessels when those vessels are in waters subject to its jurisdiction.”

Classification Society: A classification society is an industry organization, other than a flag state, that issues certificates of class and/or International Convention Certificates. The certificates of class are based on rules published by the classification society that govern the design and construction of ships and offshore installations. A classification society has specific procedures regarding the level of design review and survey that are required to allow a vessel to be “classified.” Classification indicates that the vessel met applicable class rules, international requirements, and specific national requirements. Also, some flag states delegate certain additional review and inspection responsibilities to classification societies.

Membrane Tanks: Non-self-supporting tanks that consist of a thin layer (membrane) supported through insulation by the adjacent hull structures. The membrane is designed in such a way that

thermal and other expansion or contraction is compensated for without undue stressing of the membrane.

Independent Tanks: Self-supporting tanks; they do not form part of the ship's hull and are not essential to the hull strength. There are three categories of independent tanks:

Type A — Designed primarily using recognized standards for classical ship structural analysis procedures

Type B — Designed using model tests, refined analytical tools, and analysis methods to determine stress levels, fatigue life, and crack propagation characteristics

Type C — Tanks meeting pressure vessel criteria and designed for specific vapor pressure criteria (not typically applicable to LNG carriers)

4.3.1.2 Design specifications for LNG tankers

The IMO, through its signatory nations, provides the basis for the framework of international regulations for shipping. The IMO publishes documents that outline the international requirements for vessel design and construction, operation, safety security, and crewing. There are several IMO publications and or conventions regarding design, construction, and operation of LNG tankers that are allowed to operate in U.S. waters. These conventions are:

- Convention on the International Regulations for Preventing Collisions at Sea, 1972/1981
- Safety of Life at Sea (SOLAS), 1974/1981
- Code for the Construction and Equipment of Ships Carrying Liquefied Gases in Bulk (Gas Carrier Code), 1983
- International Code for Ships Carrying Liquefied Gases in Bulk (IGC Code), 1993
- 1994/1996 Amendments to the IGC (replaced the Gas Carrier Code)
- International Convention on Standards of Training, Certification and Watchkeeping (STCW) for Seafarers, 1978
- International Management Code for the Safe Operation of Ships and for Pollution Prevention (ISM Code) – adopted by IMO Resolution A.741 (18) in 1994

The most important of these international requirements for new LNG carrier design is the IGC Code. This provides the basic requirements that flag states and classification societies then supplement with more detailed requirements.

Flag states are responsible for ensuring that vessels intending to fly their flags are designed and constructed in accordance with the applicable international standards and any unique national requirements. Flag states generally discharge their responsibilities by (1) combining design review and inspection by their personnel and (2) requiring the vessels to be constructed in accordance with the design and survey rules of a classification society of which they approve. Flag states then have an ongoing responsibility for safe vessel operation and maintenance. This requires the vessel to be periodically inspected and certified by the flag state and likely requires periodic survey by the classification society also. Such inspections also confirm that the ship is adequately staffed (based on international and national requirements) and that the vessel crew has received specific training and certification (where required).

Port states impose laws and regulations specific to their individual ports and areas of jurisdiction. In the case of vessels wanting to enter the United States, the USCG exercises port state control. As part of port state control measures, a port state can impound or delay a vessel for a number of reasons, including, but not limited to, safety issues, pollution issues, operational restrictions/concerns, vessel condition, crew member issues such as immigration status, and security issues.

Industry organizations (like the vessel charterers and other participants in the LNG value chain) may also perform periodic audits of vessel safety and compliance with applicable requirements. These inspections serve not only to help ensure safety but also contribute to reliable operation in the LNG trade. A contributor to the safety of the industry is the Society of International Gas Tanker and Terminal Operators (SIGTTO), which publishes recommended practices in areas important to the safety of LNG vessels and terminals.

The remainder of this section discusses some of the design features of LNG carriers that help prevent significant releases if incidents should occur.

4.3.2 Design Features Pertinent to Release Prevention

Double Hull Construction: All LNG carriers (both currently in service and planned) provide double hull construction, providing a significant measure of protection against LNG release due to external damage, such as could occur in groundings, collisions, or allisions (i.e., striking a fixed object). The IGC Code requires cargo tanks to be protected from damage due to collision or grounding by being located at least a specified minimum distance inboard from the ship's shell plating. Also, gas carriers are required by the IGC Code to survive the normal effects of flooding that could be caused by external damage to the hull. Typically a grounding, collision, or allision occurs due to a (1) failure of the propulsion and/or steering system, (2) failure of navigational equipment, or (3) human error. The various authorities extensively regulate propulsion and steering systems. Maintenance and inspection of such equipment are the first step in preventing failures that would lead to the grounding of an LNG carrier. To ensure that such actions occur, flag states require periodic inspections of the vessels in their registry. Also, port states may perform their own inspections or require evidence of routine inspections to allow the vessel entry into ports under their jurisdiction. Entry into port would not typically be allowed if there were deficiencies in this equipment. Also, LNG carriers are generally guided into ports and restricted waterways by local pilots with extensive experience in the port area. This reduces the likelihood of navigational failures or human errors by normal tanker crews. Docking and departing of LNG tankers also generally involve the use of harbor tugs to assist in maneuvering the LNG carrier. Also, in the United States, LNG carrier arrivals and departures are subject to operational plans developed and enforced by the cognizant USCG Marine Safety Office (MSO). These plans generally mandate safety zones and restrict traffic in the area of any LNG tanker.

Segregation of Cargo Areas and Piping: The IGC Code requires that hold spaces (i.e., the enclosed space in the ship structure where the cargo containment system is situated) be separated from machinery and boiler spaces, accommodations, service spaces, control stations, chain lockers, drinking and domestic water tanks, and stores. There are also specific requirements for segregation of cargo piping systems from other piping systems in order to prevent the transfer of cargo or cargo vapor into or through other piping systems. Appropriate locations for accommodations, service and machinery spaces, and control stations are also defined in the IGC Code.

Accessibility for Inspection Access: In order to facilitate inspection of various structures and equipment in gas carriers, the IGC Code requires arrangements that allow visual inspection of at least one side of the inner hull structure and insulation located in hold spaces. Adequate access to cargo tanks to allow internal inspection is also required. The ability to access these areas allows periodic surveys and inspections to be performed in order to identify any damage or deterioration that has occurred. This in turn helps any identified problems to be corrected before they become safety issues for the vessel.

Leak Detection for Gas Carrier Hold Spaces: The IGC Code requires hold spaces and insulation areas where cargo leakage could occur to be equipped with gas detection and low temperature alarms.

Cargo Containment Design Requirements: The IGC Code mandates development of a cargo containment design that addresses a design vapor pressure for the containment system that considers the cargo vapor pressure and the maximum allowable relief valve setting. Also, the selection of materials for cargo tank construction must be based on a defined minimum design temperature, and it must be shown that the cargo tank temperature cannot be lowered below the design temperature. Design loads for the cargo containment must be based on specific combinations of potential loads (e.g., internal pressure, external pressure, dynamic loads due to ship motion, thermal loads, sloshing loads, ship deflection loads, weight distribution).

Structural Analysis Requirements: The IGC Code mandates that structural analyses be performed for each type of cargo containment design to address the specific loads of concern for that type of cargo containment design. The IGC Code also defines the allowable stresses for independent cargo tanks.

Secondary Barrier Provisions: LNG carriers built to the IGC Code require a secondary cargo barrier. The design intent for the secondary barrier is to contain an envisaged leakage of liquid cargo (generally for up to 15 days) to prevent lowering of the temperature of the ship structure to an unsafe level. Membrane and Type A independent tanks require a full secondary barrier. Independent Type B tanks (i.e., self-supporting tanks that are designed using model tests, refined analytical tools, and analysis methods) only require a partial secondary barrier. In all cases, the vessel inner hull that is adjacent to cargo tanks must be protected against contact from liquid cargo (e.g., either a full second barrier or appropriate spray shield and routing of potential leakage).

Low Temperature Provisions: In addition to the requirements to handle envisaged leakage, the IGC Code requires a combination of proper material selection, adequate insulation, and use of heating systems (which must include standby heating in the event of a failure of the normal heating system) to ensure that hull structures are not exposed to temperatures below their design temperature. The design must consider that the secondary barrier is at the cargo temperature with the lowest design ambient air and seawater temperatures.

Construction and Testing Requirements for Cargo Containers: The IGC Code includes construction and testing requirements that address welding, workmanship, quality assurance, hydropneumatic or hydrostatic pressure testing, leak testing, and nondestructive testing of welds.

Pressure Vessel and Piping System Requirements: The IGC Code contains provisions for general design requirements, piping thickness, design pressure rating, allowable stresses and stress analyses, type testing, fabrication and joining, welding, postweld heat treatment, nondestructive

testing, hydrostatic testing, and leak testing of piping systems and pressure vessels. These requirements are designed to ensure that the piping is appropriately designed and fabricated. Other IGC requirements specify the types of isolation valves required on connections to cargo tanks.

Emergency Shutdown Valves and Shutdown Systems: The IGC Code requires remotely controlled emergency shutdown valves on the ship for stopping liquid and vapor transfers between the ship and shore. Cargo pumps and compressors must be arranged to shut down automatically if the emergency shutdown system closes the emergency shutdown valves. In addition, there must be a remotely operated shutdown valve at each cargo hose connection used in transfers. The emergency shutdown control system must be capable of being actuated by a single control in either of two locations on the ship. It must also be actuated by fusible links that will respond in the event of a fire in locations, including tank domes and loading stations.

Cargo Pressure/Temperature Control: The IGC Code requires pressure control for the cargo system in order to keep the cargo tank pressure under the tank design pressure or the maximum allowable relief valve setting (MARVS). The pressure control system can (1) employ mechanical refrigeration or (2) use the boil-off vapor as fuel for shipboard use or for a waste heat system. Per the IGC Code, a flag administration can allow other means to control cargo tank pressure, such as venting LNG vapor to the atmosphere. Of course, operators would only consider this as a secondary means of pressure/temperature control. However, the USCG requires LNG cargo systems to be used in U.S. waters to be capable of maintaining the cargo for at least 21 days without venting. This is intended to eliminate the need to vent flammable vapors while in U.S. ports.

Pressure Relief Systems: The IGC Code requires pressure relief systems for cargo tanks that are independent of the pressure control systems described previously. For LNG cargo tanks of the size typically used on LNG carriers, the IGC Code requires at least two pressure relief valves of appropriate capacity. The valves have to be provided with vent piping that minimizes the potential for accumulation of LNG vapor on deck or ingress of vapor into areas where it might create a dangerous condition. The IGC Code mandates that the pressure relief valves have a combined relieving capacity of the greater of (1) the maximum capacity of the cargo tank inerting system or (2) the vapor generation rate due to fire exposure of the tank.

Vacuum Protection Systems: The IGC Code requires that any LNG cargo tank not designed for the maximum pressure differential that could be developed by (1) pumping out a tank without vapor return, (2) operating a refrigeration system, or (3) sending boil-off vapor to machinery spaces, be provided with a vacuum protection system. Acceptable vacuum protection systems under the IGC Code include use of two independent pressure switches that alarm and actuate to stop any suction of liquid or vapor from the cargo tank and shut down refrigeration equipment. Another vacuum protection option is to provide vacuum relief valves that are sized for the maximum discharge rate from the cargo tank. Since operation of a vacuum relief valve would introduce air into the tank, in practice, ship pressure control systems are designed to prevent negative pressure situations in the tank well before vacuum relief valves operate.

Vessel Fire Protection Systems: Per the IGC Code, LNG carriers require a firewater main system and hydrants/hose stations with the ability to supply at least two jets of water to any part of the deck in the cargo area and parts of the cargo containment and tank covers above the deck. The firewater supply system also has to supply water for a water spray system that provides water for cooling, fire prevention, and crew protection in specific areas. LNG carriers also require a fixed dry chemical powder-type extinguishing system to allow the crew to fight fires on the deck in the cargo

area and cargo handling areas. In addition, the cargo compressor room, which is located on deck, is fitted with a CO_2 smothering system.

Cargo Tank Instrumentation: In order to allow an LNG carrier crew to monitor cargo tank conditions, the IGC Code requires a variety of instrumentation. These include:

- Gas detection equipment capable of alerting the crew to leakage of LNG from the primary barrier (i.e., instruments to detect LNG vapor between the primary and secondary barriers)
- At least one liquid level gauging device for each tank
- A high liquid level alarm (independent of other level devices) that gives audible and visual warning and shuts off flow into the cargo tank when it is actuated. This serves to help prevent the tank from becoming liquid-full
- Cargo tank pressure gauges, marked with maximum and minimum pressures, providing both high and low pressure (if the tank requires vacuum protection)
- Two temperature indicating devices (one at the bottom and one at the top of the cargo tank) marked to show the minimum cargo tank design temperature
- Temperature indicating devices and alarms to monitor for leaks of LNG into the insulation between primary and secondary LNG cargo tank barriers or onto the hull structure adjacent to the cargo tank

This instrumentation, along with the pressure relief and vacuum pressure protection systems described earlier, provides a major role in preventing LNG cargo tank upsets or human errors from damaging the tank or resulting in a large scale release.

Vessel Gas Detection Systems: In addition to gas detection discussed previously, the IGC Code requires a permanently installed gas detection system with audible and visual alarms for areas, including cargo compressor rooms, motor rooms, cargo control rooms, enclosed spaces in the cargo area, specific ventilation hoods and gas ducts in the propulsion machinery space for the fuel gas system, and air locks. These detectors are required to activate alarms when 30% of the LFL is reached. Ships also are required to have at least two sets of portable gas detectors.

Gas Detection and Safety Shutdown Systems for Terminal Operations: LNG unloading systems and docks are equipped with LNG vapor detection, fire detection, and associated safety shutdown systems that shut down pumping operations and close valves to isolate the transfer lines. The shutdown systems can be actuated by the ship's crew or LNG terminal personnel. In most cases, these systems also respond automatically to any detection of LNG in the atmosphere by shutting down pumping operations and closing valves to isolate the LNG transfer lines. The systems can also be actuated by the ship's crew or LNG terminal personnel. This serves to limit the amount of LNG that would be released in a leak that occurred during the unloading process.

Emergency Release Couplings: Current designs for LNG terminals have emergency release couplings that are fitted between the ship's cargo manifold and the receiving station. These couplings are designed to release if vessel movement exceeds predetermined limits. If the couplings release, the

resulting LNG loss to the atmosphere is designed to be very small (e.g., approximately 1 gal). As LNG is a cryogenic liquid that has the capacity to cause severe embrittlement of steel structures, the areas of an LNG carrier deck likely to be contacted by a leak of LNG are protected with drip trays constructed of materials suitable for withstanding LNG exposure.

4.3.3 Operational Measures Pertinent to Accidental Release Prevention

In addition to design features, the international and national maritime authorities have recognized the need for operational measures that prevent or at least reduce the likelihood of LNG incidents. These measures include:

- Training
- Procedures
- Inspections

Training – Minimum training requirements for crews of LNG carriers are specified in the IMO STCW Convention referenced previously. This level of training is generally exceeded by the training specified by the flag state and the shipping company. LNG carrier crews are considered some of the most professional and competent in the international shipping business, recognizing the important role they play in safe operations.

Procedures – International ships over 500 gross tons subject to SOLAS (including LNG carriers) are required by IMO to meet the ISM Code. This safety management approach requires development of safety and environmental policies, along with the assignment of responsibilities, development of procedures, performance of training, and periodic audits and reviews to evaluate compliance with those requirements. The ISM Code explicitly addresses the need to prepare for responding to emergency situations like fire and LNG releases.

Inspections **–** Inspections for vessels occur from a variety of sources. Flag states and classification societies both have requirements for periodic inspections and surveys. Port state control activities often include safety inspections of vessels desiring to enter a port. These third-party inspections are in addition to inspections and audits required under vessel and shipping company ISM programs or by charterers concerned with ensuring safe, reliable voyages on which the success of their investment depends.

4.3.4 Security Measures that Help Prevent Release Incidents Due to Deliberate Attacks

Some of the design features and operational measures described in the previous sections play a role in preventing LNG releases even when terrorist acts are considered (e.g., double hull structures). However, this section describes the international and U.S. requirements for security measures applicable to LNG carriers.

After the events of 9-11, the IMO added Chapter XI-2 to the SOLAS Convention to provide the International Ship and Port Facility Security (ISPS) Code. Applicable to LNG vessels, the ISPS Code requires actions by flag states, port states, shipping companies, and port facilities to reduce the likelihood of terrorism acts against maritime assets. Effective July 1, 2004, the ISPS Code requires:

- Security levels
- Ship security plans

- Ship security alarm systems
- Automatic identification systems
- Port security plans
- Declarations of security
- Facility security plans

These security measures are discussed below.

Security levels – Flag states and port states are required to provide security-related information to their vessels and port facilities in the form of a designation of security levels. The three security levels represent the assessment of the likelihood of a terrorist event being attempted against maritime assets. Each level is intended to trigger specific security measures that are defined in ship, port, and port facility security plans.

Ship security plans – Flag states are required to review and approve ship security plans developed by the operator of each SOLAS vessel in international service that is larger than 500 gross tons (which includes all LNG carriers). These plans must address security measures for:

- Access to the ship by ship personnel, passengers, visitors, etc.
- Restricted areas on the ship
- Handling of cargo
- Delivery of ship's stores
- Handling unaccompanied baggage
- Monitoring the security of the ship

These measures are intended to protect the ship and to prevent the ship from being used as a weapon against other maritime targets (e.g., other vessels, bridges, terminals). The ship security plan implementation must be evaluated by an onboard verification by the flag state or a security organization recognized by the flag state before an International Ship Security Certificate (ISSC) can be issued for that vessel.

Ship security alarm systems – Each vessel subject to the ISPS Code must carry on board equipment to provide a ship security alarm (SSA) that the ship's crew can activate if terrorists board the vessel. The alarm, which is does not sound aboard the vessel, is intended to alert responsible authorities (e.g., the USCG or other designated authority) that a security incident is underway.

Automatic identification systems (AISs) – AIS equipment has been in the process of being introduced over the last few years. It consists of a transponder on each vessel that provides a signal identifying vessel name, location, cargo, heading, etc. Originally intended to help reduce vessel collisions and make port state control activities easier, it is recognized as another step that contributes to port security. As such, application of AISs was accelerated for some vessels as part of the changes to SOLAS made when the ISPS Code was introduced. For U.S. ports where vessel traffic systems or other AIS base stations are implemented, the AIS transponders allow the USCG to have real-time radar systems that provide a higher level of information than just the radar images.

Port security plans – Each port served by international vessels subject to the ISPS Code is required to have a port facility security officer and to develop a port facility security plan. The plan must specify the security measures expected at local port facilities and the measures expected by international vessels that interface (e.g., load, unload, refuel, transfer passengers) with those facilities. In the United States, the applicable USCG Captain of the Port (COTP) serves as the port

facility security officer and, in conjunction with a port security committee, is responsible for developing a port security plan. Among other things, the port security plan identifies the individual facilities within the port that will require their own facility security plan. Also, port security plans define what operational controls (e.g., security zones, escorts, sea marshals) apply to various kinds of vessels to enter the port. The USCG also uses the requirement for an Advanced Notice of Arrival (ANOA) from vessels entering U.S. ports from foreign departure locations as a tool in port state control. The ANOA information allows the USCG to select vessels based on their route, cargo, security, and safety history, and other pertinent information in order to plan security inspections, escorting, and boarding of sea marshals or other USCG personnel as appropriate.

Declarations of security – Nationwide, the USCG has mandated that all visits by vessels like LNG carriers require a declaration of security (DoS) that must be prepared by the ship and the facility it is to call upon. A DoS defines the security responsibilities for both the facility and the ship for the period of time the vessel is at that facility. It has to be coordinated between the ship security officer and the facility security officer and signed prior to any interface activities (e.g., cargo transfers or personnel movement) between the vessel and the facility.

Facility security plans – Under the USCG maritime security regulations (33 CFR, Subchapter H), LNG facilities that receive LNG carriers will have to develop a security plan. Like the ship plans that have to meet the ISPS Code, the USCG regulations define areas the facility security plans have to address, including:

- Security administration and organization of the facility
- Personnel training
- Drills and exercises
- Records and documentation
- Response to change in security level
- Procedures for interfacing with vessels
- DoS
- Communications
- Security systems and equipment maintenance
- Security measures for access control, restricted areas, handling cargo, delivery of vessel stores and bunkers, and monitoring
- Security incident procedures
- Audits and security plan amendments

Like ship security plans, facility security plans have to be approved by the responsible government, in this case, the port state. For U.S. facilities, that requires submission of the facility security plans to the USCG for review and approval.

4.4 MITIGATION MEASURES TO HELP RESPOND TO RELEASES

For LNG releases, the industry has traditionally focused on release prevention; however, there are some measures that are pertinent to help mitigate releases once they occur. This section discusses those measures, which apply to both accidental releases and releases caused by security incidents (e.g., terrorist acts).

The primary focus in responding to LNG releases is to protect public and employee safety and secondarily to minimize the amount of damage to vessel and facility property. Some of the features previously discussed as design elements for preventing significant releases play a role once a release

occurs. These include gas detection, safety shutdown systems, and fire protection systems. Beyond those elements there are other mitigation features such as:

- Safety and security zones
- Ship and facility emergency response plans
- Coordination with USCG and local emergency responders
- Evacuation plans and procedures

Safety and security zones – Safety zones around vessels play a role in reducing the likelihood of collisions or the need for an LNG vessel to try to avoid other port traffic. Security zones help vessel and USCG resources recognize if a vessel near an LNG carrier is not willing to abide by established rules and allow the vessel to keep watch for unusual activity. They also allow the USCG to intervene with a vessel if resources are available to do so. However, either of these types of zones help in that if there is an event, they limit the proximity of recreational and commercial traffic to the LNG vessel and berthing area.

Ship and facility emergency response plans – Both LNG carriers and LNG terminals are required to develop emergency response plans, complete with personnel training and exercises. These plans serve to help ensure that prompt and effective action results if a release scenario occurs. Emergency response actions include release isolation (if possible), minimization of ignition sources (e.g., by shutting down equipment or restricting activities), and evacuation of ship crew or members of the public if deemed appropriate.

Coordination with USCG and local emergency responders – Because the ship crew may not be able to deal with all potential contingencies or possible release events, emergency response actions are typically coordinated with USCG and other local emergency response personnel located near LNG terminals where transfers will occur. Coordination, which might include joint drills, exercises, or other types of training, helps improve understanding of the types of events that could occur, the expected consequences, and how the resources of the various entities can best be combined to address those events.

Evacuation plans and procedures – If necessary, an emergency response plan will call for evacuation of locations where the emergency personnel are concerned that threats to personnel may develop. Particularly for an unignited release, emergency responders may involve law enforcement or other public resources to help notify personnel in the downwind direction to take action and move away from the area of the hazard.

5 CONCLUSIONS

5.1 REVIEW OF WORK SCOPE

- **An evaluation of published models to calculate the rate of cargo release and the spread of unconfined LNG spills on water**

  No models were identified that account for the multi-hull structure of an LNG carrier and the physics of a release of cryogenic LNG. In the absence of models specifically for LNG carriers, the orifice model is recommended. However, when using this model it is vital to keep in mind that the model does not match the reality of carrier construction very well, and the results should be interpreted as a rough guide to the rate of release for a given hole size. Because it does not account for the multi-hull construction of carriers, the orifice model will tend to overestimate the LNG outflow for many scenarios. See Section 2.1 for details of the release rate modeling review and recommendations.

  Several models for spreading were found in the literature, most of which are based on the assumption that spreading is dominated by the balance of the gravitational spreading force and inertial resistance to spreading. One methodology, developed by Webber and his colleagues (as described in TNO 1997), also accounts for resistance to spreading as a result of frictional forces. Our analysis of these methodologies indicates that frictional effects are important for scenarios involving large releases in short periods of time. Therefore, Webber's methodology is recommended.

  It is important to note that this methodology for estimating pool spread does not account for some aspects of spills on open water that could be important such as wind, water currents, and waves. However, no existing model for an LNG spill appropriately accounts for these effects. It should be recognized that the recommended model is based on the assumption of smooth quiescent water.

  See Section 2.2 for details of the pool spread modeling review and recommendations.

- **A determination of the effect of cargo tank hole diameter on cargo release and pool spread (including establishment of an upper limit on pool spread)**

  The example release rates presented in Section 3.1 provide some information about the effect of cargo tank hole diameter. However, the results of the sample calculations must be considered no more than a rough guide to potential release rates.

  For a given hole size (or release rate), the upper limit on pool spread depends on the duration of release. For long duration releases, the pool will spread to the point where evaporation rate (or burning rate in case of a fire) matches the release rate into the pool. This is based on a simple mass and heat balance for the pool, and effectively defines an upper limit for long-term releases. For short duration releases, the dynamics of the release are more important in identifying the upper limit. The pool spread is slowed by inertial and frictional effects but is only stopped once the pool is thin enough for surface tension effects to become important. During the spread, evaporation reduces the volume of the pool, and therefore also slows the spread. As a result of these dynamics, it is difficult to establish an upper limit for short duration releases without modeling the full spread process.

This raises the question of how to decide if a given release should be treated as long duration or short duration for modeling purposes. It is recommended to avoid the necessity of selecting either of these by modeling the pool spread in a way that handles a transient release into the pool. The integral solution to the spreading problem implemented for the example problems in this report accomplishes this and allows modeling scenarios using (1) an initial pool volume and/or (2) a constant or transient flow rate into the pool.

- **An evaluation of these models to calculate the rate of vapor generation for unconfined LNG spills on water**

  LNG spilled from a carrier onto water will form a pool at its boiling point (at atmospheric pressure) of approximately -259 ºF (-162 ºC). At this temperature the LNG will rapidly absorb heat from the water, and the heat absorbed will go directly to vaporize the LNG (at a rate determined by the heat of vaporization of the LNG). Therefore, modeling of vaporization of the LNG essentially reduces to the modeling of heat flux into the pool from the water. Of course the dynamics of pool spread (as discussed above and in Section 2.2) are also important because total evaporation rate (mass per unit time) depends on the pool area.

  Two methods are identified for estimating heat flux to a boiling LNG pool on water: (1) select a value estimated from spill tests or (2) calculate a value based on heat transfer theory. Based on review of the literature, it is recommended to estimate heat flux using heat transfer theory. Key reasons for this choice are that (1) the experimental data show significant spread, (2) the experimental data for heat flux were typically calculated from other data (rather than measured directly), and (3) a viable theoretical model from heat transfer theory is available to help fill the gap in experimental data.

  As noted above for pool spread, it is important to note that this methodology for estimating vapor generation does not account for some aspects of spills on open water that could be important such as wind, water currents, and waves.

  See Section 2.3 for details of the vapor generation modeling review and recommendations.

- **An evaluation of the models to calculate thermal radiation distances from fires involving unconfined LNG spills on water**

  Available pool fire models for hazard assessment purposes are predominantly based on the solid flame model. The fire is represented as gray-body emitter, and the geometry is approximated by an upright cylinder that is tilted as a result of wind. The point source model is also sometimes used. In this model energy generated by combustion is assumed to emanate from a single point at the center of the pool fire. The calculated energy is multiplied by a fraction that accounts for the fact that only part of the energy will be emitted as thermal radiation.

  In some circumstances the point source model can be appropriate, but its chief disadvantage is that it does not produce valid estimates for any people or structures located close to the fire. Therefore, the solid flame model is recommended.

  Two key parameters required to apply the solid flame model are the burning rate and surface emitted flux. Based on a review of experimental data the recommended values for these parameters are a burning rate of 0.058 lb/s/ft^2 (0.282 kg/s/m^2) and emissive power of 84,000 BTU/hr/ft^2 (265 kW/m^2). There is significant spread in the experimental data for these

parameters; however, comparisons only to data for the larger scale spill tests tend to indicate that these are relatively conservative choices.

See Section 2.4 for details of the pool fire modeling review and recommendations

- **An evaluation of the models to calculate the distance traveled by flammable vapors from unconfined LNG spills on water**

  This work did not involve a detailed review of dispersion models. For large releases of LNG, the cold LNG vapors are more dense than the surrounding air and tend to remain at surface. These dense-gas effects are important and must be accounted for in the model used. Several such models are available in the form of freely available, as well as commercial, software.

  For the example dispersion calculations presented in this report, the DEGADIS software was used. This model accounts for dense-gas effects and was originally developed for simulation of cryogenic flammable gas dispersion, particularly for LNG. It has been validated against a wide range of available laboratory and field test data.

  See Section 2.5 for details of the dispersion modeling review and recommendations..

- **An evaluation of the theoretical basis for current models used to calculate each of the above, and a review of the applicability of existing computer modeling to field test data**

  The theoretical basis is an important factor that was considered as part of the overall review of each modeling area and is addressed throughout Section 2.

  The time available for this work did not allow a detailed review of existing computer programs that implement the recommended methods; however, use of some existing software is discussed in Section 2. In general, validation of computer models (as well as their theoretical bases) has been very limited with regard to large LNG spills on water. There are simply very few data to validate models against, and there are no test data for spills of the large size considered by this report.

- **A review of the effects of thermal radiation levels on population and structures**

  The extent to which people are injured by exposure to thermal radiation depends on both the incident heat flux and the exposure time. A variety of data are available for estimating effects on people, including data from experiments with humans and animals and review of historical data. Section 2.7.1 summarizes some of the injury criteria developed based on these data.

  Like effects of thermal radiation on people, effects on structures also depend on incident heat flux and the exposure time. With structures, effects also depend strongly on the materials of construction (e.g., wood, steel, concrete). Section 2.8 presents some criteria from various sources for structural damage. Most of the criteria presented are for long-term exposure, which is very generally considered to be on the order of 30 minutes or more. More accurate assessment of structural damage requires performing heat balance calculations to determine the resulting surface temperature for comparison with acceptable temperatures for the particular structure.

- **A recommendation, including the selection rationale, of specific methods and a model which FERC staff may use to calculate the flammable vapor and thermal radiation hazards associated with marine transportation of LNG**

  The recommendations are made throughout Section 2, and example assessments are presented in Section 3. The detailed calculations for the examples are provided in Appendices A through D.

- **A comprehensive review of design, operational, safety, and security features and possible mitigating measures that an LNG facility and/or vessel operator employs or could provide to minimize impacts from: accidents; attacks; leaks; spills; fire; rapid phase transitions; or the spread of negatively buoyant, flammable vapor clouds**

  Section 4 of this report is dedicated to this item.

5.2 OBSERVATIONS

The methods recommended in this analysis can only provide rough estimates of the magnitude of effects for incidents involving large LNG releases on water. This is typically the case with consequence assessments, and it is important to keep in mind that the recommended methods cannot definitively describe the effects because of variability in actual incident circumstances, as well as uncertainty inherent in the methods used.

The example consequence calculations presented in Section 3 are intended only to illustrate use of the various analysis methods recommended in Section 2. The scenarios were chosen simply to exercise the various methods and are not necessarily the correct scenarios to model for specific facility siting or any other hazard assessment purpose. Furthermore, some input parameters (e.g., atmospheric conditions, surface roughness) were chosen for the examples only and may be inappropriate for a particular site and/or particular hazard assessment. When using the presented analysis methods for an actual analysis, it is important to choose scenarios and input parameters based on the analysis requirements and site conditions.

6 REFERENCES

AIChE (2000)
Center for Chemical Process Safety of the American Institute of Chemical Engineers, *Guidelines for Chemical Process Quantitative Risk Analysis*, Second Edition, ISBN 0-8169-0720-X, New York, 2000.

API (1992)
American Petroleum Institute, *Hazard Response Modeling Uncertainty (A Quantitative Method) - Volume II: Evaluation of Commonly Used Hazardous Gas Dispersion Models*, API Publication Number 4546, October 1992.

API (1997)
American Petroleum Institute (API), *Guide for Pressure-Relieving and Depressuring Systems*, Recommended Practice 521, Fourth Edition, API, Washington, D.C., March 1997.

Atallah (1997)
Sami Atallah, *Rapid Phase Transitions*, Topical Report GRI-92/0533, Gas Research Institute, October 1997.

Boyle (1972)
G.J. Boyle and A. Kneebone, *Laboratory Investigation into the Characteristics of LNG Spills on Water. Evaporation Spreading and Vapor Dispersion*, Shell Research Limited, Report of work done for American Petroleum Institute, 1972.

Briscoe (1980)
F. Briscoe and P. Shaw, "Spread and Evaporation of Liquid," *Prog. Energy Comb. Sci.*, Vol. 6, pp. 127-140, 1980.

Brown (1974)
L.E. Brown, H.R. Wesson, and J.R. Welker, "Predicting LNG Fire Radiation," *Hydrocarbon Process*, 141-143, 1974.

BS 5908 (1990)
British Standard 5908, *Code of Practice for Fire Precautions in Chemical Plant*, 1990.

Burgess (1970)
D.S. Burgess, J.N. Murphy, and M.G. Zabetakis, *Hazards Associated with the Spillage of Liquefied Natural Gas on Water*, Report No. 7448, U.S. Bureau of Mines. 1970.

Burgess (1972)
D.S. Burgess, J. Biordi, and J.N. Murphy, *Hazards of Spillage of LNG into Water*, MIPR Z-70099-9-12395, U.S. Bureau of Mines, 1972.

Cavanaugh (1994)
T.A. Cavanaugh, J.H. Siegell, and K.W. Steinberg, "Simulation of Vapor Emissions from Liquid Spills," *Journal of Hazardous Materials*, Vol. 38, pp. 41-63, 1994.

Conrado (2000)
C. Conrado and V. Vesovic, "The Influence of Chemical Composition on Vaporisation of LNG and LPG on Unconfined Water Surfaces," *Chemical Engineering Science,* Vol. 55, pp. 4549-4562, 2000.

Cumber (2002)
Peter Cumber, "Vessel Outflow Sensitivity to Composition," *Journal of Loss Prevention in the Process Industries*, 15 pp. 205–212, 2002.

Dinenno (1982)
P.J. Dinenno, "Simplified Radiation Heat Transfer Calculations from Large Open Hydrocarbon Fires," *Society of Fire Protection Engineers Annual Meeting*, 1982.

EPA (1991)
U.S. Environmental Protection Agency, *Evaluation of Dense Gas Simulation Models*, EPA-450/4-90-018, May 1991.

Fay (1973)
J.A. Fay, "Unusual Fire Hazard of LNG Tanker Spills," *Combusion Science and Technology*, 7, pp. 47-49, 1973.

Fay (2003)
J.A. Fay, "Model of Spills and Fires from LNG and Oil Tankers," *Journal of Hazardous Materials*, B96, pp. 171-188, 2003.

FEMA (1990)
Federal Emergency Management Agency, *Handbook of Chemical Hazard Analysis Procedures*, Available from Federal Emergency Management Agency, Publications Office, 500 C Street, SW, Washington, D.C. 20472.

Glastone (1977)
S. Glastone and P.J. Dolan, *The Effects of Nuclear Weapons*, third ed., Tonbridge Wells, Castle House, 1077.

GRI (1990)
Gas Research Institute, *LNG Vapor Dispersion Prediction with the DEGADIS Dense Gas Dispersion Model*, Topical Report GRI-89/0242, September 1990.

GRI (1997)
Gas Research Institute, *Evaluation of Mitigation Methods for Accidental LNG Releases. Volume 5: Using FEM3A for LNG Accident Consequence Analyses*, Topical Report GRI-96/0396.5, 1997.

Hoult (1972)
D. Hoult, "The Fire Hazard of LNG Spilled on Water," *Proceedings Conference on LNG importation and safety*, Boston, p. 87, 1972.

Kletz (1980)
T.A. Kletz, "Plant Layout and Location: Methods for Taking Hazardous Occurrences into Account," *Loss Prevention*, 13, 147, 1980.

Klimenko (1981)
V.V. Klimenko, "Film Boiling on a Horizontal Plate – New Correlation," *International Journal of Heat and Mass Transfer*, 24, 69-79, 1981.

Koopman (1979)
R.P. Koopman, B.R. Bowman, and D.L. Ermak, *Data and Calculations of Dispersion on 5 m^3 LNG Spill Tests*, UCRL-52876, 1979.

Lees (1980)
F.P. Lees, *Loss Prevention in the Process Industries*, Volume 1, Butterworth-Heinemann, Oxford, 1980.

Lees (1996)
F.P. Lees, *Loss Prevention in the Process Industries*, Second Edition, ISBN 0-7506-1547-8, Butterworth-Heinemann, Oxford, 1996.

Lehr (2004)
William Lehr and Debra Simecek-Beatty, "Comparison of Hypothetical LNG and Fuel Oil Fires on Water," *Journal of Hazardous Materials*, 107, pp. 3-9, 2004.

Lloyds (2001)
Lloyd's Register of Shipping, *Explosion and Gas Release from LNG Membrane Carriers – Generic Consequence Assessment*, MARSPEC – Risk Management, October 4, 2001.

McQueen (1972)
W. McQueen, R.H. Whipp, and W.G. May, *Spills of LNG on Water – Vaporization and Downward Drift of Combustible Mixtures*, Esso Research and Engineering Company Report No. EE61E-72, Report of work done for American Petroleum Institute, 1972.

Mecklenburgh (1985)
J.C. Mecklenburgh, *Process Plant Layout*, Godwin, London, 1985.

Mizner (1983)
G.A. Mizner and J.A. Eyre, "Radiation from Liquefied Gas Fires on Water," *Comb. Sci. and Tech.*, 35, pp. 33-57, 1983.

Moorhouse (1982)
J. Moorhouse, "Scaling Criteria for Pool Fires Derived from Large-Scale Experiments." *The Assessment of Major Hazards*, Symposium Series No. 71, The Institution of Chemical Engineers, Pergamon Press Ltd., Oxford, United Kingdom, pp. 165-179, 1982.

NFPA (1995)
Society of Fire Protection Engineering and the National Fire Protection Association, *The SFPE Handbook of Fire Protection Engineering (Second Edition)*, ISBN 0-87765-354-2 (NFPA No. HFPE-95), 1995.

NFPA (2001)
National Fire Protection Association, *Guide for Fire and Explosion Investigations*, National Fire Prevention Association Standard 921, 2001.

NFPA (2002)
National Fire Protection Association, *NFPA 68 Guide for Venting of Deflagrations*, National Fire Protection Association, 2002.

Otterman (1975)
B. Otterman, "Analysis of Large LNG Spills on Water, Part 1: Liquid Spread and Evaporation," *Cryogenics*, pp. 455-460, August, 1975.

Prichard (1992)
M.J. Prichard and T.M. Binding, "FIRE2: A New Approach for Predicting Thermal Radiation Levels from Hydrocarbon Pool Fires," *IChemE Symposium Series*, No. 130, pp. 491-505, 1992.

Prugh (1994)
R.W. Prugh, "Quantitative Evaluation of Fireball Hazards," *Process Safety Progress*, The American Institute of Chemical Engineers, Vol. 13, No. 2, pp. 83-91, April 1994.

Quest (2001, 2003)
Quest Consultants, Inc., *Modeling LNG Spills in Boston Harbor*, Letter from John Cornwell of Quest Consultants to Don Juckett of the U.S. Department of Energy, October 2, 2001; Letter from John Cornwell of Quest Consultants to Don Juckett of the U.S. Department of Energy, October 3, 2001; and Letter from John Cornwell of Quest Consultants to Clifford Tomaszewski of the Office of Natural Gas & Petroleum Import & Export Activities, November 17, 2003.

Raj (1974)
P.K. Raj and A.S. Kalelkar, *Assessment Models in Support of the Hazard Assessment Handbook*, Technical Report No. CG-D-65-74, US Coast Guard, NTIS AD776617, January 1974.

Raj (1979)
P.K. Raj, K.S. Mudan, and A.N. Moussa, *Experiments Involving Pool and Vapor Fires from Spills of LNG on Water*, Report CG-D-55-79, NTIS AD077073, U.S. Coast Guard, 1979.

Rew (1996)
P.J. Rew and W.G. Hulbert, *Development of Pool Fire Thermal Radiation Model*, HSE Contract Research Report No. 96-1996, Health and Safety Executive, 1996.

Shaw (1978)
P. Shaw and F. Briscoe, *Vaporization of Spills of Hazardous Liquids on Land and Water*, SRD/HSE-report R100, May 1978.

Thomas (1963)
P.H. Thomas, "The size of flames of natural fires", *Ninth Symposium on Combustion*, Academic Press, New York, p. 844-859, 1963.

Thomas (1965)
P.H. Thomas, *F.R. Note 600*, Fire Research Station, Borehamwood, England, 1965.

TNO (1992)
C. J. H. van den Bosch et al., *Methods for the Determination of Possible Damage to People and Objects Resulting from Releases of Hazardous Materials (TNO Green Book)*, CPR 16E (ISBN 90-5307-052-4), The Netherlands Organisation of Applied Scientific Research (TNO), The Hague, 1992.

TNO (1997)
C.J.H. van den Bosch and R.A.P.M Weterings, eds., *Methods for the Calculation of Physical Effects* (TNO Yellow Book), TNO, The Hague, The Netherlands, Third edition 1997.

Valencia-Chavez (1979)
Jaime A. Valencia-Chavez and Robert C. Reid, "The Effect of Composition on the Boiling Rates of Liquefied Natural Gas for Confined Spills on Water," *International Journal of Heat and Mass Transfer,* Vol. 22, pp. 831-838, 1979.

Vallejo (2003)
LNG Health and Safety Committee of the Disaster Council City of Vallejo, California, *Liquefied Natural Gas in Vallejo: Health and Safety Issues*, January 16, 2003.

Waite (1983)
P.J. Waite, R.J. Whitehouse, and E.B. Winn, "The Spread and Vaporization of Cryogen Liquids on Water," *Journal of Hazardous Materials*, Vol. 8, pp. 165-184, 1983.

Wayne (1991)
F.D. Wayne, "An Economical Formula for Calculating Atmospheric Infrared Transmissivities," *Journal of Loss Prevention in the Process Industries*, Volume 4, pp. 86-92, January, 1991.

Welker (1970)
J.R. Welker and C.M. Sliepcevich, *Susceptibility of Potential Target Components to Defeat by Thermal Action*. University of Oklahoma Research Institute, Report No. OURI-1578-FR, Norman Oklahoma, 1970.

World Bank (1988)
The World Bank, *Techniques for Assessing Industrial Hazards: A Manual*, World Bank Technical Paper Number 55, ISBN 0253-7454, the International Bank for Reconstruction and Development, 1818 H Street, NW, Washington, D.C. 20433, 1988.

Appendix A

Film Boiling Heat Transfer Calculations

LNG Boiling Heat Flux for Spill on Water

Ambient Conditions

Ambient temperature	$T_a := (100 + 459.67)\cdot R$	$T_a = 559.67R$
Ambient pressure	$p_a := 101325\,Pa$	$p_a = 14.7psi$
Temperature of water	$T_w := (20 + 273.15)\cdot K$	$T_w = 293.15K$

Constants and Conversion Factors

Unit conversions $kJ \equiv 1000\cdot joule$ $lbmole \equiv 1$ $kgmole \equiv \frac{kg}{lb}\cdot lbmole$ $kW \equiv 1000\cdot watt$

Universal gas constant $R_u \equiv 1545\cdot\frac{ft\cdot lbf}{lbmole\cdot R}$

Material Properties

Molecular weight $M := 16.043\frac{kg}{kgmole}$

Normal boiling point $T_b := 111.66\,K$ $T_b = 200.988R$

Vapor density (at T_b, using ideal gas law) $\rho_v := \frac{p_a}{\frac{R_u}{M}\cdot T_b}$ $\rho_v = 1.751\frac{kg}{m^3}$ $\rho_v = 0.109\frac{lb}{ft^3}$

Vapor viscosity (at T_b) $\mu_v := 4.362\cdot 10^{-6}\,Pa\,sec$

Kinematic viscosity of vapor (at T_b) $\nu_v := \frac{\mu_v}{\rho_v}$ $\nu_v = 2.491\times 10^{-6}\frac{m^2}{sec}$

Density of Liquid (at T_b) $\rho_l := 422.5\frac{kg}{m^3}$

Heat of vaporization $h_{fg} := 509331.9\frac{joule}{kg}$

Surface Tension (at T_b) $\sigma := 0.0133\frac{newton}{m}$

Thermal conductivity of vapor $\lambda_v := 0.01269\frac{watt}{m\cdot K}$

Heat capacity of vapor $C_p := 2075.56\frac{joule}{kg\cdot K}$

Vapor thermal diffusivity $\alpha_v := \frac{\lambda_v}{\rho_v\cdot C_p}$ $\alpha_v = 3.491\times 10^{-6}\frac{m^2}{sec}$

Film Boiling Heat Flux

Use the model/correlation of Klimenko, as given by TNO (1997).

Length scale for vapor bubble formation $l_c := 2\pi\left[\frac{\sigma}{g\cdot(\rho_l - \rho_v)}\right]^{.5}$ $l_c = 0.011\text{m}$

Galileo number $Ga := \frac{g\cdot l_c^{3}}{\nu_v^{2}}$ $Ga = 2.269\times 10^{6}$

Archimedes number $Ar := Ga\cdot\frac{(\rho_l - \rho_v)}{\rho_v}$ $Ar = 5.452\times 10^{8}$

Prandtl number $Pr_v := \frac{\nu_v}{\alpha_v}$ $Pr_v = 0.713$

Dimensionless heat of vaporization $L_{vR} := \frac{h_{fg}}{C_p\cdot(T_w - T_b)}$ $L_{vR} = 1.352$

Nusselt number

$$F_1 := 1\cdot(L_{vR} \le 1.4) + \left(\frac{L_{vR}}{1.4}\right)^{\frac{1}{3}}\cdot(L_{vR} > 1.4) \qquad F_2 := 1\cdot(L_{vR} \le 2) + \left(\frac{L_{vR}}{2}\right)^{\frac{1}{2}}\cdot(L_{vR} > 2)$$

$$Nu := 0.19\cdot(Ar\cdot Pr_v)^{\frac{1}{3}}\cdot F_1\cdot(Ar \le 10^{8}) + 0.0086\sqrt{Ar}\cdot Pr_v^{\frac{1}{3}}\cdot(Ar > 10^{8}) \qquad Nu = 179.4$$

Heat transfer coefficient $h_{film} := \lambda_v\cdot\frac{Nu}{l_c}$ $h_{film} = 201.8\frac{\text{watt}}{\text{m}^2\cdot\text{K}}$

Heat flux $Q_{film} := h_{film}\cdot(T_w - T_b)$ $Q_{film} = 36.6\frac{\text{kW}}{\text{m}^2}$

Appendix B

Example Release Rate Calculations

LNG Release Rates Based on Flow Through an Orifice

Model release using flow through an orifice with flow rate dropping as height of liquid above hole decreases. Assume that cross sectional area of tank (in horizontal plane) is approximately constant.

Density of Liquid (at boiling point) $\rho_1 := 422.5 \cdot \frac{kg}{m^3}$

Total volume in the tank above the hole $V_{spill} := 12500 \cdot m^3$ $V_{spill} = 4.41 \times 10^5\ ft^3$

Initial liquid height above the hole $h_{init} := 13 \cdot m$ $h_{init} = 42.7\ ft$

Tank area in horizontal plane $A_{tank} := \frac{V_{spill}}{h_{init}}$ $A_{tank} = 962\ m^2$ $A_{tank} = 1.03 \times 10^4\ ft^2$

Discharge coefficient $C_d := 1$

Function for flow through an orifice driven only by gravity $Q_o(d_{hole}, h) := C_d \cdot \rho_1 \cdot \pi \cdot \left(\frac{d_{hole}}{2}\right)^2 \cdot \sqrt{2g \cdot h}$

Function to determine flow rate versus time, taking into account the decreasing head

Time step $dt := 0.1 \cdot sec$

$flow(d_{hole}) :=$

$V_0 \leftarrow V_{spill}$

$h_0 \leftarrow h_{init}$

$q_0 \leftarrow Q_o(d_{hole}, h_0)$

$t_0 \leftarrow 0 \cdot sec$

$i \leftarrow 0$

while $V_i > 0$

$i \leftarrow i + 1$

$t_i \leftarrow i \cdot dt$

$V_i \leftarrow V_{i-1} - \frac{q_{i-1} \cdot dt}{\rho_1}$

$V_i \leftarrow 0$ if $V_i < 0$

$h_i \leftarrow \frac{V_i}{A_{tank}}$

$q_i \leftarrow Q_o(d_{hole}, h_i)$

$M^{\langle 0 \rangle} \leftarrow \frac{t}{min}$

$M^{\langle 1 \rangle} \leftarrow \frac{q}{\frac{kg}{sec}}$

$M^{\langle 2 \rangle} \leftarrow \frac{V}{m^3}$

$$\left| M^{\langle 3 \rangle} \leftarrow \frac{h}{m} \right| \quad M$$

Hole size		Initial flow rate	Time for full release
$d_1 := 0.5 \cdot m$	$d_1 = 1.64\,ft$	$\max\left(flow\left(d_1\right)^{\langle 1 \rangle}\right) = 1325$	$\max\left(flow\left(d_1\right)^{\langle 0 \rangle}\right) = 133$
$d_2 := 1 \cdot m$	$d_2 = 3.28\,ft$	$\max\left(flow\left(d_2\right)^{\langle 1 \rangle}\right) = 5299$	$\max\left(flow\left(d_2\right)^{\langle 0 \rangle}\right) = 33$
$d_3 := 5 \cdot m$	$d_3 = 16.4\,ft$	$\max\left(flow\left(d_3\right)^{\langle 1 \rangle}\right) = 132466$	$\max\left(flow\left(d_3\right)^{\langle 0 \rangle}\right) = 1.3$

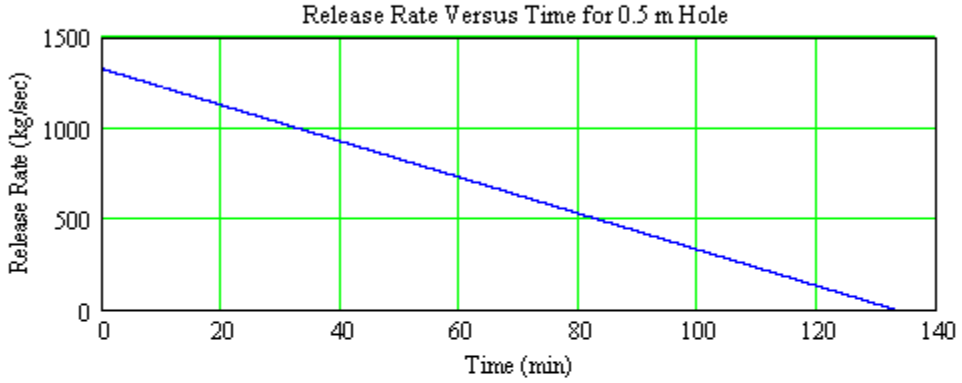

Initial flow rate:
2,900 lb/sec
(1,300 kg/sec)

Time to release
4.4×10^5 ft^3
(12,500 m^3):
130 min

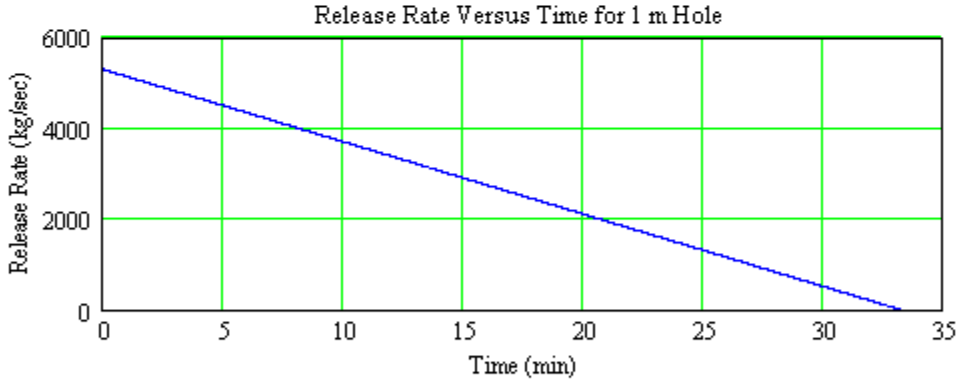

Initial flow rate:
12,000 lb/sec
(5,300 kg/sec)

Time to release
4.4×10^5 ft^3
(12,500 m^3):
33 min

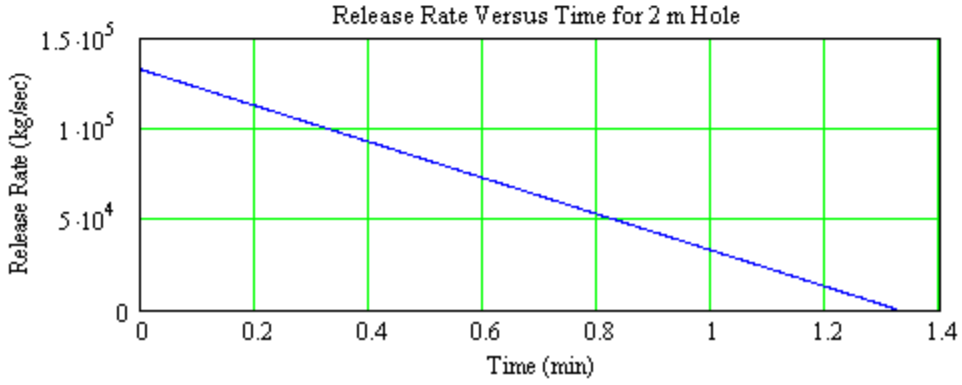

Initial flow rate:
290,000 lb/sec
(130,000 kg/sec)

Time to release
4.4×10^5 ft^3
(12,500 m^3):
1.3 min

Appendix C

Example Pool Fire Calculations

LNG Source Term and Pool Fire Calculations

- **Vessel Release and Deinventory**
- **Pool Spread and Evaporation (Webber Methodology)**
- **Pool Fire**

Scenario Definition

Spill Definition

Instantaneous pool volume	$V_{instant} := 0 \cdot m^3$	
Hole diameter	$d_{hole} := 1 \cdot m$	$d_{hole} = 3.28\,ft$
Initial liquid height above the hole	$h_{init} := 13 \cdot m$	$h_{init} = 42.7\,ft$
Volume to release through hole (i.e., volume above the hole)	$V_{spill} := 12500 \cdot m^3$	

Ambient Conditions for Pool Fire Analysis

Ambient pressure	$p_a := 101325 \cdot Pa$	$p_a = 14.7\,psi$
Ambient temperature	$T_a := (80 + 459.67) \cdot R$	$T_a = 539.67\,R$
Relative humidity	$RH := 0.7$	
Wind speed	$u_w := 20 \cdot mph$	$u_w = 8.941 \frac{m}{sec}$
Ref. height for wind speed	$Z_r := 10 \cdot m$	
Wind speed at 1.6 m (power of 0.3 for wind profile assumes urban conditions and class F stability)	$u_{w\_1.6} := u_w \cdot \left(\frac{1.6 \cdot m}{Z_r}\right)^{0.3}$	$u_{w\_1.6} = 11.5\,mph$
Molecular weight of air	$M_{air} := 28.964 \cdot \frac{kg}{kgmole}$	
Ambient air density	$\rho_a := \frac{p_a \cdot M_{air}}{R_u \cdot T_a}$	$\rho_a = 0.074 \frac{lb}{ft^3}$ $\rho_a = 1.178 \frac{kg}{m^3}$

Constants and Conversion Factors

Unit conversions	$kJ \equiv 1000 \cdot joule$	$lbmole \equiv 1$	$kgmole \equiv \frac{kg}{lb} \cdot lbmole$	$kW \equiv 1000 \cdot watt$
Universal gas constant	$R_u \equiv 1545 \cdot \frac{ft \cdot lbf}{lbmole \cdot R}$			

Material Properties

Molecular weight	$M := 16.043 \cdot \frac{kg}{kgmole}$	
Normal boiling point	$T_b := 111.66 \cdot K$	$T_b = 200.988\,R$

Vapor density (at T_b, using ideal gas law)	$\rho_v := \frac{p_a}{\frac{R_u}{M}\cdot T_b}$	$\rho_v = 1.751\,\frac{kg}{m^3}$	$\rho_v = 0.109\,\frac{lb}{ft^3}$
Vapor viscosity (at T_b)	$\mu_v := 4.362\cdot 10^{-6}\,Pa\,sec$		
Kinematic viscosity of vapor (at T_b)	$\nu_v := \frac{\mu_v}{\rho_v}$	$\nu_v = 2.491\times 10^{-6}\,\frac{m^2}{sec}$	
Density of Liquid (at T_b)	$\rho_l := 422.5\cdot\frac{kg}{m^3}$		
Liquid viscosity (at T_b)	$\mu_l := 1.168\cdot 10^{-4}\,Pa\,sec$		
Kinematic viscosity of vapor (at T_b)	$\nu_l := \frac{\mu_l}{\rho_l}$	$\nu_l = 2.764\times 10^{-7}\,\frac{m^2}{sec}$	
Heat of vaporization	$h_{fg} := 509331.9\cdot\frac{joule}{kg}$		
Surface Tension (at T_b)	$\sigma := 0.0133\,\frac{newton}{m}$		
Thermal conductivity of vapor	$\lambda_v := 0.01269\,\frac{watt}{m\cdot K}$		
Heat capacity of vapor	$C_p := 2075.56\,\frac{joule}{kg\cdot K}$		
Vapor thermal diffusivity	$\alpha_v := \frac{\lambda_v}{\rho_v\cdot C_p}$	$\alpha_v = 3.491\times 10^{-6}\,\frac{m^2}{sec}$	
Seawater density	$\rho_w := 1025\cdot\frac{kg}{m^3}$		
Water viscosity	$\mu_w := 1.021\cdot 10^{-3}\,Pa\,sec$		
Water kinematic viscosity of vapor	$\nu_w := \frac{\mu_w}{\rho_w}$	$\nu_w = 9.961\times 10^{-7}\,\frac{m^2}{sec}$	

Vessel Release and Deinventory

Hole diameter Specified above under Scenario Definition	$d_{hole} = 1\,m$	$d_{hole} = 3.28\,ft$
Total volume in the tank above the hole Specified above under Scenario Definition	$V_{spill} = 12500\,m^3$	

Initial liquid height above the hole
Specified above under Scenario Definition

$h_{init} = 13\,m$

Tank area in horizontal plane
Assuming that cross sectional area of tank (in horizontal plane) is approximately constant.

$A_{tank} := \frac{V_{spill}}{h_{init}}$ $\quad A_{tank} = 962\,m^2$

Discharge coefficient

$C_d := 1$

Function for flow through an orifice driven only by gravity

$Q_o(h) := C_d \cdot \rho_1 \cdot \pi \cdot \left(\frac{d_{hole}}{2}\right)^2 \cdot \sqrt{2g \cdot h}$

Time step

$dt := 0.1 \cdot sec$

Determine flow rate versus time, taking into account the decreasing head

$$
\begin{aligned}
flow := \;& V_0 \leftarrow V_{spill} \\
& h_0 \leftarrow h_{init} \\
& q_0 \leftarrow Q_o(h_0) \\
& t_0 \leftarrow 0 \cdot sec \\
& i \leftarrow 0 \\
& \text{while } V_i > 0 \\
& \quad i \leftarrow i + 1 \\
& \quad t_i \leftarrow i \cdot dt \\
& \quad V_i \leftarrow V_{i-1} - \frac{q_{i-1} \cdot dt}{\rho_1} \\
& \quad V_i \leftarrow 0 \text{ if } V_i < 0 \\
& \quad h_i \leftarrow \frac{V_i}{A_{tank}} \\
& \quad q_i \leftarrow Q_o(h_i) \\
& M^{\langle 0 \rangle} \leftarrow \frac{t}{sec} \\
& M^{\langle 1 \rangle} \leftarrow \frac{q}{\frac{kg}{sec}} \\
& M^{\langle 2 \rangle} \leftarrow \frac{V}{m^3} \\
& M^{\langle 3 \rangle} \leftarrow \frac{h}{m} \\
& M
\end{aligned}
$$

t q v h

flow =

	0	1	2	3
0	0	$5.299 \cdot 10^3$	$1.25 \cdot 10^4$	13
1	0.1	$5.298 \cdot 10^3$	$1.25 \cdot 10^4$	12.999
2	0.2	$5.298 \cdot 10^3$	$1.25 \cdot 10^4$	12.997
3	0.3	$5.298 \cdot 10^3$	$1.25 \cdot 10^4$	12.996
4	0.4	$5.298 \cdot 10^3$	$1.249 \cdot 10^4$	12.995
5	0.5	$5.297 \cdot 10^3$	$1.249 \cdot 10^4$	12.993
6	0.6	$5.297 \cdot 10^3$	$1.249 \cdot 10^4$	12.992
7	0.7	$5.297 \cdot 10^3$	$1.249 \cdot 10^4$	12.991
8	0.8	$5.297 \cdot 10^3$	$1.249 \cdot 10^4$	12.99
9	0.9	$5.296 \cdot 10^3$	$1.249 \cdot 10^4$	12.988
10	1	$5.296 \cdot 10^3$	$1.249 \cdot 10^4$	12.987
11	1.1	$5.296 \cdot 10^3$	$1.249 \cdot 10^4$	12.986
12	1.2	$5.295 \cdot 10^3$	$1.248 \cdot 10^4$	12.984
13	1.3	$5.295 \cdot 10^3$	$1.248 \cdot 10^4$	12.983
14	1.4	$5.295 \cdot 10^3$	$1.248 \cdot 10^4$	12.982
15	1.5	$5.295 \cdot 10^3$	$1.248 \cdot 10^4$	12.98

Plot release rate versus time

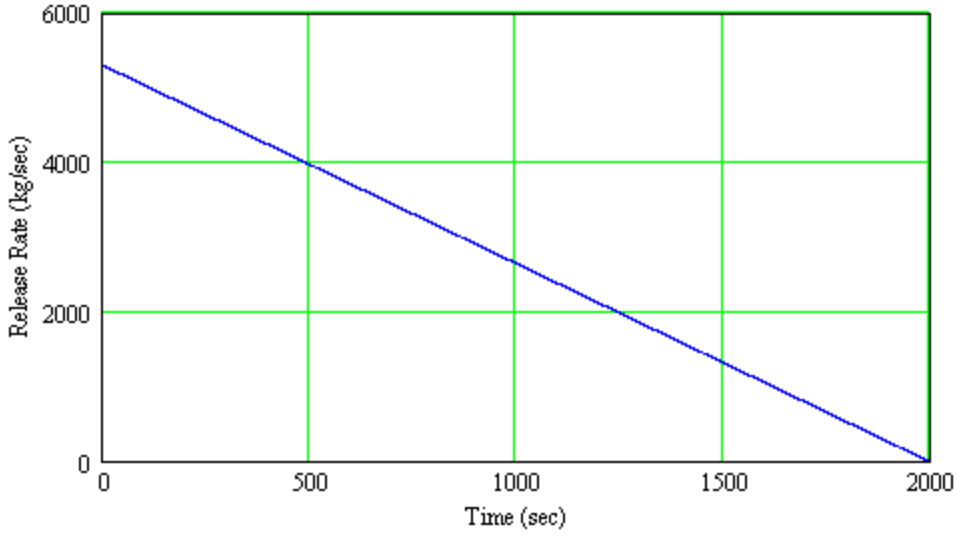

Time to release entire volume $t_{end} := \max(flow^{\langle 0 \rangle}) \cdot sec$ $t_{end} = 1993\,sec$ $t_{end} = 33.2\,min$

Function for evaporation rate as a function of time for use in pool spread calculations

$$q_S(t) := \begin{cases} 0 \cdot \frac{kg}{sec} & \text{if } t > t_{end} \\ linterp\left(flow^{\langle 0 \rangle}, flow^{\langle 1 \rangle}, \frac{t}{sec}\right) \cdot \frac{kg}{sec} & \text{otherwise} \end{cases}$$

Burning rate and surface emitted flux for an LNG pool fire on water

Burning rate
Chosen based on review of experimental data

$$m_b := 0.282 \cdot \frac{kg}{m^2 \cdot sec} \qquad m_b = 0.058 \frac{lb}{ft^2 \cdot sec}$$

Surface emitted flux
Chosen based on review of experimental data

$$E_s := 265 \cdot \frac{kW}{m^2} \qquad E_s = 84005 \frac{BTU}{ft^2 \cdot hr}$$

Heat flux to produce above burning rate

$$Q_{fire} := m_b \cdot h_{fg} \qquad Q_{fire} = 143.6 \frac{kW}{m^2} \qquad Q_{fire} = 45531 \frac{BTU}{ft^2 \cdot hr}$$

Mass burning rate as a function of pool radius

$$m_f(r) := \pi \cdot r^2 \cdot m_b$$

Spread Equations

Reduced gravitational acceleration
(TNO, 1997, Eqn. 3.34)

$$g_r := g \cdot \frac{(\rho_w - \rho_l)}{\rho_w} \qquad g_r = 5.76 \frac{m}{s^2} \qquad g_r = 18.9 \frac{ft}{s^2}$$

Minimum frontal depth based on surface tension
(TNO, 1997, Eqn. 3.48)

$$h_\sigma := \sqrt{\frac{\sigma}{g \cdot \rho_l}} \qquad h_\sigma = 0.18\,cm \qquad h_\sigma = 0.0705\,in$$

Minimum frontal depth based on viscous effects
(TNO, 1997, Eqn. 3.11)

$$h_c(q_S) := \left(\frac{6 \cdot \nu_l \cdot q_S}{\rho_l \cdot \pi \cdot g}\right)^{0.25}$$

Choose minimum depth
(TNO, 1997, Eqn. 3.49)

$$h_{0max}(q) := \max(h_\sigma, h_c(q))$$

Pool shape factor

$$s(u,h,h_{0max}) := \begin{cases} 1 & \text{if } h < 0.01 \cdot m \\ \text{otherwise} & \\ \quad Fr \leftarrow 1.078 & \\ \quad N \leftarrow \dfrac{u^2}{2 \cdot Fr^2 \cdot g_r \cdot h} & \text{if } u > 0 \\ \quad N \leftarrow 0 & \text{otherwise} \\ \quad s \leftarrow N + \sqrt{N^2 + \left(\dfrac{h_{0max}}{h}\right)^2} & \\ \quad s & \end{cases}$$

Gravity term coefficient
(TNO, 1997, Eqn. 3.63)

$$\Phi(s) := (1 - s) \cdot (s \le 2) + \left(\frac{-s^2}{4}\right)(s > 2)$$

TNO, 1997, Eqn. 3.46

$$j(s) := 1 \cdot (s \ge 2) + \frac{2}{s} \cdot (s < 2)$$

Resistance for laminar flow (TNO, 1997, Eqns. 3.64, 3.65b, 3.66, 3.68W, and 3.69)

$$ff(u,h,s,r) := \begin{cases} 1 & \text{if } r = 0\cdot m \\ \text{otherwise} & \\ \quad \begin{cases} 1 & \text{if } h < 0.001\cdot m \\ \text{otherwise} & \\ \quad \begin{cases} 1 & \text{if } u < 0.000001\cdot \frac{m}{sec} \\ \text{otherwise} & \\ \quad \begin{cases} f \leftarrow 0.2 \\ \text{root}\left(\frac{\mu_1}{\mu_w}\cdot\sqrt{\frac{u\cdot h^2}{\nu_w\cdot r}}\cdot\frac{1}{j(s)}\cdot f^{\frac{3}{2}} - 1 + f, f\right) \end{cases} \end{cases} \end{cases}$$

$$C_{FL}(u,h,s,r) := \begin{cases} 0\cdot\frac{m}{sec^2} & \text{if } h \le 0 \\ 2.35\cdot j(s)\cdot 0.66\cdot \nu_l\cdot\frac{u}{h^2}\cdot(1 - ff(u,h,s,r)) & \text{otherwise} \end{cases}$$

Resistance for turbulent flow (TNO, 1997, Eqns. 3.70 and 3.71)

$$C_{FT}(u,h,s) := \begin{cases} 0\cdot\frac{m}{sec^2} & \text{if } h \le 0 \\ \frac{4.49\cdot j(s)\cdot 0.0015\cdot u^2}{h} & \text{otherwise} \end{cases}$$

Resistance term (TNO, 1997, Eqn. 3.72)

$$C_F(u,C_{FT},C_{FL}) := \text{sign}(u)\cdot\max(C_{FT},C_{FL})$$

Acceleration of the leading edge of the pool (TNO, 1997, Eqn. 3.62)

$$a(\Phi,h,r,C_F) := \frac{4\cdot\Phi\cdot g_r\cdot h}{r} - C_F$$

Acceleration as a function of current speed, radius, height, and mass addition rate

$$acc(u,r,h,q) := \begin{cases} h_{0max} \leftarrow h_{0max}(q) \\ s \leftarrow s(u,h,h_{0max}) \\ \Phi \leftarrow \Phi(s) \\ C_{FT} \leftarrow C_{FT}(u,h,s) \\ C_{FL} \leftarrow C_{FL}(u,h,s,r) \\ C_F \leftarrow C_F(u,C_{FT},C_{FL}) \\ a(\Phi,h,r,C_F) \end{cases}$$

Spill Definition for Pool Calculations

Initial pool volume Specified above under Scenario Definition	$V_I := V_{instant}$	$V_I = 0\,m^3$
Spill rate as a function of time	Defined above under Vessel Release and Deinventory	
Time step	$dt := 0.1 \cdot sec$	

Pool Spread and Evaporation Algorithm

$pool :=$

$t_0 \leftarrow 0 \cdot sec$

$V_0 \leftarrow V_I$

$r_0 \leftarrow \left(V_0\right)^{\frac{1}{3}}$

$h_0 \leftarrow \frac{V_0}{\pi \cdot \left(r_0\right)^2}$

$u_0 \leftarrow 0 \cdot \frac{m}{sec}$

$q_0 \leftarrow q_S(0 \cdot sec)$

$a_0 \leftarrow acc\left(u_0, r_0, h_0, q_0\right)$

$e_0 \leftarrow m_f\left(r_0\right)$

$V_{add_0} \leftarrow \frac{q_0 \cdot dt}{\rho_1}$

$V_{evap_0} \leftarrow \frac{e_0 \cdot dt}{\rho_1}$

$SourceMatched \leftarrow 0$

$i \leftarrow 0$

while $(i < 1) \vee \left(V_i > 0 \cdot m^3\right)$

- $i \leftarrow i + 1$
- $t_i \leftarrow i \cdot dt$
- $V_i \leftarrow V_{i-1} + V_{add_{i-1}} - V_{evap_{i-1}}$
- $V_i \leftarrow 0 \cdot m^3$ if $V_i < 0$
- if $SourceMatched = 1$
  - $r_i \leftarrow r_{i-1}$

$$h_i \leftarrow \frac{V_i}{\pi \cdot (r_i)^2}$$

$$q_i \leftarrow q_S(i \cdot dt)$$

$$h_{min} \leftarrow h_{0max}(q_i)$$

if $h_i < h_{min}$ if $q_i > 0$

$$h_i \leftarrow h_{min}$$

$$r_i \leftarrow \sqrt{\frac{V_i}{\pi \cdot h_i}}$$

$$e_i \leftarrow m_F(r_i)$$

$$V_{add_i} \leftarrow \frac{q_i \cdot dt}{\rho_1}$$

$$V_{evap_i} \leftarrow \frac{e_i \cdot dt}{\rho_1}$$

if $\left(V_i + V_{add_i} - V_{evap_i}\right) \le 0 \cdot m^3$ if $q_i > 0 \cdot \frac{kg}{sec}$

$$r_i \leftarrow \sqrt{\frac{q_i \cdot h_{fg}}{\pi \cdot Q_{fire}}}$$

$$h_i \leftarrow \frac{V_i}{\pi \cdot (r_i)^2}$$

$$e_i \leftarrow q_i$$

$$V_{evap_i} \leftarrow V_{add_i}$$

otherwise

$$r_i \leftarrow r_{i-1} + u_{i-1} \cdot dt$$

$$r_i \leftarrow (V_i)^{\frac{1}{3}} \text{ if } r_i = 0 \cdot m$$

$$h_i \leftarrow \frac{V_i}{\pi \cdot (r_i)^2}$$

$$u_i \leftarrow u_{i-1} + a_{i-1} \cdot dt$$

$$q_i \leftarrow q_S(i \cdot dt)$$

$$e_i \leftarrow m_F(r_i)$$

$$a_i \leftarrow \mathrm{acc}(u_i, r_i, h_i, q_i)$$

if $\left[\left(q_i > 0 \cdot \frac{kg}{sec}\right) \wedge \left(q_i \le e_i\right)\right]$

$$\mathrm{SourceMatched} \leftarrow 1$$

$$r_i \leftarrow \sqrt{\frac{q_i \cdot h_{fg}}{\pi \cdot Q_{fire}}}$$

$$h_i \leftarrow \frac{V_i}{\pi \cdot (r_i)^2}$$

$$e_i \leftarrow q_i$$

$$u_i \leftarrow 0 \cdot \frac{m}{sec}$$

$$a_i \leftarrow 0 \cdot \frac{m}{sec^2}$$

$$V_{add_i} \leftarrow \frac{q_i \cdot dt}{\rho_1}$$

$$V_{evap_i} \leftarrow \frac{e_i \cdot dt}{\rho_1}$$

$$M^{\langle 0 \rangle} \leftarrow \frac{t}{sec}$$

$$M^{\langle 1 \rangle} \leftarrow \frac{V}{m^3}$$

$$M^{\langle 2 \rangle} \leftarrow \frac{r}{m}$$

$$M^{\langle 3 \rangle} \leftarrow \frac{h}{m}$$

$$M^{\langle 4 \rangle} \leftarrow \frac{q}{\frac{kg}{sec}}$$

$$M^{\langle 5 \rangle} \leftarrow \frac{e}{\frac{kg}{sec}}$$

M

Pool Spread and Evaporation Results

Time for complete evaporation $t_{total} := \max(pool^{\langle 0 \rangle}) \cdot sec$ $t_{total} = 1999\,sec$ $t_{total} = 33.3\,min$

Maximum pool radius $r_{max} := \max(pool^{\langle 2 \rangle}) \cdot m$ $r_{max} = 74\,m$ $r_{max} = 241\,ft$

pool =

	t	V	r	h	q	e
	0	1	2	3	4	5
0	0	0	0	0	$5.299 \cdot 10^3$	0
1	0.1	1.254	1.078	0.343	$5.298 \cdot 10^3$	1.03
2	0.2	2.508	1.078	0.686	$5.298 \cdot 10^3$	1.03
3	0.3	3.762	1.146	0.912	$5.298 \cdot 10^3$	1.163
4	0.4	5.015	1.342	0.886	$5.298 \cdot 10^3$	1.596
5	0.5	6.269	1.605	0.774	$5.297 \cdot 10^3$	2.283
6	0.6	7.522	1.842	0.706	$5.297 \cdot 10^3$	3.006
7	0.7	8.775	2.069	0.653	$5.297 \cdot 10^3$	3.791
8	0.8	10.028	2.287	0.61	$5.297 \cdot 10^3$	4.633
9	0.9	11.28	2.497	0.576	$5.296 \cdot 10^3$	5.525
10	1	12.533	2.702	0.547	$5.296 \cdot 10^3$	6.467
11	1.1	13.785	2.901	0.521	$5.296 \cdot 10^3$	7.454
12	1.2	15.036	3.095	0.5	$5.295 \cdot 10^3$	8.485
13	1.3	16.288	3.285	0.481	$5.295 \cdot 10^3$	9.558
14	1.4	17.539	3.471	0.463	$5.295 \cdot 10^3$	10.671

Plot evaporation rate versus time

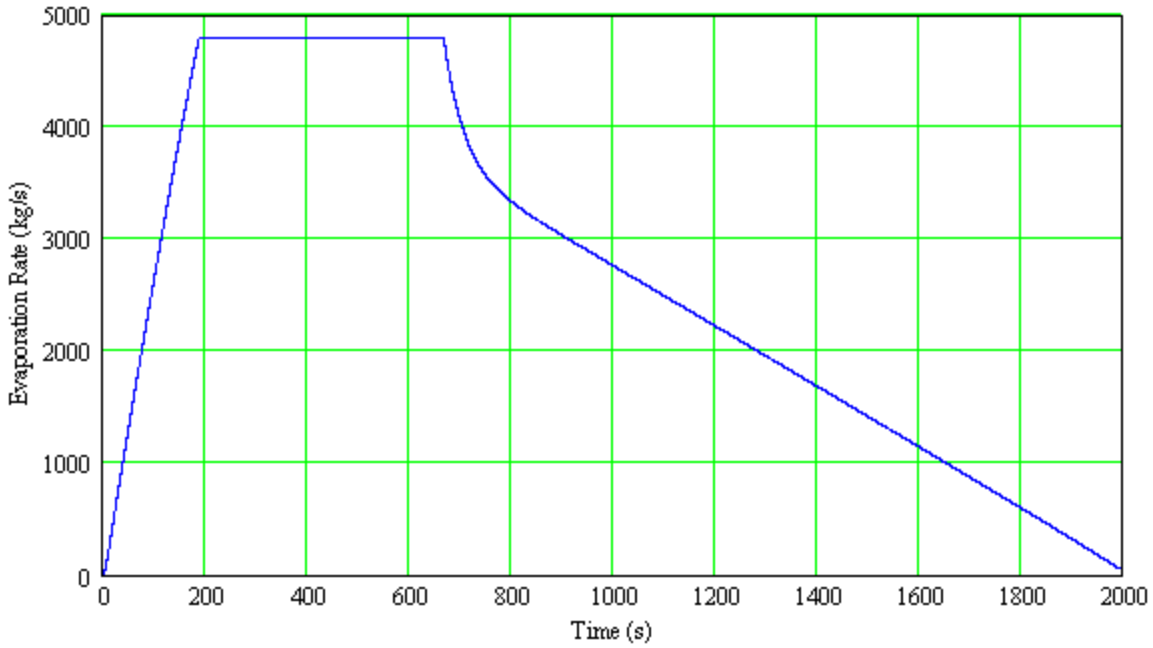

Plot pool radius versus time

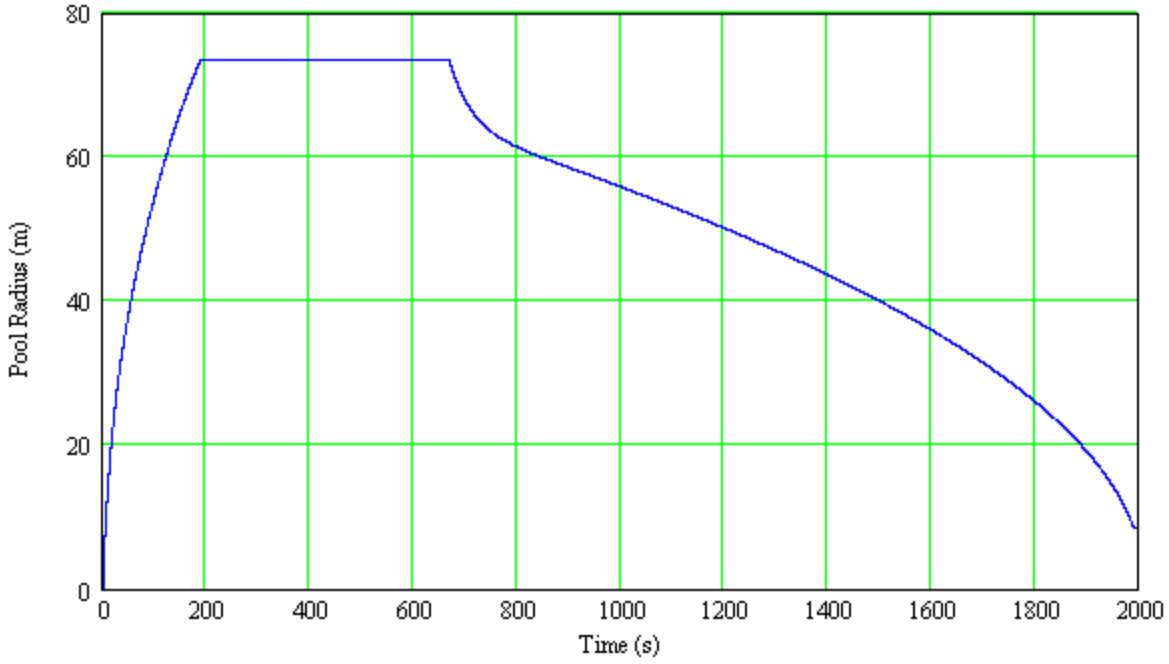

Pool Fire

Functions for pool radius and diameter from spread results

$$r(t) := \text{linterp}\left(\text{pool}^{\langle 0\rangle}, \text{pool}^{\langle 2\rangle}, \frac{t}{\text{sec}}\right)\cdot m \qquad d(t) := 2\cdot r(t)$$

Flame Length

Nondimensional wind velocity
(NFPA, 1995, Sec. 3, Ch.11, Eqn. 15)

$$u_s(t) := \frac{u_{w\_1.6}}{\left(\frac{g\cdot m_b\cdot d(t)}{\rho_v}\right)^{\frac{1}{3}}}$$

Flame length
(NFPA, 1995, Sec. 3, Ch.11, Eqn. 14)

$$a(t) := 55\cdot d(t)\cdot\left(\frac{m_b}{\rho_a\cdot\sqrt{g\cdot d(t)}}\right)^{0.67}\cdot\left(u_s(t)\right)^{-0.21}$$

Flame Tilt

Tilt angle from vertical
(Rew, 1996, Eqn. 2.18)

$$\theta(t) := \text{root}\left[\frac{\tan(\theta)}{\cos(\theta)} - 3.13\cdot\left(\frac{u_w^{\,2}}{g\cdot d(t)}\right)^{0.431}, \theta, 0\text{deg}, 45\text{deg}\right]\cdot\text{rad}$$

Flame Drag

Extension of base of the flame downwind. This function gives ratio of extended diameter to base diameter
(NFPA, 1995, Sec. 3, Ch.11, Eqn. 22)

$$D(t) := 1.25\cdot\left(\frac{u_w^{\,2}}{g\cdot d(t)}\right)^{0.069}\cdot\left(\frac{\rho_v}{\rho_a}\right)^{0.48}$$

Atmospheric Transmissivity

Define function for saturation pressure of water
(AICHE, 2000, Eqn. 2.2.43, p. 209)

$$P_{v\_water}(T_a) := \left[1013.25 \cdot (RH) \cdot \exp\left(14.4114 - \frac{5328}{\frac{T_a}{K}}\right)\right] \cdot Pa$$

Define function for atmospheric transmissivity
(AICHE, 2000, Eqn. 2.2.42, p. 209)

$$\tau_0(x) := 2.02 \cdot \left[RH \cdot P_{v\_water}(T_a) \cdot Pa^{-1} \cdot (x) \cdot m^{-1}\right]^{-0.09}$$

For short distances, the correlation may calculate a transmissivity > 1

$$\tau(x) := \tau_0(x) \cdot \left(\tau_0(x) \le 1.0\right) + 1.0 \cdot \left(\tau_0(x) > 1.0\right)$$

Cylindrical Flame Model Geometric View Factors

Geometric view factor for a cylindrical flam
(NFPA, 1995, Se
3, Ch.11)

$$F(x_r, t) :=$$

$$X \leftarrow \frac{a(t)}{r(t)}$$

$$Y \leftarrow \frac{x_r - r(t) \cdot (D(t) - 1)}{r(t)}$$

$$\theta \leftarrow \theta(t)$$

$$A \leftarrow (X)^2 + (Y + 1)^2 - 2 \cdot X \cdot (Y + 1) \cdot \sin(\theta)$$

$$B \leftarrow (X)^2 + (Y - 1)^2 - 2 \cdot X \cdot (Y - 1) \cdot \sin(\theta)$$

$$C \leftarrow 1 + \left(Y^2 - 1\right) \cdot \cos(\theta)^2$$

$$V_1 \leftarrow \frac{X \cdot \cos(\theta)}{Y - X \cdot \sin(\theta)} \cdot \left[\frac{(X)^2 + (Y + 1)^2 - 2 \cdot Y \cdot (1 + X \cdot \sin(\theta))}{\pi \cdot \sqrt{A \cdot B}}\right] \cdot \operatorname{atan}\left[\sqrt{\frac{A \cdot (Y - 1)}{B \cdot (Y + 1)}}\right]$$

$$V_2 \leftarrow \frac{\cos(\theta)}{\pi \cdot \sqrt{C}} \cdot \left[\operatorname{atan}\left[\frac{X \cdot Y - \left(Y^2 - 1\right) \cdot \sin(\theta)}{\sqrt{Y^2 - 1} \cdot \sqrt{C}}\right] + \operatorname{atan}\left(\frac{\sqrt{Y^2 - 1} \cdot \sin(\theta)}{\sqrt{C}}\right)\right]$$

$$V_3 \leftarrow \frac{-X \cdot \cos(\theta)}{\pi \cdot (Y - X \cdot \sin(\theta))} \cdot \operatorname{atan}\left(\sqrt{\frac{Y - 1}{Y + 1}}\right)$$

$$F_v \leftarrow V_1 + V_2 + V_3$$

$$H_1 \leftarrow \frac{1}{\pi} \cdot \operatorname{atan}\left(\sqrt{\frac{Y + 1}{Y - 1}}\right)$$

$$H_2 \leftarrow -\left[\frac{(X)^2 + (Y + 1)^2 - 2 \cdot (Y + 1 + X \cdot Y \cdot \sin(\theta))}{\pi \cdot \sqrt{A \cdot B}}\right] \cdot \operatorname{atan}\left[\sqrt{\frac{A \cdot (Y - 1)}{B \cdot (Y + 1)}}\right]$$

$$H_3 \leftarrow \frac{\sin(\theta)}{\pi \cdot \sqrt{C}} \cdot \left[\operatorname{atan}\left[\frac{X \cdot Y - \left(Y^2 - 1\right) \cdot \sin(\theta)}{\sqrt{Y^2 - 1} \cdot \sqrt{C}}\right] + \operatorname{atan}\left(\frac{\sqrt{Y^2 - 1} \cdot \sin(\theta)}{\sqrt{C}}\right)\right]$$

$$F_h \leftarrow H_1 + H_2 + H_3$$

$$\sqrt{F_v^2 + F_h^2}$$

Calculate Thermal Flux Downwind

Function for thermal flux $I_{th}(x_r,t) := \tau(x_r - D(t)\cdot r(t))\cdot F(x_r,t)\cdot E_s$

Calculate flux at a series of points using the maximum pool radius

Look up time for maximum radius $t_{rmax} := \frac{t_{total}}{3}$ (initial guess) $t_{rmax} := root(r_{max} - r(t_{rmax}), t_{rmax})$

Calculate flux at a series of points $i \equiv 0..50$ $x_i := [(i+1)\cdot 200\cdot m] + 10\cdot m$ $I_i := I_{th}(x_i, t_{rmax})$

Plot incident flux versus distance for maximum pool radius

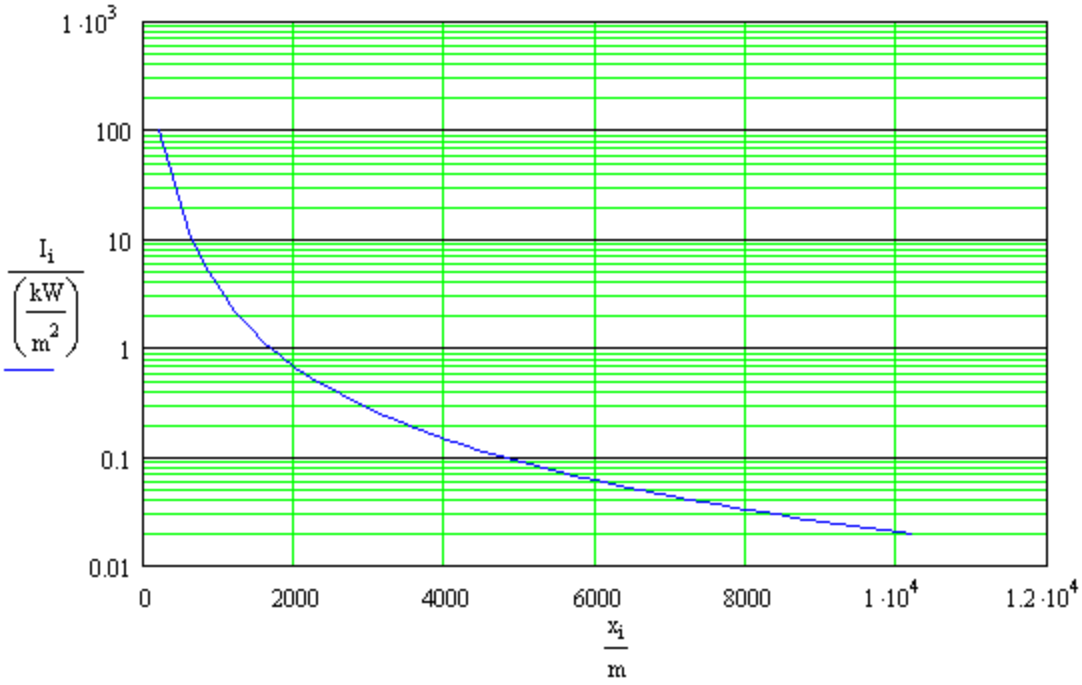

Maximum flame length $a(t_{rmax}) = 282\,m$ $a(t_{rmax}) = 924\,ft$

Tilt angle at time of maximum length $\theta(t_{rmax}) = 36.03\,deg$

Flame drag at time of maximum length (ratio of extended diameter to base diameter) $D(t_{rmax}) = 1.24$

Plot incident flux versus time at 300, 500, and 1000 m $t_i := (i + 1) \cdot \frac{t_{total}}{51}$

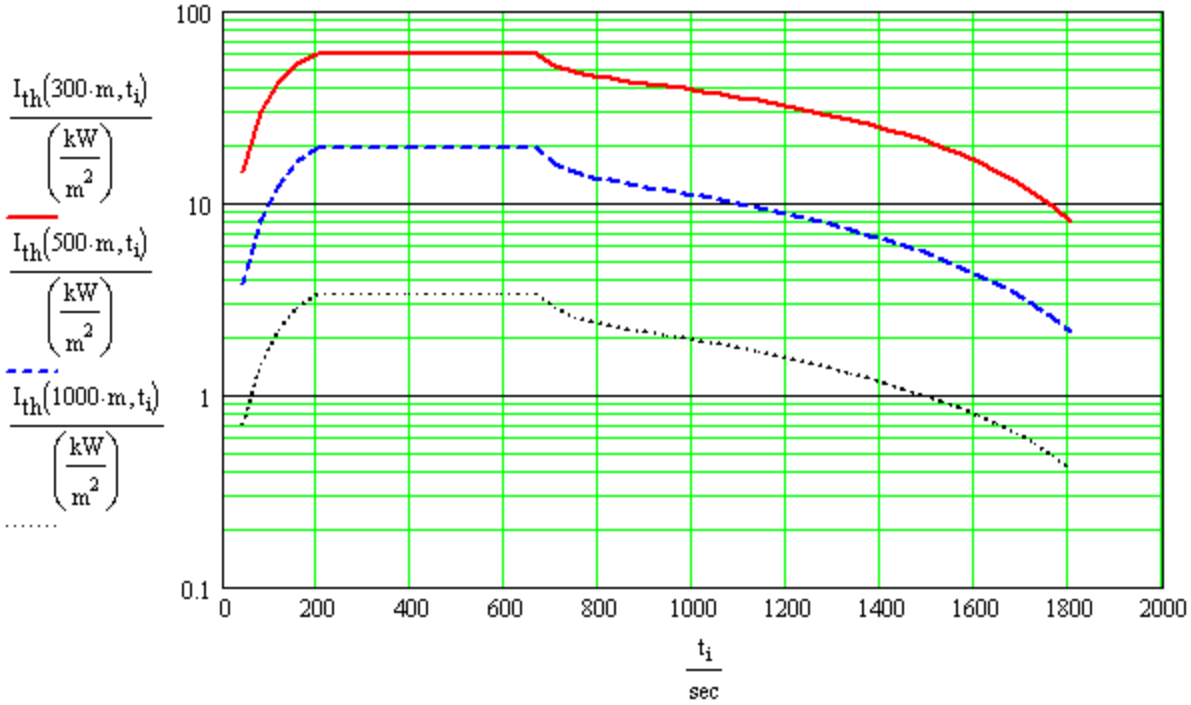

Determine the ground-level distances to the thermal flux level(s) of concern using maximum radius

$x_r := 200 \cdot m$ (initial guess) $R_{loc}(I_{loc}) := root(I_{loc} - I_{th}(x_r, t_{rmax}), x_r)$

Distances to the thermal flux levels of concern

	38 kW/m²	**25 kW/m²**	**12 kW/m²**	**5 kW/m²**
LOC defined	$I_{loc1} := 38 \cdot \frac{kW}{m^2}$	$I_{loc2} := 25 \cdot \frac{kW}{m^2}$	$I_{loc3} := 12 \cdot \frac{kW}{m^2}$	$I_{loc4} := 5 \cdot \frac{kW}{m^2}$
	$I_{loc1} = 12046 \frac{BTU}{hr \cdot ft^2}$	$I_{loc2} = 7925 \frac{BTU}{hr \cdot ft^2}$	$I_{loc3} = 3804 \frac{BTU}{hr \cdot ft^2}$	$I_{loc4} = 1585 \frac{BTU}{hr \cdot ft^2}$
Calculate distance	$R_{loc1} := R_{loc}(I_{loc1})$	$R_{loc2} := R_{loc}(I_{loc2})$	$R_{loc3} := R_{loc}(I_{loc3})$	$R_{loc4} := R_{loc}(I_{loc4})$
	$R_{loc1} = 375\,m$	$R_{loc2} = 450\,m$	$R_{loc3} = 604\,m$	$R_{loc4} = 855\,m$
	$R_{loc1} = 1230\,ft$	$R_{loc2} = 1476\,ft$	$R_{loc3} = 1982\,ft$	$R_{loc4} = 2804\,ft$
	$R_{loc1} = 0.23\,mi$	$R_{loc2} = 0.28\,mi$	$R_{loc3} = 0.38\,mi$	$R_{loc4} = 0.53\,mi$

LNG Source Term and Pool Fire Calculations

- **Vessel Release and Deinventory**
- **Pool Spread and Evaporation (Webber Methodology)**
- **Pool Fire**

Scenario Definition

Spill Definition

Instantaneous pool volume	$V_{instant} := 0 \cdot m^3$	
Hole diameter	$d_{hole} := 5 \cdot m$	$d_{hole} = 16.4\,ft$
Initial liquid height above the hole	$h_{init} := 13 \cdot m$	$h_{init} = 42.7\,ft$
Volume to release through hole (i.e., volume above the hole)	$V_{spill} := 12500 \cdot m^3$	

Ambient Conditions for Pool Fire Analysis

Ambient pressure	$p_a := 101325 \cdot Pa$	$p_a = 14.7\,psi$
Ambient temperature	$T_a := (80 + 459.67) \cdot R$	$T_a = 539.67\,R$
Relative humidity	$RH := 0.7$	
Wind speed	$u_w := 20 \cdot mph$	$u_w = 8.941 \frac{m}{sec}$
Ref. height for wind speed	$Z_r := 10 \cdot m$	
Wind speed at 1.6 m (power of 0.3 for wind profile assumes urban conditions and class F stability)	$u_{w\_1.6} := u_w \cdot \left(\frac{1.6 \cdot m}{Z_r}\right)^{0.3}$	$u_{w\_1.6} = 11.5\,mph$
Molecular weight of air	$M_{air} := 28.964 \cdot \frac{kg}{kgmole}$	
Ambient air density	$\rho_a := \frac{p_a \cdot M_{air}}{R_u \cdot T_a}$	$\rho_a = 0.074 \frac{lb}{ft^3}$ $\rho_a = 1.178 \frac{kg}{m^3}$

Constants and Conversion Factors

Unit conversions	$kJ \equiv 1000 \cdot joule$	$lbmole \equiv 1$	$kgmole \equiv \frac{kg}{lb} \cdot lbmole$	$kW \equiv 1000 \cdot watt$
Universal gas constant	$R_u \equiv 1545 \cdot \frac{ft \cdot lbf}{lbmole \cdot R}$			

Material Properties

Molecular weight	$M := 16.043 \cdot \frac{kg}{kgmole}$	
Normal boiling point	$T_b := 111.66 \cdot K$	$T_b = 200.988\,R$

Vapor density (at T_b, using ideal gas law)	$\rho_v := \frac{p_a}{\frac{R_u}{M}\cdot T_b}$	$\rho_v = 1.751\,\frac{kg}{m^3}$	$\rho_v = 0.109\,\frac{lb}{ft^3}$
Vapor viscosity (at T_b)	$\mu_v := 4.362\cdot 10^{-6}\,Pa\,sec$		
Kinematic viscosity of vapor (at T_b)	$\nu_v := \frac{\mu_v}{\rho_v}$	$\nu_v = 2.491\times 10^{-6}\,\frac{m^2}{sec}$	
Density of Liquid (at T_b)	$\rho_l := 422.5\cdot\frac{kg}{m^3}$		
Liquid viscosity (at T_b)	$\mu_l := 1.168\cdot 10^{-4}\,Pa\,sec$		
Kinematic viscosity of vapor (at T_b)	$\nu_l := \frac{\mu_l}{\rho_l}$	$\nu_l = 2.764\times 10^{-7}\,\frac{m^2}{sec}$	
Heat of vaporization	$h_{fg} := 509331.9\cdot\frac{joule}{kg}$		
Surface Tension (at T_b)	$\sigma := 0.0133\,\frac{newton}{m}$		
Thermal conductivity of vapor	$\lambda_v := 0.01269\,\frac{watt}{m\cdot K}$		
Heat capacity of vapor	$C_p := 2075.56\,\frac{joule}{kg\cdot K}$		
Vapor thermal diffusivity	$\alpha_v := \frac{\lambda_v}{\rho_v\cdot C_p}$	$\alpha_v = 3.491\times 10^{-6}\,\frac{m^2}{sec}$	
Seawater density	$\rho_w := 1025\cdot\frac{kg}{m^3}$		
Water viscosity	$\mu_w := 1.021\cdot 10^{-3}\,Pa\,sec$		
Water kinematic viscosity of vapor	$\nu_w := \frac{\mu_w}{\rho_w}$	$\nu_w = 9.961\times 10^{-7}\,\frac{m^2}{sec}$	

Vessel Release and Deinventory

Hole diameter Specified above under Scenario Definition	$d_{hole} = 5\,m$	$d_{hole} = 16.4\,ft$
Total volume in the tank above the hole Specified above under Scenario Definition	$V_{spill} = 12500\,m^3$	

Initial liquid height above the hole
Specified above under Scenario Definition

$h_{init} = 13\,m$

Tank area in horizontal plane
Assuming that cross sectional area of tank (in horizontal plane) is approximately constant.

$A_{tank} := \frac{V_{spill}}{h_{init}}$ $\quad A_{tank} = 962\,m^2$

Discharge coefficient

$C_d := 1$

Function for flow through an orifice driven only by gravity

$Q_o(h) := C_d \cdot \rho_1 \cdot \pi \cdot \left(\frac{d_{hole}}{2}\right)^2 \cdot \sqrt{2g \cdot h}$

Time step

$dt := 0.1 \cdot sec$

Determine flow rate versus time, taking into account the decreasing head

$$
\begin{aligned}
flow := \;& V_0 \leftarrow V_{spill} \\
& h_0 \leftarrow h_{init} \\
& q_0 \leftarrow Q_o(h_0) \\
& t_0 \leftarrow 0 \cdot sec \\
& i \leftarrow 0 \\
& \text{while } V_i > 0 \\
& \quad i \leftarrow i + 1 \\
& \quad t_i \leftarrow i \cdot dt \\
& \quad V_i \leftarrow V_{i-1} - \frac{q_{i-1} \cdot dt}{\rho_1} \\
& \quad V_i \leftarrow 0 \text{ if } V_i < 0 \\
& \quad h_i \leftarrow \frac{V_i}{A_{tank}} \\
& \quad q_i \leftarrow Q_o(h_i) \\
& M^{\langle 0 \rangle} \leftarrow \frac{t}{sec} \\
& M^{\langle 1 \rangle} \leftarrow \frac{q}{\frac{kg}{sec}} \\
& M^{\langle 2 \rangle} \leftarrow \frac{V}{m^3} \\
& M^{\langle 3 \rangle} \leftarrow \frac{h}{m} \\
& M
\end{aligned}
$$

flow =

	t	q	v	h
0	0	$1.325 \cdot 10^5$	$1.25 \cdot 10^4$	13
1	0.1	$1.323 \cdot 10^5$	$1.247 \cdot 10^4$	12.967
2	0.2	$1.321 \cdot 10^5$	$1.244 \cdot 10^4$	12.935
3	0.3	$1.32 \cdot 10^5$	$1.241 \cdot 10^4$	12.902
4	0.4	$1.318 \cdot 10^5$	$1.237 \cdot 10^4$	12.87
5	0.5	$1.316 \cdot 10^5$	$1.234 \cdot 10^4$	12.837
6	0.6	$1.315 \cdot 10^5$	$1.231 \cdot 10^4$	12.805
7	0.7	$1.313 \cdot 10^5$	$1.228 \cdot 10^4$	12.773
8	0.8	$1.311 \cdot 10^5$	$1.225 \cdot 10^4$	12.74
9	0.9	$1.31 \cdot 10^5$	$1.222 \cdot 10^4$	12.708
10	1	$1.308 \cdot 10^5$	$1.219 \cdot 10^4$	12.676
11	1.1	$1.306 \cdot 10^5$	$1.216 \cdot 10^4$	12.644
12	1.2	$1.305 \cdot 10^5$	$1.213 \cdot 10^4$	12.611
13	1.3	$1.303 \cdot 10^5$	$1.21 \cdot 10^4$	12.579
14	1.4	$1.301 \cdot 10^5$	$1.206 \cdot 10^4$	12.547
15	1.5	$1.3 \cdot 10^5$	$1.203 \cdot 10^4$	12.515

Plot release rate versus time

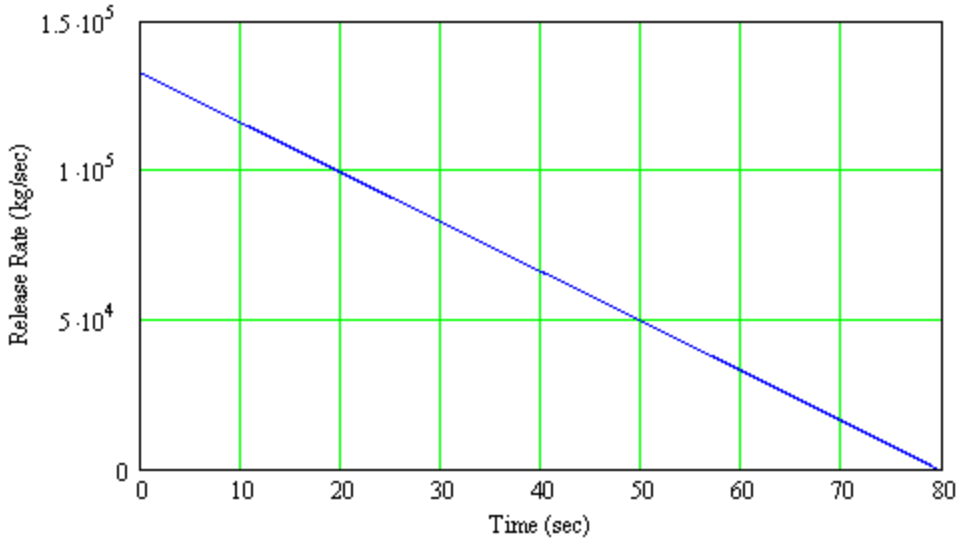

Time to release entire volume $t_{end} := \max(flow^{\langle 0 \rangle}) \cdot sec$ $t_{end} = 79\,sec$ $t_{end} = 1.3\,min$

Function for evaporation rate as a function of time for use in pool spread calculations

$$q_S(t) := \begin{cases} 0 \cdot \frac{kg}{sec} & \text{if } t > t_{end} \\ linterp\left(flow^{\langle 0 \rangle}, flow^{\langle 1 \rangle}, \frac{t}{sec}\right) \cdot \frac{kg}{sec} & \text{otherwise} \end{cases}$$

Burning rate and surface emitted flux for an LNG pool fire on water

Burning rate
Chosen based on review of experimental data

$$m_b := 0.282 \cdot \frac{kg}{m^2 \cdot sec} \qquad m_b = 0.058 \frac{lb}{ft^2 \cdot sec}$$

Surface emitted flux
Chosen based on review of experimental data

$$E_s := 265 \cdot \frac{kW}{m^2} \qquad E_s = 84005 \frac{BTU}{ft^2 \cdot hr}$$

Heat flux to produce above burning rate

$$Q_{fire} := m_b \cdot h_{fg} \qquad Q_{fire} = 143.6 \frac{kW}{m^2} \qquad Q_{fire} = 45531 \frac{BTU}{ft^2 \cdot hr}$$

Mass burning rate as a function of pool radius

$$m_f(r) := \pi \cdot r^2 \cdot m_b$$

Spread Equations

Reduced gravitational acceleration
(TNO, 1997, Eqn. 3.34)

$$g_r := g \cdot \frac{(\rho_w - \rho_l)}{\rho_w} \qquad g_r = 5.76 \frac{m}{s^2} \qquad g_r = 18.9 \frac{ft}{s^2}$$

Minimum frontal depth based on surface tension
(TNO, 1997, Eqn. 3.48)

$$h_\sigma := \sqrt{\frac{\sigma}{g \cdot \rho_l}} \qquad h_\sigma = 0.18\,cm \qquad h_\sigma = 0.0705\,in$$

Minimum frontal depth based on viscous effects
(TNO, 1997, Eqn. 3.11)

$$h_c(q_S) := \left(\frac{6 \cdot \nu_l \cdot q_S}{\rho_l \cdot \pi \cdot g}\right)^{0.25}$$

Choose minimum depth
(TNO, 1997, Eqn. 3.49)

$$h_{0max}(q) := \max(h_\sigma, h_c(q))$$

Pool shape factor

$$s(u,h,h_{0max}) := \begin{cases} 1 & \text{if } h < 0.01 \cdot m \\ \text{otherwise} & \\ \quad Fr \leftarrow 1.078 & \\ \quad N \leftarrow \dfrac{u^2}{2 \cdot Fr^2 \cdot g_r \cdot h} & \text{if } u > 0 \\ \quad N \leftarrow 0 & \text{otherwise} \\ \quad s \leftarrow N + \sqrt{N^2 + \left(\dfrac{h_{0max}}{h}\right)^2} & \\ \quad s & \end{cases}$$

Gravity term coefficient
(TNO, 1997, Eqn. 3.63)

$$\Phi(s) := (1 - s) \cdot (s \le 2) + \left(\frac{-s^2}{4}\right)(s > 2)$$

TNO, 1997, Eqn. 3.46

$$j(s) := 1 \cdot (s \ge 2) + \frac{2}{s} \cdot (s < 2)$$

Resistance for laminar flow (TNO, 1997, Eqns. 3.64, 3.65b, 3.66, 3.68W, and 3.69)

$$ff(u,h,s,r) := \begin{cases} 1 & \text{if } r = 0\cdot m \\ \text{otherwise} & \\ \quad \begin{cases} 1 & \text{if } h < 0.001\cdot m \\ \text{otherwise} & \\ \quad \begin{cases} 1 & \text{if } u < 0.000001\cdot \frac{m}{sec} \\ \text{otherwise} & \\ \quad f \leftarrow 0.2 \\ \quad \text{root}\left(\frac{\mu_1}{\mu_w}\cdot\sqrt{\frac{u\cdot h^2}{\nu_w\cdot r}}\cdot\frac{1}{j(s)}\cdot f^{\frac{3}{2}} - 1 + f, f\right) \end{cases} \end{cases} \end{cases}$$

$$C_{FL}(u,h,s,r) := \begin{cases} 0\cdot\frac{m}{sec^2} & \text{if } h \le 0 \\ 2.35\cdot j(s)\cdot 0.66\cdot \nu_l\cdot\frac{u}{h^2}\cdot(1 - ff(u,h,s,r)) & \text{otherwise} \end{cases}$$

Resistance for turbulent flow (TNO, 1997, Eqns. 3.70 and 3.71)

$$C_{FT}(u,h,s) := \begin{cases} 0\cdot\frac{m}{sec^2} & \text{if } h \le 0 \\ \frac{4.49\cdot j(s)\cdot 0.0015\cdot u^2}{h} & \text{otherwise} \end{cases}$$

Resistance term (TNO, 1997, Eqn. 3.72)

$$C_F(u,C_{FT},C_{FL}) := \text{sign}(u)\cdot\max(C_{FT},C_{FL})$$

Acceleration of the leading edge of the pool (TNO, 1997, Eqn. 3.62)

$$a(\Phi,h,r,C_F) := \frac{4\cdot\Phi\cdot g_r\cdot h}{r} - C_F$$

Acceleration as a function of current speed, radius, height, and mass addition rate

$$acc(u,r,h,q) := \begin{cases} h_{0max} \leftarrow h_{0max}(q) \\ s \leftarrow s(u,h,h_{0max}) \\ \Phi \leftarrow \Phi(s) \\ C_{FT} \leftarrow C_{FT}(u,h,s) \\ C_{FL} \leftarrow C_{FL}(u,h,s,r) \\ C_F \leftarrow C_F(u,C_{FT},C_{FL}) \\ a(\Phi,h,r,C_F) \end{cases}$$

Spill Definition for Pool Calculations

Initial pool volume Specified above under Scenario Definition	$V_I := V_{instant}$ $V_I = 0\,m^3$
Spill rate as a function of time	Defined above under Vessel Release and Deinventory
Time step	$dt := 0.1 \cdot sec$

Pool Spread and Evaporation Algorithm

$pool :=$

$t_0 \leftarrow 0 \cdot sec$

$V_0 \leftarrow V_I$

$r_0 \leftarrow \left(V_0\right)^{\frac{1}{3}}$

$h_0 \leftarrow \frac{V_0}{\pi \cdot \left(r_0\right)^2}$

$u_0 \leftarrow 0 \cdot \frac{m}{sec}$

$q_0 \leftarrow q_S(0 \cdot sec)$

$h_{min_0} \leftarrow h_{0max}\left(q_0\right)$

$a_0 \leftarrow acc\left(u_0, r_0, h_0, q_0\right)$

$e_0 \leftarrow m_f\left(r_0\right)$

$V_{add_0} \leftarrow \frac{q_0 \cdot dt}{\rho_1}$

$V_{evap_0} \leftarrow \frac{e_0 \cdot dt}{\rho_1}$

$i \leftarrow 0$

while $(i < 1) \vee \left(V_i > 0 \cdot m^3\right)$

- $i \leftarrow i + 1$
- $t_i \leftarrow i \cdot dt$
- $V_i \leftarrow V_{i-1} + V_{add_{i-1}} - V_{evap_{i-1}}$
- $V_i \leftarrow 0 \cdot m^3$ if $V_i < 0$
- $r_i \leftarrow r_{i-1} + u_{i-1} \cdot dt$

$$r_i \leftarrow \left(V_i\right)^{\frac{1}{3}} \quad \text{if } r_i = 0 \cdot m$$

$$h_i \leftarrow \frac{V_i}{\pi \cdot \left(r_i\right)^2}$$

$$u_i \leftarrow u_{i-1} + a_{i-1} \cdot dt$$

$$q_i \leftarrow q_S(i \cdot dt)$$

$$e_i \leftarrow m_f\left(r_i\right)$$

$$a_i \leftarrow acc\left(u_i, r_i, h_i, q_i\right)$$

$$V_{add_i} \leftarrow \frac{q_i \cdot dt}{\rho_1}$$

$$V_{evap_i} \leftarrow \frac{e_i \cdot dt}{\rho_1}$$

$$M^{\langle 0 \rangle} \leftarrow \frac{t}{sec}$$

$$M^{\langle 1 \rangle} \leftarrow \frac{V}{m^3}$$

$$M^{\langle 2 \rangle} \leftarrow \frac{r}{m}$$

$$M^{\langle 3 \rangle} \leftarrow \frac{h}{m}$$

$$M^{\langle 4 \rangle} \leftarrow \frac{q}{\frac{kg}{sec}}$$

$$M^{\langle 5 \rangle} \leftarrow \frac{e}{\frac{kg}{sec}}$$

M

Pool Spread and Evaporation Results

Time for complete evaporation $t_{total} := \max(pool^{\langle 0 \rangle}) \cdot sec$ $t_{total} = 417\,sec$ $t_{total} = 6.9\,min$

Maximum pool radius $r_{max} := \max(pool^{\langle 2 \rangle}) \cdot m$ $r_{max} = 134\,m$ $r_{max} = 440\,ft$

pool =

	t	V	r	h	q	e
0	0	0	0	0	$1.325 \cdot 10^5$	0
1	0.1	31.353	3.153	1.004	$1.323 \cdot 10^5$	8.809
2	0.2	62.664	3.153	2.006	$1.321 \cdot 10^5$	8.809
3	0.3	93.936	3.222	2.88	$1.32 \cdot 10^5$	9.197
4	0.4	125.169	3.429	3.389	$1.318 \cdot 10^5$	10.416
5	0.5	156.362	3.795	3.456	$1.316 \cdot 10^5$	12.758
6	0.6	187.515	4.253	3.3	$1.315 \cdot 10^5$	16.026
7	0.7	218.628	4.73	3.111	$1.313 \cdot 10^5$	19.821
8	0.8	249.701	5.201	2.939	$1.311 \cdot 10^5$	23.962
9	0.9	280.733	5.661	2.789	$1.31 \cdot 10^5$	28.39
10	1	311.725	6.11	2.658	$1.308 \cdot 10^5$	33.076
11	1.1	342.677	6.549	2.543	$1.306 \cdot 10^5$	38.001
12	1.2	373.588	6.979	2.441	$1.305 \cdot 10^5$	43.154
13	1.3	404.458	7.401	2.351	$1.303 \cdot 10^5$	48.521
14	1.4	435.288	7.814	2.269	$1.301 \cdot 10^5$	54.094

Plot evaporation rate versus time

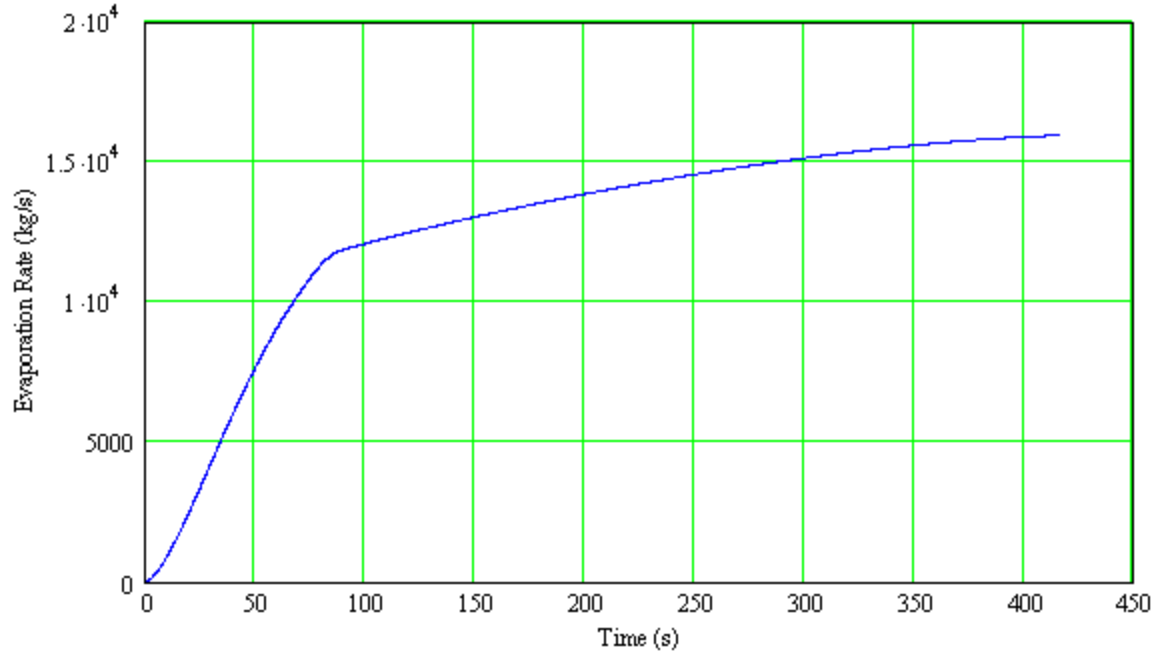

Plot pool radius versus time

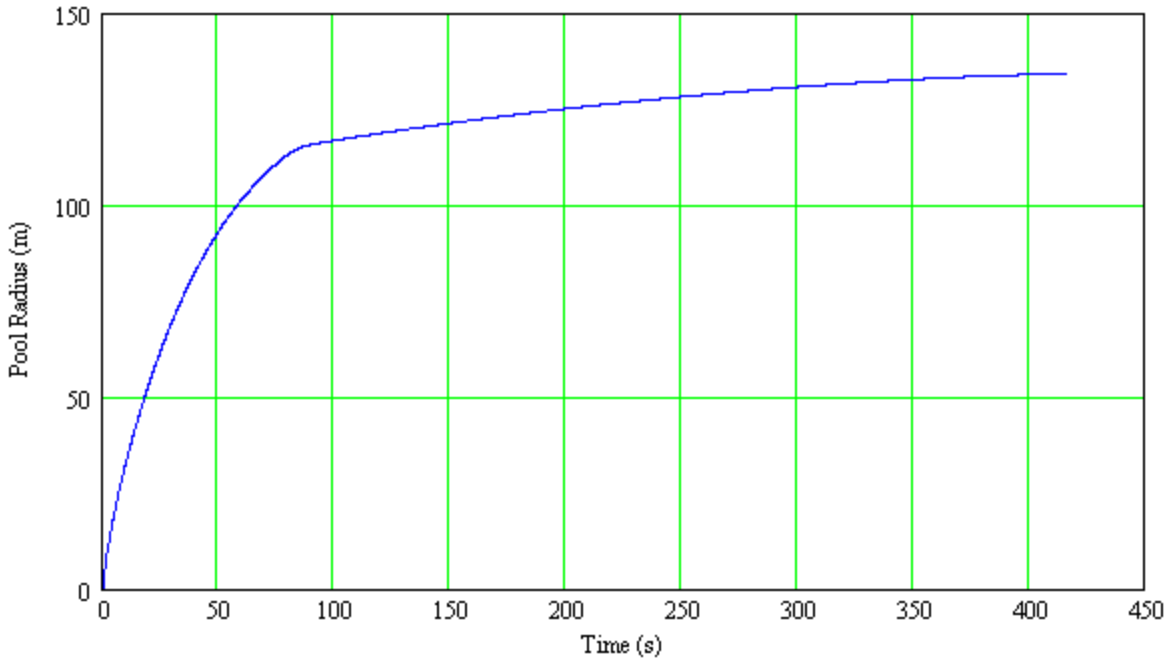

Pool Fire

Functions for pool radius and diameter from spread results

$$r(t) := \text{linterp}\left(pool^{\langle 0 \rangle}, pool^{\langle 2 \rangle}, \frac{t}{sec}\right) \cdot m \qquad d(t) := 2 \cdot r(t)$$

Flame Length

Nondimensional wind velocity
(NFPA, 1995, Sec. 3, Ch.11, Eqn. 15)

$$u_s(t) := \frac{u_{w\_1.6}}{\left(\frac{g \cdot m_b \cdot d(t)}{\rho_v}\right)^{\frac{1}{3}}}$$

Flame length
(NFPA, 1995, Sec. 3, Ch.11, Eqn. 14)

$$a(t) := 55 \cdot d(t) \cdot \left(\frac{m_b}{\rho_a \cdot \sqrt{g \cdot d(t)}}\right)^{0.67} \cdot \left(u_s(t)\right)^{-0.21}$$

Flame Tilt

Tilt angle from vertical
(Rew, 1996, Eqn. 2.18)

$$\theta(t) := \text{root}\left[\frac{\tan(\theta)}{\cos(\theta)} - 3.13 \cdot \left(\frac{u_w^{\,2}}{g \cdot d(t)}\right)^{0.431}, \theta, 0deg, 45deg\right] \cdot rad$$

Flame Drag

Extension of base of the flame downwind. This function gives ratio of extended diameter to base diameter
(NFPA, 1995, Sec. 3, Ch.11, Eqn. 22)

$$D(t) := 1.25 \cdot \left(\frac{u_w^{\,2}}{g \cdot d(t)}\right)^{0.069} \cdot \left(\frac{\rho_v}{\rho_a}\right)^{0.48}$$

Atmospheric Transmissivity

Define function for saturation pressure of water
(AICHE, 2000, Eqn. 2.2.43, p. 209)

$$P_{v\_water}(T_a) := \left[1013.25 \cdot (RH) \cdot \exp\left(14.4114 - \frac{5328}{\frac{T_a}{K}}\right)\right] \cdot Pa$$

Define function for atmospheric transmissivity
(AICHE, 2000, Eqn. 2.2.42, p. 209)

$$\tau_0(x) := 2.02 \cdot \left[RH \cdot P_{v\_water}(T_a) \cdot Pa^{-1} \cdot (x) \cdot m^{-1}\right]^{-0.09}$$

For short distances, the correlation may calculate a transmissivity > 1

$$\tau(x) := \tau_0(x) \cdot \left(\tau_0(x) \le 1.0\right) + 1.0 \cdot \left(\tau_0(x) > 1.0\right)$$

Cylindrical Flame Model Geometric View Factors

$$F(x_r, t) :=$$

Geometric view factor for a cylindrical flam
(NFPA, 1995, Se
3, Ch.11)

$$X \leftarrow \frac{a(t)}{r(t)}$$

$$Y \leftarrow \frac{x_r - r(t) \cdot (D(t) - 1)}{r(t)}$$

$$\theta \leftarrow \theta(t)$$

$$A \leftarrow (X)^2 + (Y+1)^2 - 2 \cdot X \cdot (Y+1) \cdot \sin(\theta)$$

$$B \leftarrow (X)^2 + (Y-1)^2 - 2 \cdot X \cdot (Y-1) \cdot \sin(\theta)$$

$$C \leftarrow 1 + \left(Y^2 - 1\right) \cdot \cos(\theta)^2$$

$$V_1 \leftarrow \frac{X \cdot \cos(\theta)}{Y - X \cdot \sin(\theta)} \cdot \left[\frac{(X)^2 + (Y+1)^2 - 2 \cdot Y \cdot (1 + X \cdot \sin(\theta))}{\pi \cdot \sqrt{A \cdot B}}\right] \cdot \operatorname{atan}\left[\sqrt{\frac{A \cdot (Y-1)}{B \cdot (Y+1)}}\right]$$

$$V_2 \leftarrow \frac{\cos(\theta)}{\pi \cdot \sqrt{C}} \cdot \left[\operatorname{atan}\left[\frac{X \cdot Y - \left(Y^2 - 1\right) \cdot \sin(\theta)}{\sqrt{Y^2 - 1} \cdot \sqrt{C}}\right] + \operatorname{atan}\left(\frac{\sqrt{Y^2 - 1} \cdot \sin(\theta)}{\sqrt{C}}\right)\right]$$

$$V_3 \leftarrow \frac{-X \cdot \cos(\theta)}{\pi \cdot (Y - X \cdot \sin(\theta))} \cdot \operatorname{atan}\left(\sqrt{\frac{Y-1}{Y+1}}\right)$$

$$F_v \leftarrow V_1 + V_2 + V_3$$

$$H_1 \leftarrow \frac{1}{\pi} \cdot \operatorname{atan}\left(\sqrt{\frac{Y+1}{Y-1}}\right)$$

$$H_2 \leftarrow -\left[\frac{(X)^2 + (Y+1)^2 - 2 \cdot (Y + 1 + X \cdot Y \cdot \sin(\theta))}{\pi \cdot \sqrt{A \cdot B}}\right] \cdot \operatorname{atan}\left[\sqrt{\frac{A \cdot (Y-1)}{B \cdot (Y+1)}}\right]$$

$$H_3 \leftarrow \frac{\sin(\theta)}{\pi \cdot \sqrt{C}} \cdot \left[\operatorname{atan}\left[\frac{X \cdot Y - \left(Y^2 - 1\right) \cdot \sin(\theta)}{\sqrt{Y^2 - 1} \cdot \sqrt{C}}\right] + \operatorname{atan}\left(\frac{\sqrt{Y^2 - 1} \cdot \sin(\theta)}{\sqrt{C}}\right)\right]$$

$$F_h \leftarrow H_1 + H_2 + H_3$$

$$\sqrt{F_v^2 + F_h^2}$$

Calculate Thermal Flux Downwind

Function for thermal flux $I_{th}(x_r,t) := \tau(x_r - D(t)\cdot r(t))\cdot F(x_r,t)\cdot E_s$

Calculate flux at a series of points using the maximum pool radius

Look up time for maximum radius $t_{rmax} := \frac{t_{total}}{2}$ (initial guess) $t_{rmax} := root(r_{max} - r(t_{rmax}), t_{rmax})$

Calculate flux at a series of points $i \equiv 0..50$ $x_i := [(i+1)\cdot 200\cdot m] + 10\cdot m$ $I_i := I_{th}(x_i, t_{rmax})$

Plot incident flux versus distance for maximum pool radius

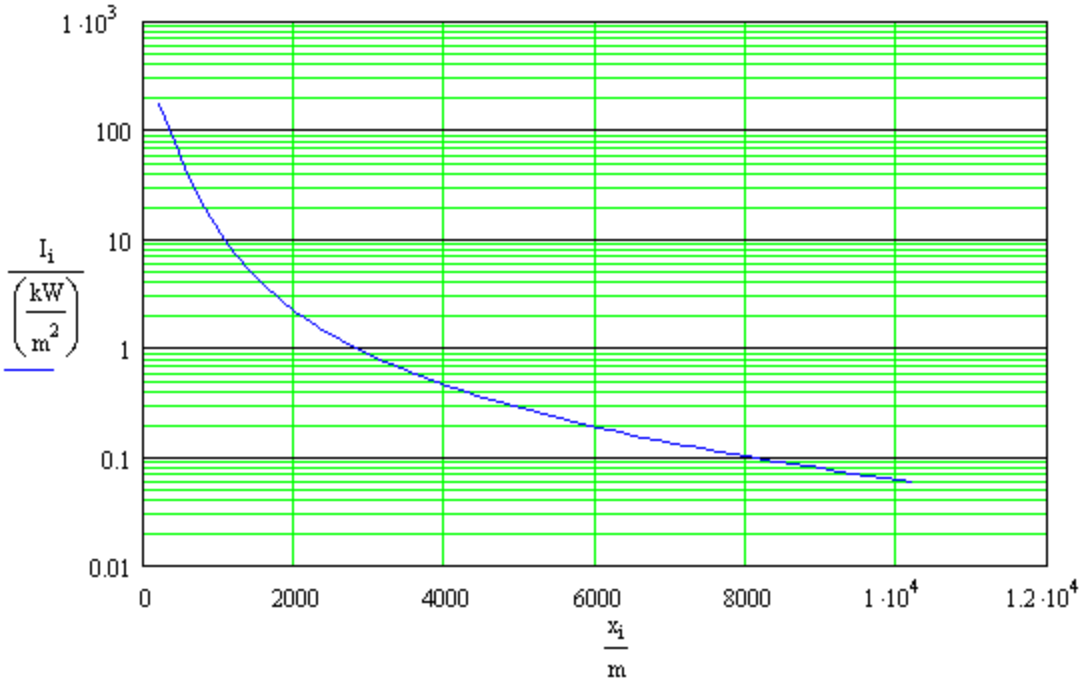

Maximum flame length $a(t_{rmax}) = 438\,m$ $a(t_{rmax}) = 1437\,ft$

Tilt angle at time of maximum length $\theta(t_{rmax}) = 30.8\,deg$

Flame drag at time of maximum length (ratio of extended diameter to base diameter) $D(t_{rmax}) = 1.19$

Plot incident flux versus time at 500, 1000, and 2000 m $t_i := (i + 1) \cdot \frac{t_{total}}{51}$

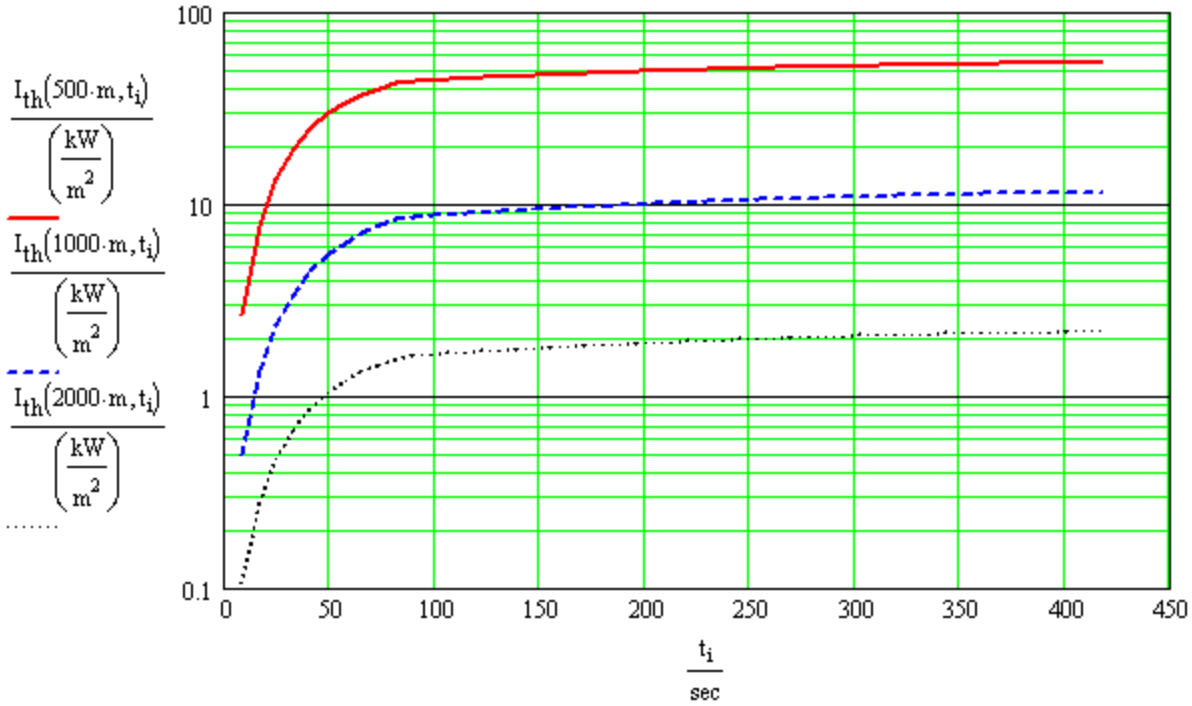

Determine the ground-level distances to the thermal flux level(s) of concern using maximum radius

$x_r := 200 \cdot m$ (initial guess) $R_{loc}(I_{loc}) := root(I_{loc} - I_{th}(x_r, t_{rmax}), x_r)$

Distances to the thermal flux levels of concern

	38 kW/m²	**25 kW/m²**	**12 kW/m²**	**5 kW/m²**
LOC defined	$I_{loc1} := 38 \cdot \frac{kW}{m^2}$	$I_{loc2} := 25 \cdot \frac{kW}{m^2}$	$I_{loc3} := 12 \cdot \frac{kW}{m^2}$	$I_{loc4} := 5 \cdot \frac{kW}{m^2}$
	$I_{loc1} = 12046 \frac{BTU}{hr \cdot ft^2}$	$I_{loc2} = 7925 \frac{BTU}{hr \cdot ft^2}$	$I_{loc3} = 3804 \frac{BTU}{hr \cdot ft^2}$	$I_{loc4} = 1585 \frac{BTU}{hr \cdot ft^2}$
Calculate distance	$R_{loc1} := R_{loc}(I_{loc1})$	$R_{loc2} := R_{loc}(I_{loc2})$	$R_{loc3} := R_{loc}(I_{loc3})$	$R_{loc4} := R_{loc}(I_{loc4})$
	$R_{loc1} = 599\,m$	$R_{loc2} = 723\,m$	$R_{loc3} = 982\,m$	$R_{loc4} = 1406\,m$
	$R_{loc1} = 1965\,ft$	$R_{loc2} = 2373\,ft$	$R_{loc3} = 3223\,ft$	$R_{loc4} = 4614\,ft$
	$R_{loc1} = 0.37\,mi$	$R_{loc2} = 0.45\,mi$	$R_{loc3} = 0.61\,mi$	$R_{loc4} = 0.87\,mi$

Appendix D

Example Source Term Calculations for Flammable Vapor Dispersion

LNG Source Term and Dispersion Modeling Input Data

- **Vessel Release and Deinventory**
- **Film Boiling Heat Flux**
- **Pool Spread and Evaporation (Webber Methodology)**
- **DEGADIS Source Term Input Data**

Scenario Definition

Spill Definition

Instantaneous pool volume: $V_{instant} := 0 \cdot m^3$

Hole diameter: $d_{hole} := 1 \cdot m$ $d_{hole} = 3.28\,ft$

Initial liquid height above the hole: $h_{init} := 13 \cdot m$ $h_{init} = 42.7\,ft$

Volume to release through hole (i.e., volume above the hole): $V_{spill} := 12500 \cdot m^3$

Ambient Conditions

Ambient pressure: $p_a := 101325 \cdot Pa$ $p_a = 14.7\,psi$

Temperature of water: $T_w := (70 + 459.67) \cdot R$ $T_w = 529.67\,R$

Constants and Conversion Factors

Unit conversions: $kJ \equiv 1000 \cdot joule$ $lbmole \equiv 1$ $kgmole \equiv \frac{kg}{lb} \cdot lbmole$ $kW \equiv 1000 \cdot watt$

Universal gas constant: $R_u \equiv 1545 \cdot \frac{ft \cdot lbf}{lbmole \cdot R}$

Material Properties

Molecular weight: $M := 16.043 \cdot \frac{kg}{kgmole}$

Normal boiling point: $T_b := 111.66 \cdot K$ $T_b = 200.988\,R$

Vapor density (at T_b, using ideal gas law): $\rho_v := \frac{p_a}{\frac{R_u}{M} \cdot T_b}$ $\rho_v = 1.751 \frac{kg}{m^3}$ $\rho_v = 0.109 \frac{lb}{ft^3}$

Vapor viscosity (at T_b): $\mu_v := 4.362 \cdot 10^{-6} Pa\,sec$

Kinematic viscosity of vapor (at T_b): $\nu_v := \frac{\mu_v}{\rho_v}$ $\nu_v = 2.491 \times 10^{-6} \frac{m^2}{sec}$

Density of Liquid (at T_b): $\rho_l := 422.5 \cdot \frac{kg}{m^3}$

Liquid viscosity (at T_b): $\mu_l := 1.168 \cdot 10^{-4} Pa\,sec$

Kinematic viscosity of vapor (at T_b)

$$\nu_l := \frac{\mu_l}{\rho_l} \qquad \nu_l = 2.764 \times 10^{-7}\ \frac{m^2}{sec}$$

Heat of vaporization

$$h_{fg} := 509331.9 \cdot \frac{joule}{kg}$$

Surface Tension (at T_b)

$$\sigma := 0.0133\ \frac{newton}{m}$$

Thermal conductivity of vapor

$$\lambda_v := 0.01269\ \frac{watt}{m \cdot K}$$

Heat capacity of vapor

$$C_p := 2075.56\ \frac{joule}{kg \cdot K}$$

Vapor thermal diffusivity

$$\alpha_v := \frac{\lambda_v}{\rho_v \cdot C_p} \qquad \alpha_v = 3.491 \times 10^{-6}\ \frac{m^2}{sec}$$

Seawater density

$$\rho_w := 1025 \cdot \frac{kg}{m^3}$$

Water viscosity

$$\mu_w := 1.021 \cdot 10^{-3}\ Pa\,sec$$

Water kinematic viscosity of vapor

$$\nu_w := \frac{\mu_w}{\rho_w} \qquad \nu_w = 9.961 \times 10^{-7}\ \frac{m^2}{sec}$$

Vessel Release and Deinventory

Hole diameter
Specified above under Scenario Definition

$$d_{hole} = 1\,m \qquad d_{hole} = 3.281\,ft$$

Total volume in the tank above the hole
Specified above under Scenario Definition

$$V_{spill} = 12500\,m^3$$

Initial liquid height above the hole
Specified above under Scenario Definition

$$h_{init} = 13\,m$$

Tank area in horizontal plane
Assuming that cross sectional area of tank (in horizontal plane) is approximately constant.

$$A_{tank} := \frac{V_{spill}}{h_{init}} \qquad A_{tank} = 962\,m^2$$

Discharge coefficient

$$C_d := 1$$

Function for flow through an orifice driven only by gravity

$$Q_o(h) := C_d \cdot \rho_l \cdot \pi \cdot \left(\frac{d_{hole}}{2}\right)^2 \cdot \sqrt{2g \cdot h}$$

Time step

$$dt := 0.1 \cdot sec$$

Determine flow rate versus time, taking into account the decreasing head

$$
\begin{aligned}
\text{flow} := \;& V_0 \leftarrow V_{spill} \\
& h_0 \leftarrow h_{init} \\
& q_0 \leftarrow Q_o(h_0) \\
& t_0 \leftarrow 0 \cdot sec \\
& i \leftarrow 0 \\
& \text{while } V_i > 0 \\
& \quad i \leftarrow i + 1 \\
& \quad t_i \leftarrow i \cdot dt \\
& \quad V_i \leftarrow V_{i-1} - \frac{q_{i-1} \cdot dt}{\rho_1} \\
& \quad V_i \leftarrow 0 \text{ if } V_i < 0 \\
& \quad h_i \leftarrow \frac{V_i}{A_{tank}} \\
& \quad q_i \leftarrow Q_o(h_i) \\
& M^{\langle 0 \rangle} \leftarrow \frac{t}{sec} \\
& M^{\langle 1 \rangle} \leftarrow \frac{q}{\frac{kg}{sec}} \\
& M^{\langle 2 \rangle} \leftarrow \frac{V}{m^3} \\
& M^{\langle 3 \rangle} \leftarrow \frac{h}{m} \\
& M
\end{aligned}
$$

flow =

	t	q	v	h
	0	1	2	3
0	0	$5.299 \cdot 10^3$	$1.25 \cdot 10^4$	13
1	0.1	$5.298 \cdot 10^3$	$1.25 \cdot 10^4$	12.999
2	0.2	$5.298 \cdot 10^3$	$1.25 \cdot 10^4$	12.997
3	0.3	$5.298 \cdot 10^3$	$1.25 \cdot 10^4$	12.996
4	0.4	$5.298 \cdot 10^3$	$1.249 \cdot 10^4$	12.995
5	0.5	$5.297 \cdot 10^3$	$1.249 \cdot 10^4$	12.993
6	0.6	$5.297 \cdot 10^3$	$1.249 \cdot 10^4$	12.992
7	0.7	$5.297 \cdot 10^3$	$1.249 \cdot 10^4$	12.991
8	0.8	$5.297 \cdot 10^3$	$1.249 \cdot 10^4$	12.99
9	0.9	$5.296 \cdot 10^3$	$1.249 \cdot 10^4$	12.988

Plot release rate versus time

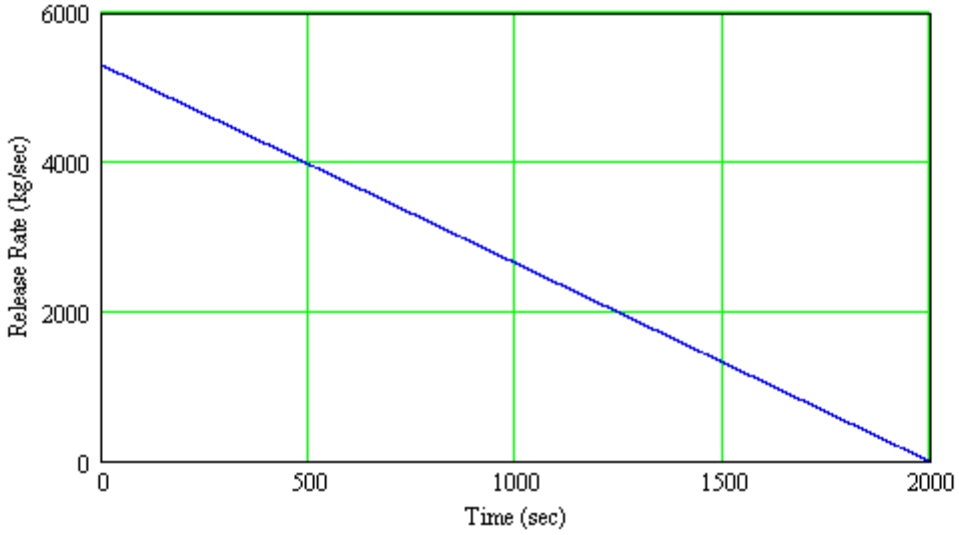

Time to release entire volume $t_{end} := \max\left(flow^{\langle 0 \rangle}\right) \cdot sec$ $t_{end} = 1993\,sec$ $t_{end} = 33.2\,min$

Function for evaporation rate as a function of time for use in pool spread calculations

$$q_S(t) := \begin{cases} 0 \cdot \frac{kg}{sec} & \text{if } t > t_{end} \\ linterp\left(flow^{\langle 0 \rangle}, flow^{\langle 1 \rangle}, \frac{t}{sec}\right) \cdot \frac{kg}{sec} & \text{otherwise} \end{cases}$$

Film Boiling Heat Flux and Evaporation Rate

Use the model/correlation of Klimenko, as given by TNO (1997).

Length scale for vapor bubble formation $l_c := 2\pi\left[\frac{\sigma}{g \cdot (\rho_l - \rho_v)}\right]^{.5}$ $l_c = 0.011\,m$

Galileo number $Ga := \frac{g \cdot l_c^{\,3}}{\nu_v^{\,2}}$ $Ga = 2.269 \times 10^6$

Archimedes number $Ar := Ga \cdot \frac{(\rho_l - \rho_v)}{\rho_v}$ $Ar = 5.452 \times 10^8$

Prandtl number $Pr_v := \frac{\nu_v}{\alpha_v}$ $Pr_v = 0.713$

Dimensionless heat of vaporization $L_{vR} := \frac{h_{fg}}{C_p \cdot (T_w - T_b)}$ $L_{vR} = 1.344$

Nusselt number

$$F_1 := 1\cdot\left(L_{vR} \le 1.4\right) + \left(\frac{L_{vR}}{1.4}\right)^{\frac{1}{3}}\cdot\left(L_{vR} > 1.4\right) \qquad F_2 := 1\cdot\left(L_{vR} \le 2\right) + \left(\frac{L_{vR}}{2}\right)^{\frac{1}{2}}\cdot\left(L_{vR} > 2\right)$$

$$Nu := 0.19\cdot\left(Ar\cdot Pr_v\right)^{\frac{1}{3}}\cdot F_1\cdot\left(Ar \le 10^8\right) + 0.0086\cdot\sqrt{Ar}\cdot Pr_v^{\frac{1}{3}}\cdot\left(Ar > 10^8\right) \qquad Nu = 179.4$$

Heat transfer coefficient $h_{film} := \lambda_v\cdot\frac{Nu}{l_c}$ $h_{film} = 201.8\,\frac{watt}{m^2\cdot K}$

Heat flux $Q_{film} := h_{film}\cdot\left(T_w - T_b\right)$ $Q_{film} = 36.9\,\frac{kW}{m^2}$

Evaporation mass flux $M_{film} := \frac{Q_{film}}{h_{fg}}$ $M_{film} = 0.072\,\frac{kg}{m^2\cdot sec}$

Mass evaporation rate as a function of pool radius $m_e(r) := \frac{\pi\cdot\left(r^2\right)\cdot Q_{film}}{h_{fg}}$

Spread Equations

Reduced gravitational acceleration (TNO 3.34) $g_r := g\cdot\frac{\left(\rho_w - \rho_l\right)}{\rho_w}$

Minimum frontal depth based on surface tension (TNO 3.48) $h_\sigma := \sqrt{\frac{\sigma}{g\cdot\rho_l}}$ $h_\sigma = 0.18\,cm$

Minimum frontal depth based on viscous effects (TNO 3.11) $h_c\left(q_S\right) := \left(\frac{6\cdot\nu_l\cdot q_S}{\rho_l\cdot\pi\cdot g}\right)^{0.25}$

Choose minimum depth (TNO 3.49) $h_{0max}(q) := \max\left(h_\sigma, h_c(q)\right)$

Pool shape factor $s\left(u,h,h_{0max}\right) :=$

1 if $h < 0.01\cdot m$

otherwise

$Fr \leftarrow 1.078$

$N \leftarrow \frac{u^2}{2\cdot Fr^2\cdot g_r\cdot h}$ if $u > 0$

$N \leftarrow 0$ otherwise

$s \leftarrow N + \sqrt{N^2 + \left(\frac{h_{0max}}{h}\right)^2}$

s

Gravity term coefficient (TNO 3.63)

$$\Phi(s) := (1 - s)\cdot(s \le 2) + \left(\frac{-s^2}{4}\right)(s > 2)$$

TNO (3.46)

$$j(s) := 1\cdot(s \ge 2) + \frac{2}{s}\cdot(s < 2)$$

Resistance for laminar flow (TNO 3.64, 3.65b, 3.66, 3.68W, and 3.69)

$$ff(u,h,s,r) := \left|\begin{array}{l} 1 \text{ if } r = 0\cdot m \\ \text{otherwise} \\ \quad \left|\begin{array}{l} 1 \text{ if } h < 0.001\cdot m \\ \text{otherwise} \\ \quad \left|\begin{array}{l} 1 \text{ if } u < 0.000001\cdot\frac{m}{sec} \\ \text{otherwise} \\ \quad \left|\begin{array}{l} f \leftarrow 0.2 \\ \text{root}\left(\frac{\mu_1}{\mu_w}\cdot\sqrt{\frac{u\cdot h^2}{\nu_w\cdot r}}\cdot\frac{1}{j(s)}\cdot f^{\frac{3}{2}} - 1 + f, f\right) \end{array}\right. \end{array}\right. \end{array}\right.$$

$$C_{FL}(u,h,s,r) := \left|\begin{array}{ll} 0\cdot\frac{m}{sec^2} & \text{if } h \le 0 \\ 2.35\cdot j(s)\cdot 0.66\cdot\nu_1\cdot\frac{u}{h^2}\cdot(1 - ff(u,h,s,r)) & \text{otherwise} \end{array}\right.$$

Resistance for turbulent flow (TNO 3.70 and 3.71)

$$C_{FT}(u,h,s) := \left|\begin{array}{ll} 0\cdot\frac{m}{sec^2} & \text{if } h \le 0 \\ \frac{4.49\cdot j(s)\cdot 0.0015\cdot u^2}{h} & \text{otherwise} \end{array}\right.$$

Resistance term (TNO 3.72)

$$C_F(u,C_{FT},C_{FL}) := \text{sign}(u)\cdot\max(C_{FT},C_{FL})$$

Acceleration of the leading edge of the pool (TNO 3.62)

$$a(\Phi,h,r,C_F) := \frac{4\cdot\Phi\cdot g_r\cdot h}{r} - C_F$$

Acceleration as a function of current speed, radius, height, and mass addition rate

$$acc(u,r,h,q) := \left|\begin{array}{l} h_{0max} \leftarrow h_{0max}(q) \\ s \leftarrow s(u,h,h_{0max}) \\ \Phi \leftarrow \Phi(s) \\ C_{FT} \leftarrow C_{FT}(u,h,s) \\ C_{FL} \leftarrow C_{FL}(u,h,s,r) \\ C_F \leftarrow C_F(u,C_{FT},C_{FL}) \\ a(\Phi,h,r,C_F) \end{array}\right.$$

Spill Definition for Pool Calculations

Initial pool volume
Specified above under Scenario Definition

$V_I := V_{instant}$ $V_I = 0\,m^3$

Spill rate as a function of time

Defined above under
Vessel Release and Deinventory

Time step

$dt := 0.1 \cdot sec$

Pool Spread and Evaporation Algorithm

pool :=

$t_0 \leftarrow 0 \cdot sec$

$V_0 \leftarrow V_I$

$r_0 \leftarrow (V_0)^{\frac{1}{3}}$

$h_0 \leftarrow \frac{V_0}{\pi \cdot (r_0)^2}$

$u_0 \leftarrow 0 \cdot \frac{m}{sec}$

$q_0 \leftarrow q_S(0 \cdot sec)$

$a_0 \leftarrow acc(u_0, r_0, h_0, q_0)$

$e_0 \leftarrow m_e(r_0)$

$V_{add_0} \leftarrow \frac{q_0 \cdot dt}{\rho_1}$

$V_{evap_0} \leftarrow \frac{e_0 \cdot dt}{\rho_1}$

$SourceMatched \leftarrow 0$

$i \leftarrow 0$

while $(i < 1) \vee (V_i > 0 \cdot m^3)$

- $i \leftarrow i + 1$
- $t_i \leftarrow i \cdot dt$
- $V_i \leftarrow V_{i-1} + V_{add_{i-1}} - V_{evap_{i-1}}$
- $V_i \leftarrow 0 \cdot m^3$ if $V_i < 0$
- if $SourceMatched = 1$
  - $r_i \leftarrow r_{i-1}$

$$h_i \leftarrow \frac{V_i}{\pi \cdot (r_i)^2}$$

$$q_i \leftarrow q_S(i \cdot dt)$$

$$h_{min} \leftarrow h_{0max}(q_i)$$

if $h_i < h_{min}$ if $q_i > 0$

$$h_i \leftarrow h_{min}$$

$$r_i \leftarrow \sqrt{\frac{V_i}{\pi \cdot h_i}}$$

$$e_i \leftarrow m_e(r_i)$$

$$V_{add_i} \leftarrow \frac{q_i \cdot dt}{\rho_1}$$

$$V_{evap_i} \leftarrow \frac{e_i \cdot dt}{\rho_1}$$

if $\left(V_i + V_{add_i} - V_{evap_i}\right) \le 0 \cdot m^3$ if $q_i > 0 \cdot \frac{kg}{sec}$

$$r_i \leftarrow \sqrt{\frac{q_i \cdot h_{fg}}{\pi \cdot Q_{film}}}$$

$$h_i \leftarrow \frac{V_i}{\pi \cdot (r_i)^2}$$

$$e_i \leftarrow q_i$$

$$V_{evap_i} \leftarrow V_{add_i}$$

otherwise

$$r_i \leftarrow r_{i-1} + u_{i-1} \cdot dt$$

$$r_i \leftarrow (V_i)^{\frac{1}{3}} \quad \text{if } r_i = 0 \cdot m$$

$$h_i \leftarrow \frac{V_i}{\pi \cdot (r_i)^2}$$

$$u_i \leftarrow u_{i-1} + a_{i-1} \cdot dt$$

$$q_i \leftarrow q_S(i \cdot dt)$$

$$e_i \leftarrow m_e(r_i)$$

$a_i \leftarrow acc(u_i, r_i, h_i, q_i)$

if $\left[\left(q_i > 0 \cdot \frac{kg}{sec}\right) \wedge \left(q_i \le e_i\right)\right]$

SourceMatched $\leftarrow 1$

$r_i \leftarrow \sqrt{\frac{q_i \cdot h_{fg}}{\pi \cdot Q_{film}}}$

$h_i \leftarrow \frac{V_i}{\pi \cdot (r_i)^2}$

$e_i \leftarrow q_i$

$u_i \leftarrow 0 \cdot \frac{m}{sec}$

$a_i \leftarrow 0 \cdot \frac{m}{sec^2}$

$V_{add_i} \leftarrow \frac{q_i \cdot dt}{\rho_1}$

$V_{evap_i} \leftarrow \frac{e_i \cdot dt}{\rho_1}$

$M^{\langle 0 \rangle} \leftarrow \frac{t}{sec}$

$M^{\langle 1 \rangle} \leftarrow \frac{V}{m^3}$

$M^{\langle 2 \rangle} \leftarrow \frac{r}{m}$

$M^{\langle 3 \rangle} \leftarrow \frac{h}{m}$

$M^{\langle 4 \rangle} \leftarrow \frac{q}{\frac{kg}{sec}}$

$M^{\langle 5 \rangle} \leftarrow \frac{e}{\frac{kg}{sec}}$

M

Pool Spread and Evaporation Results

Time for complete evaporation $t_{total} := \max(pool^{\langle 0 \rangle}) \cdot sec$ $t_{total} = 2028\ sec$ $t_{total} = 33.8\ min$

Maximum pool radius $r_{max} := \max(pool^{\langle 2 \rangle}) \cdot m$ $r_{max} = 131\ m$ $r_{max} = 430\ ft$

pool =

	t	V	r	h	q	e
	0	1	2	3	4	5
0	0	0	0	0	$5.299 \cdot 10^3$	0
1	0.1	1.254	1.078	0.343	$5.298 \cdot 10^3$	0.264
2	0.2	2.508	1.078	0.686	$5.298 \cdot 10^3$	0.264
3	0.3	3.762	1.146	0.912	$5.298 \cdot 10^3$	0.298
4	0.4	5.016	1.342	0.886	$5.298 \cdot 10^3$	0.41
5	0.5	6.27	1.605	0.775	$5.297 \cdot 10^3$	0.586
6	0.6	7.523	1.842	0.706	$5.297 \cdot 10^3$	0.771
7	0.7	8.777	2.069	0.653	$5.297 \cdot 10^3$	0.973
8	0.8	10.03	2.287	0.611	$5.297 \cdot 10^3$	1.189
9	0.9	11.284	2.497	0.576	$5.296 \cdot 10^3$	1.418
10	1	12.537	2.702	0.547	$5.296 \cdot 10^3$	1.66
11	1.1	13.79	2.901	0.522	$5.296 \cdot 10^3$	1.913
12	1.2	15.043	3.095	0.5	$5.295 \cdot 10^3$	2.178
13	1.3	16.296	3.285	0.481	$5.295 \cdot 10^3$	2.453
14	1.4	17.548	3.471	0.464	$5.295 \cdot 10^3$	2.739

Plot evaporation rate versus time

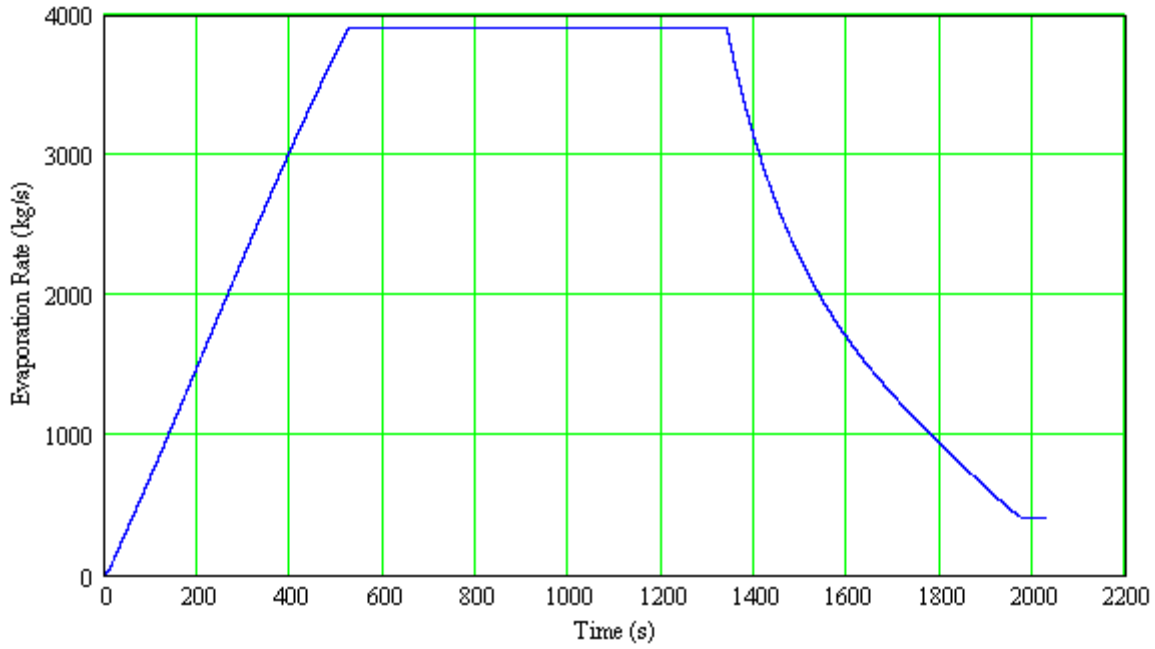

Plot pool radius versus time

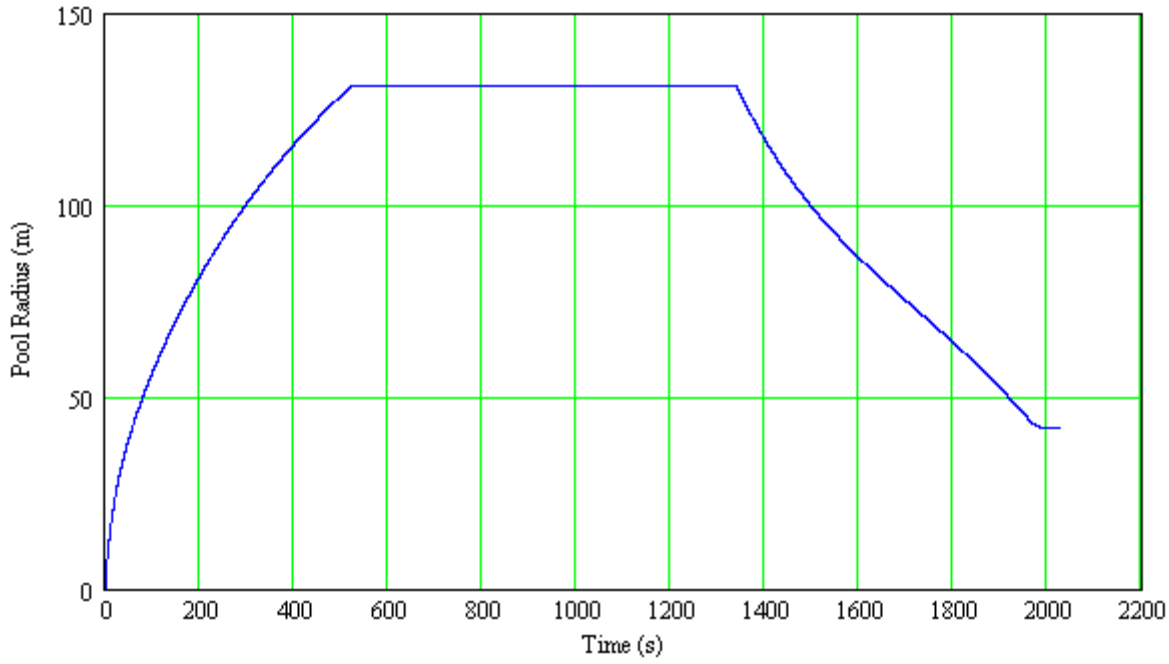

Transient Source Term for DEGADIS

Time step $step := \frac{t_{total}}{38}$ $step = 53.379\ s$

For each time step, use the evaporation rate and pool radius for the midpoint

$deg :=$ for $i \in 0..37$

$t_i \leftarrow i \cdot \frac{step}{sec}$

$t_{mid} \leftarrow t_i + \frac{step}{2 \cdot sec}$

$e_i \leftarrow linterp(pool^{\langle 0 \rangle}, pool^{\langle 5 \rangle}, t_{mid})$

$r_i \leftarrow linterp(pool^{\langle 0 \rangle}, pool^{\langle 2 \rangle}, t_{mid})$

$t_{38} \leftarrow \frac{38 \cdot step}{sec}$

$t_{39} \leftarrow t_{38} + 1$

$M^{\langle 0 \rangle} \leftarrow t$

$M^{\langle 1 \rangle} \leftarrow e$

$M^{\langle 2 \rangle} \leftarrow r$

M

deg =

	0	1	2
0	0.00	172.20	27.52
1	53.38	569.00	50.03
2	106.76	978.90	65.62
3	160.14	1397.89	78.42
4	213.52	1818.77	89.44
5	266.89	2236.28	99.18
6	320.27	2646.29	107.89
7	373.65	3045.32	115.74
8	427.03	3430.27	122.84
9	480.41	3798.20	129.26
10	533.79	3907.11	131.10
11	587.17	3907.11	131.10
12	640.55	3907.11	131.10
13	693.93	3907.11	131.10
14	747.31	3907.11	131.10
15	800.68	3907.11	131.10
16	854.06	3907.11	131.10
17	907.44	3907.11	131.10
18	960.82	3907.11	131.10
19	1014.20	3907.11	131.10
20	1067.58	3907.11	131.10
21	1120.96	3907.11	131.10
22	1174.34	3907.11	131.10
23	1227.72	3907.11	131.10
24	1281.09	3907.11	131.10
25	1334.47	3576.64	125.43
26	1387.85	2945.41	113.83
27	1441.23	2470.13	104.24
28	1494.61	2101.46	96.14
29	1547.99	1805.19	89.11
30	1601.37	1557.63	82.77
31	1654.75	1342.52	76.85
32	1708.13	1148.67	71.08
33	1761.51	968.44	65.27
34	1814.88	796.67	59.20
35	1868.26	630.25	52.65
36	1921.64	470.98	45.52
37	1975.02	404.51	42.18
38	2028.40	0.00	0.00
39	2029.40	0.00	0.00

Write data to text file for input to DEGADIS

WRITEPRN("deg.txt") := deg

Note that DEGADIS requires the number of data points at the top of the file, so before input to DEGADIS, a new line should be added to the top of this file with the number 40.

LNG Source Term and Dispersion Modeling Input Data

- **Vessel Release and Deinventory**
- **Film Boiling Heat Flux**
- **Pool Spread and Evaporation (Webber Methodology)**
- **DEGADIS Source Term Input Data**

Scenario Definition

Spill Definition

Instantaneous pool volume $V_{instant} := 0 \cdot m^3$

Hole diameter $d_{hole} := 5 \cdot m$ $d_{hole} = 16.4\,ft$

Initial liquid height above the hole $h_{init} := 13 \cdot m$ $h_{init} = 42.7\,ft$

Volume to release through hole (i.e., volume above the hole) $V_{spill} := 12500 \cdot m^3$

Ambient Conditions

Ambient pressure $p_a := 101325 \cdot Pa$ $p_a = 14.7\,psi$

Temperature of water $T_w := (70 + 459.67) \cdot R$ $T_w = 529.67\,R$

Constants and Conversion Factors

Unit conversions $kJ \equiv 1000 \cdot joule$ $lbmole \equiv 1$ $kgmole \equiv \frac{kg}{lb} \cdot lbmole$ $kW \equiv 1000 \cdot watt$

Universal gas constant $R_u \equiv 1545 \cdot \frac{ft \cdot lbf}{lbmole \cdot R}$

Material Properties

Molecular weight $M := 16.043 \cdot \frac{kg}{kgmole}$

Normal boiling point $T_b := 111.66 \cdot K$ $T_b = 200.988\,R$

Vapor density (at T_b, using ideal gas law) $\rho_v := \frac{p_a}{\frac{R_u}{M} \cdot T_b}$ $\rho_v = 1.751 \frac{kg}{m^3}$ $\rho_v = 0.109 \frac{lb}{ft^3}$

Vapor viscosity (at T_b) $\mu_v := 4.362 \cdot 10^{-6} Pa\,sec$

Kinematic viscosity of vapor (at T_b) $\nu_v := \frac{\mu_v}{\rho_v}$ $\nu_v = 2.491 \times 10^{-6} \frac{m^2}{sec}$

Density of Liquid (at T_b) $\rho_l := 422.5 \cdot \frac{kg}{m^3}$

Liquid viscosity (at T_b) $\mu_l := 1.168 \cdot 10^{-4} Pa\,sec$

Kinematic viscosity of vapor (at T_b)

$$\nu_1 := \frac{\mu_1}{\rho_1} \qquad \nu_1 = 2.764 \times 10^{-7}\ \frac{m^2}{sec}$$

Heat of vaporization

$$h_{fg} := 509331.9 \cdot \frac{joule}{kg}$$

Surface Tension (at T_b)

$$\sigma := 0.0133\ \frac{newton}{m}$$

Thermal conductivity of vapor

$$\lambda_v := 0.01269\ \frac{watt}{m \cdot K}$$

Heat capacity of vapor

$$C_p := 2075.56\ \frac{joule}{kg \cdot K}$$

Vapor thermal diffusivity

$$\alpha_v := \frac{\lambda_v}{\rho_v \cdot C_p} \qquad \alpha_v = 3.491 \times 10^{-6}\ \frac{m^2}{sec}$$

Seawater density

$$\rho_w := 1025 \cdot \frac{kg}{m^3}$$

Water viscosity

$$\mu_w := 1.021 \cdot 10^{-3}\ Pa\,sec$$

Water kinematic viscosity of vapor

$$\nu_w := \frac{\mu_w}{\rho_w} \qquad \nu_w = 9.961 \times 10^{-7}\ \frac{m^2}{sec}$$

Vessel Release and Deinventory

Hole diameter
Specified above under Scenario Definition

$$d_{hole} = 5\,m \qquad d_{hole} = 16.404\,ft$$

Total volume in the tank above the hole
Specified above under Scenario Definition

$$V_{spill} = 12500\,m^3$$

Initial liquid height above the hole
Specified above under Scenario Definition

$$h_{init} = 13\,m$$

Tank area in horizontal plane
Assuming that cross sectional area of tank (in horizontal plane) is approximately constant.

$$A_{tank} := \frac{V_{spill}}{h_{init}} \qquad A_{tank} = 962\,m^2$$

Discharge coefficient

$$C_d := 1$$

Function for flow through an orifice driven only by gravity

$$Q_o(h) := C_d \cdot \rho_1 \cdot \pi \cdot \left(\frac{d_{hole}}{2}\right)^2 \cdot \sqrt{2g \cdot h}$$

Time step

$$dt := 0.1 \cdot sec$$

Determine flow rate versus time, taking into account the decreasing head

$$
\begin{aligned}
\text{flow} := \;& V_0 \leftarrow V_{spill} \\
& h_0 \leftarrow h_{init} \\
& q_0 \leftarrow Q_o(h_0) \\
& t_0 \leftarrow 0 \cdot sec \\
& i \leftarrow 0 \\
& \text{while } V_i > 0 \\
& \quad i \leftarrow i + 1 \\
& \quad t_i \leftarrow i \cdot dt \\
& \quad V_i \leftarrow V_{i-1} - \frac{q_{i-1} \cdot dt}{\rho_1} \\
& \quad V_i \leftarrow 0 \text{ if } V_i < 0 \\
& \quad h_i \leftarrow \frac{V_i}{A_{tank}} \\
& \quad q_i \leftarrow Q_o(h_i) \\
& M^{\langle 0 \rangle} \leftarrow \frac{t}{sec} \\
& M^{\langle 1 \rangle} \leftarrow \frac{q}{\frac{kg}{sec}} \\
& M^{\langle 2 \rangle} \leftarrow \frac{V}{m^3} \\
& M^{\langle 3 \rangle} \leftarrow \frac{h}{m} \\
& M
\end{aligned}
$$

flow =

	t	q	v	h
	0	1	2	3
0	0	$1.325 \cdot 10^5$	$1.25 \cdot 10^4$	13
1	0.1	$1.323 \cdot 10^5$	$1.247 \cdot 10^4$	12.967
2	0.2	$1.321 \cdot 10^5$	$1.244 \cdot 10^4$	12.935
3	0.3	$1.32 \cdot 10^5$	$1.241 \cdot 10^4$	12.902
4	0.4	$1.318 \cdot 10^5$	$1.237 \cdot 10^4$	12.87
5	0.5	$1.316 \cdot 10^5$	$1.234 \cdot 10^4$	12.837
6	0.6	$1.315 \cdot 10^5$	$1.231 \cdot 10^4$	12.805
7	0.7	$1.313 \cdot 10^5$	$1.228 \cdot 10^4$	12.773
8	0.8	$1.311 \cdot 10^5$	$1.225 \cdot 10^4$	12.74
9	0.9	$1.31 \cdot 10^5$	$1.222 \cdot 10^4$	12.708

Plot release rate versus time

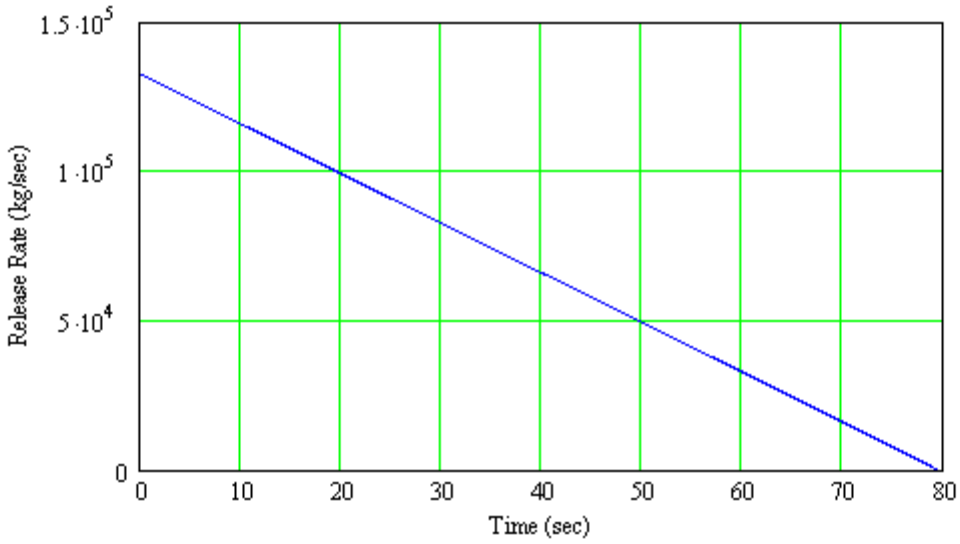

Time to release entire volume $t_{end} := \max\left(flow^{\langle 0 \rangle}\right) \cdot sec$ $t_{end} = 79\,sec$ $t_{end} = 1.3\,min$

Function for evaporation rate as a function of time for use in pool spread calculations

$$qs(t) := \begin{cases} 0 \cdot \frac{kg}{sec} & \text{if } t > t_{end} \\ \text{linterp}\left(flow^{\langle 0 \rangle}, flow^{\langle 1 \rangle}, \frac{t}{sec}\right) \cdot \frac{kg}{sec} & \text{otherwise} \end{cases}$$

Film Boiling Heat Flux and Evaporation Rate

Use the model/correlation of Klimenko, as given by TNO (1997).

Length scale for vapor bubble formation $l_c := 2\pi\left[\frac{\sigma}{g \cdot (\rho_l - \rho_v)}\right]^{.5}$ $l_c = 0.011\,m$

Galileo number $Ga := \frac{g \cdot l_c^{\,3}}{\nu_v^{\,2}}$ $Ga = 2.269 \times 10^6$

Archimedes number $Ar := Ga \cdot \frac{(\rho_l - \rho_v)}{\rho_v}$ $Ar = 5.452 \times 10^8$

Prandtl number $Pr_v := \frac{\nu_v}{\alpha_v}$ $Pr_v = 0.713$

Dimensionless heat of vaporization $L_{vR} := \frac{h_{fg}}{C_p \cdot (T_w - T_b)}$ $L_{vR} = 1.344$

Nusselt number

$$F_1 := 1\cdot\left(L_{vR} \le 1.4\right) + \left(\frac{L_{vR}}{1.4}\right)^{\frac{1}{3}}\cdot\left(L_{vR} > 1.4\right) \qquad F_2 := 1\cdot\left(L_{vR} \le 2\right) + \left(\frac{L_{vR}}{2}\right)^{\frac{1}{2}}\cdot\left(L_{vR} > 2\right)$$

$$Nu := 0.19\cdot\left(Ar\cdot Pr_v\right)^{\frac{1}{3}}\cdot F_1\cdot\left(Ar \le 10^8\right) + 0.0086\cdot\sqrt{Ar}\cdot Pr_v^{\frac{1}{3}}\cdot\left(Ar > 10^8\right) \qquad Nu = 179.4$$

Heat transfer coefficient $h_{film} := \lambda_v\cdot\frac{Nu}{l_c}$ $h_{film} = 201.8\,\frac{watt}{m^2\cdot K}$

Heat flux $Q_{film} := h_{film}\cdot\left(T_w - T_b\right)$ $Q_{film} = 36.9\,\frac{kW}{m^2}$

Evaporation mass flux $M_{film} := \frac{Q_{film}}{h_{fg}}$ $M_{film} = 0.072\,\frac{kg}{m^2\cdot sec}$

Mass evaporation rate as a function of pool radius $m_e(r) := \frac{\pi\cdot\left(r^2\right)\cdot Q_{film}}{h_{fg}}$

Spread Equations

Reduced gravitational acceleration (TNO 3.34) $g_r := g\cdot\frac{\left(\rho_w - \rho_l\right)}{\rho_w}$

Minimum frontal depth based on surface tension (TNO 3.48) $h_\sigma := \sqrt{\frac{\sigma}{g\cdot\rho_l}}$ $h_\sigma = 0.18\,cm$

Minimum frontal depth based on viscous effects (TNO 3.11) $h_c\left(q_S\right) := \left(\frac{6\cdot\nu_l\cdot q_S}{\rho_l\cdot\pi\cdot g}\right)^{0.25}$

Choose minimum depth (TNO 3.49) $h_{0max}(q) := \max\left(h_\sigma, h_c(q)\right)$

Pool shape factor $s\left(u,h,h_{0max}\right) :=$

1 if $h < 0.01\cdot m$

otherwise

$Fr \leftarrow 1.078$

$N \leftarrow \frac{u^2}{2\cdot Fr^2\cdot g_r\cdot h}$ if $u > 0$

$N \leftarrow 0$ otherwise

$s \leftarrow N + \sqrt{N^2 + \left(\frac{h_{0max}}{h}\right)^2}$

s

Gravity term coefficient (TNO 3.63)

$$\Phi(s) := (1 - s)\cdot(s \le 2) + \left(\frac{-s^2}{4}\right)(s > 2)$$

TNO (3.46)

$$j(s) := 1\cdot(s \ge 2) + \frac{2}{s}\cdot(s < 2)$$

Resistance for laminar flow (TNO 3.64, 3.65b, 3.66, 3.68W, and 3.69)

$$ff(u,h,s,r) := \left|\begin{array}{l} 1 \text{ if } r = 0\cdot m \\ \text{otherwise} \\ \quad \left|\begin{array}{l} 1 \text{ if } h < 0.001\cdot m \\ \text{otherwise} \\ \quad \left|\begin{array}{l} 1 \text{ if } u < 0.000001\cdot \frac{m}{sec} \\ \text{otherwise} \\ \quad \left|\begin{array}{l} f \leftarrow 0.2 \\ \text{root}\left(\frac{\mu_1}{\mu_w}\cdot\sqrt{\frac{u\cdot h^2}{\nu_w\cdot r}}\cdot\frac{1}{j(s)}\cdot f^{\frac{3}{2}} - 1 + f, f\right) \end{array}\right. \end{array}\right. \end{array}\right.$$

$$C_{FL}(u,h,s,r) := \left|\begin{array}{ll} 0\cdot\frac{m}{sec^2} & \text{if } h \le 0 \\ 2.35\cdot j(s)\cdot 0.66\cdot\nu_1\cdot\frac{u}{h^2}\cdot(1 - ff(u,h,s,r)) & \text{otherwise} \end{array}\right.$$

Resistance for turbulent flow (TNO 3.70 and 3.71)

$$C_{FT}(u,h,s) := \left|\begin{array}{ll} 0\cdot\frac{m}{sec^2} & \text{if } h \le 0 \\ \frac{4.49\cdot j(s)\cdot 0.0015\cdot u^2}{h} & \text{otherwise} \end{array}\right.$$

Resistance term (TNO 3.72)

$$C_F(u,C_{FT},C_{FL}) := \text{sign}(u)\cdot\max(C_{FT},C_{FL})$$

Acceleration of the leading edge of the pool (TNO 3.62)

$$a(\Phi,h,r,C_F) := \frac{4\cdot\Phi\cdot g_r\cdot h}{r} - C_F$$

Acceleration as a function of current speed, radius, height, and mass addition rate

$$acc(u,r,h,q) := \left|\begin{array}{l} h_{0max} \leftarrow h_{0max}(q) \\ s \leftarrow s(u,h,h_{0max}) \\ \Phi \leftarrow \Phi(s) \\ C_{FT} \leftarrow C_{FT}(u,h,s) \\ C_{FL} \leftarrow C_{FL}(u,h,s,r) \\ C_F \leftarrow C_F(u,C_{FT},C_{FL}) \\ a(\Phi,h,r,C_F) \end{array}\right.$$

Spill Definition for Pool Calculations

Initial pool volume
Specified above under Scenario Definition

$V_I := V_{instant}$ $V_I = 0\,m^3$

Spill rate as a function of time

Defined above under
Vessel Release and Deinventory

Time step

$dt := 0.1 \cdot sec$

Pool Spread and Evaporation Algorithm

$pool :=$ $t_0 \leftarrow 0 \cdot sec$

$V_0 \leftarrow V_I$

$r_0 \leftarrow \left(V_0\right)^{\frac{1}{3}}$

$h_0 \leftarrow \frac{V_0}{\pi \cdot \left(r_0\right)^2}$

$u_0 \leftarrow 0 \cdot \frac{m}{sec}$

$q_0 \leftarrow q_S(0 \cdot sec)$

$h_{min_0} \leftarrow h_{0max}\left(q_0\right)$

$a_0 \leftarrow acc\left(u_0, r_0, h_0, q_0\right)$

$e_0 \leftarrow m_e\left(r_0\right)$

$V_{add_0} \leftarrow \frac{q_0 \cdot dt}{\rho_1}$

$V_{evap_0} \leftarrow \frac{e_0 \cdot dt}{\rho_1}$

$i \leftarrow 0$

while $(i < 1) \vee \left(V_i > 0 \cdot m^3\right)$

- $i \leftarrow i + 1$
- $t_i \leftarrow i \cdot dt$
- $V_i \leftarrow V_{i-1} + V_{add_{i-1}} - V_{evap_{i-1}}$
- $V_i \leftarrow 0 \cdot m^3$ if $V_i < 0$
- $r_i \leftarrow r_{i-1} + u_{i-1} \cdot dt$

$$r_i \leftarrow \left(V_i\right)^{\frac{1}{3}} \quad \text{if } r_i = 0 \cdot m$$

$$h_i \leftarrow \frac{V_i}{\pi \cdot \left(r_i\right)^2}$$

$$u_i \leftarrow u_{i-1} + a_{i-1} \cdot dt$$

$$q_i \leftarrow q_S(i \cdot dt)$$

$$e_i \leftarrow m_e\left(r_i\right)$$

$$a_i \leftarrow acc\left(u_i, r_i, h_i, q_i\right)$$

$$V_{add_i} \leftarrow \frac{q_i \cdot dt}{\rho_1}$$

$$V_{evap_i} \leftarrow \frac{e_i \cdot dt}{\rho_1}$$

$$M^{\langle 0 \rangle} \leftarrow \frac{t}{sec}$$

$$M^{\langle 1 \rangle} \leftarrow \frac{V}{m^3}$$

$$M^{\langle 2 \rangle} \leftarrow \frac{r}{m}$$

$$M^{\langle 3 \rangle} \leftarrow \frac{h}{m}$$

$$M^{\langle 4 \rangle} \leftarrow \frac{q}{\frac{kg}{sec}}$$

$$M^{\langle 5 \rangle} \leftarrow \frac{e}{\frac{kg}{sec}}$$

M

Pool Spread and Evaporation Results

Time for complete evaporation	$t_{total} := \max\left(pool^{\langle 0 \rangle}\right) \cdot sec$	$t_{total} = 1100\,sec$	$t_{total} = 18.3\,min$
Maximum pool radius	$r_{max} := \max\left(pool^{\langle 2 \rangle}\right) \cdot m$	$r_{max} = 166.146\,m$	

pool =

	t	V	r	h	q	e
	0	1	2	3	4	5
0	0	0	0	0	$1.325 \cdot 10^5$	0
1	0.1	31.353	3.153	1.004	$1.323 \cdot 10^5$	2.26
2	0.2	62.666	3.153	2.006	$1.321 \cdot 10^5$	2.26
3	0.3	93.939	3.222	2.88	$1.32 \cdot 10^5$	2.36
4	0.4	125.174	3.429	3.389	$1.318 \cdot 10^5$	2.673
5	0.5	156.368	3.795	3.456	$1.316 \cdot 10^5$	3.274
6	0.6	187.524	4.253	3.3	$1.315 \cdot 10^5$	4.112
7	0.7	218.64	4.73	3.111	$1.313 \cdot 10^5$	5.086
8	0.8	249.716	5.201	2.939	$1.311 \cdot 10^5$	6.149
9	0.9	280.752	5.661	2.789	$1.31 \cdot 10^5$	7.285
10	1	311.75	6.11	2.658	$1.308 \cdot 10^5$	8.488
11	1.1	342.707	6.549	2.543	$1.306 \cdot 10^5$	9.752
12	1.2	373.625	6.979	2.442	$1.305 \cdot 10^5$	11.074
13	1.3	404.503	7.401	2.351	$1.303 \cdot 10^5$	12.451
14	1.4	435.341	7.814	2.269	$1.301 \cdot 10^5$	13.881

Plot evaporation rate versus time

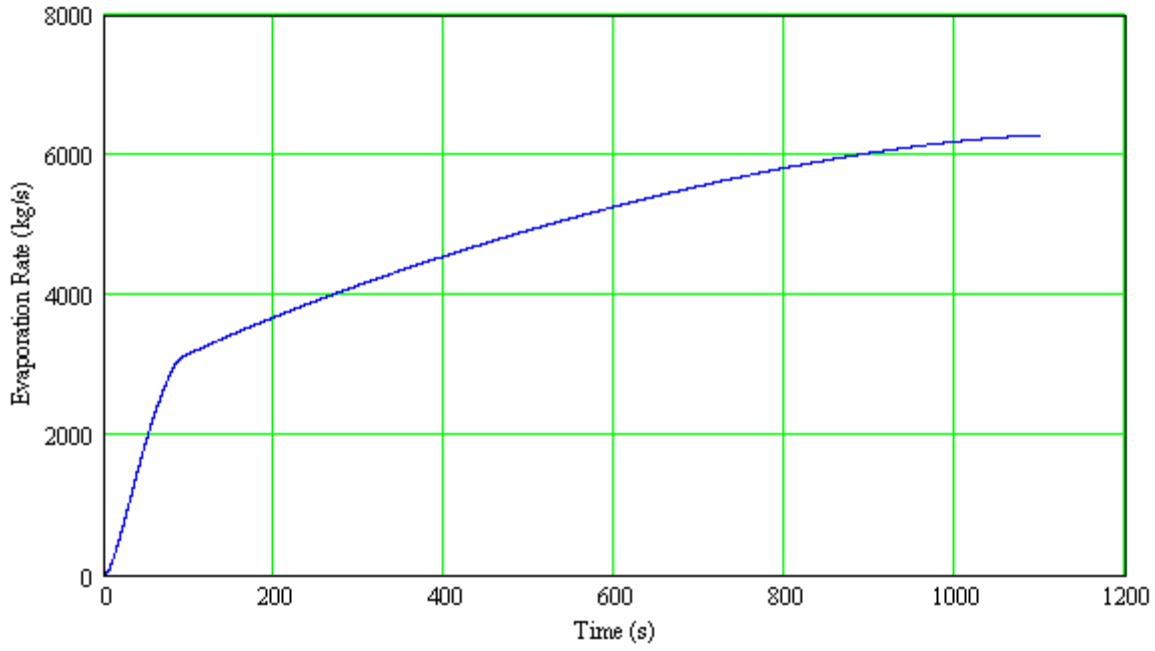

Plot pool radius versus time

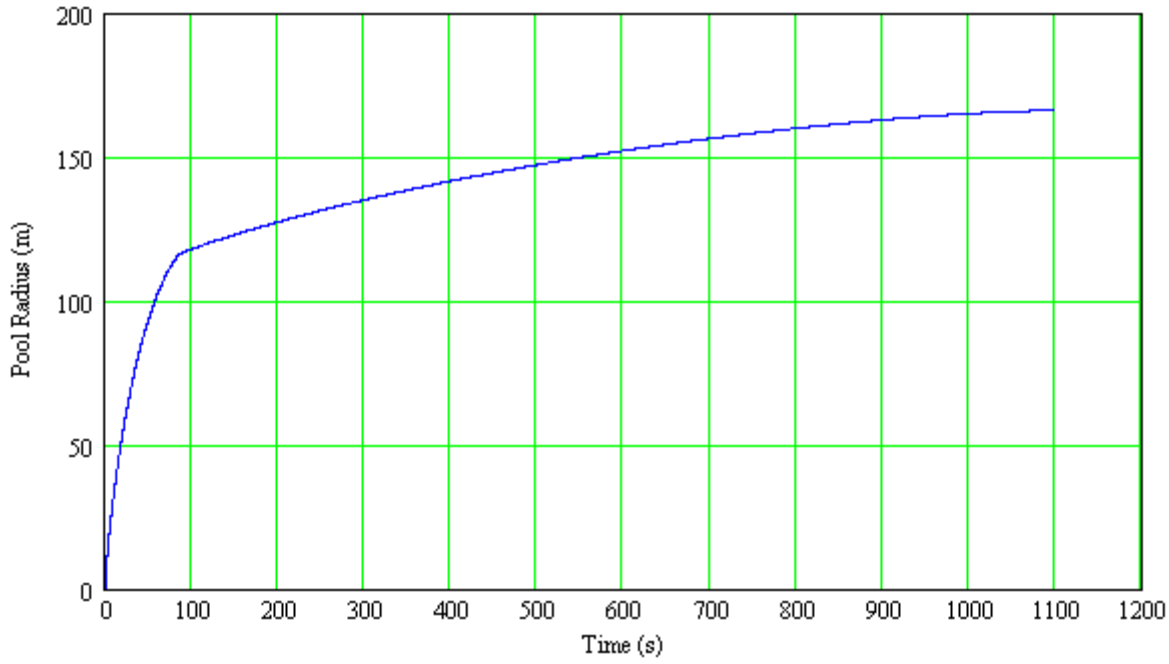

Transient Source Term for DEGADIS

Time step $step := \frac{t_{total}}{38}$ $step = 28.955\ s$

For each time step, use the evaporation rate and pool radius for the midpoint

$deg :=$ for $i \in 0..37$

$t_i \leftarrow i \cdot \frac{step}{sec}$

$t_{mid} \leftarrow t_i + \frac{step}{2 \cdot sec}$

$e_i \leftarrow linterp(pool^{\langle 0 \rangle}, pool^{\langle 5 \rangle}, t_{mid})$

$r_i \leftarrow linterp(pool^{\langle 0 \rangle}, pool^{\langle 2 \rangle}, t_{mid})$

$t_{38} \leftarrow \frac{38 \cdot step}{sec}$

$t_{39} \leftarrow t_{38} + 1$

$M^{\langle 0 \rangle} \leftarrow t$

$M^{\langle 1 \rangle} \leftarrow e$

$M^{\langle 2 \rangle} \leftarrow r$

M

deg =

	0	1	2
0	0.00	419.43	42.95
1	28.96	1714.92	86.85
2	57.91	2756.31	110.11
3	86.87	3175.33	118.18
4	115.82	3334.98	121.12
5	144.78	3487.11	123.85
6	173.73	3632.94	126.41
7	202.69	3773.32	128.83
8	231.64	3908.82	131.13
9	260.60	4039.89	133.31
10	289.55	4166.85	135.38
11	318.51	4289.94	137.37
12	347.46	4409.37	139.27
13	376.42	4525.29	141.09
14	405.37	4637.82	142.83
15	434.33	4747.04	144.50
16	463.28	4853.03	146.11
17	492.24	4955.83	147.65
18	521.19	5055.49	149.12
19	550.15	5152.01	150.54
20	579.11	5245.40	151.90
21	608.06	5335.66	153.20
22	637.02	5422.76	154.45
23	665.97	5506.67	155.64
24	694.93	5587.33	156.77
25	723.88	5664.70	157.85
26	752.84	5738.70	158.88
27	781.79	5809.22	159.85
28	810.75	5876.16	160.77
29	839.70	5939.37	161.64
30	868.66	5998.68	162.44
31	897.61	6053.89	163.19
32	926.57	6104.72	163.87
33	955.52	6150.83	164.49
34	984.48	6191.76	165.03
35	1013.43	6226.85	165.50
36	1042.39	6254.38	165.87
37	1071.34	6271.06	166.09
38	1100.30	0.00	0.00
39	1101.30	0.00	0.00

Write data to text file for input to DEGADIS

WRITEPRN("deg.txt") := deg

Note that DEGADIS requires the number of data points at the top of the file, so before input to DEGADIS, a new line should be added to the top of this file with the number 40.